Using Finite Element Methods to study Anterior Cruciate Ligament Injuries: Understanding the role of ACL modulus and Tibial Surface Geometry on ACL loading

By

Jesal N. Parekh

A dissertation submitted in partial fulfillment
of the requirements for the degree of
Doctor of Philosophy
(Kinesiology)
in The University of Michigan
2013

Doctoral Committee:
Assistant Professor Mark Palmer, Co-Chair
Assistant Professor Scott McLean, Co-Chair
Professor James Ashton-Miller
Professor Ellen Arruda

DEDICATION

To teachers, mentors, friends and family.

TABLE OF CONTENTS

DEDICATION ii
LIST OF FIGURES v
LIST OF TABLES viii
ABSTRACT ix
CHAPTER I 1
Introduction 1
Specific Aims and Hypotheses 5
Theoretical Basis 10
CHAPTER II 16
Literature Review 16
The Knee 16
Anterior Cruciate Ligament (ACL) 24
ACL Injuries 25
Computational Modeling 33
CHAPTER III 37
Preliminary Tests 37
CHAPTER IV 43
Development of a Finite Element Model of the Knee 43
Introduction 43
Overview of the experiment by Oh et al. (2011) 44
Essential features of a desired model 45
Methods 48
Validation 56
Chapter V 59
Effect of ACL Modulus on ACL Strain during Impact Loading 59
Introduction 59

Methods 60
Results 62
Discussion 65
Chapter VI 67
Effect of Tibial Surface Geometry on ACL Strain during Impact Loading 67
Introduction 67
Methods 68
Results 70
Discussion 73
Chapter VII 77
Combined Effect of Tibial Surface Geometry and ACL Modulus on ACL Strain during Impact Loading 77
Introduction 77
Methods 78
Results 79
Discussion 84
Chapter VIII 87
General Discussion 87
Significance and Innovation 87
Summary of Results 90
Assumptions and Limitations 91
Future Work 93
BIBLIOGRAPHY 96

LIST OF FIGURES

Figure 1: Schematic representation of cadaveric test device used by Oh et al (2011). Note the inverted limb for distal-to-proximal impact. 6

Figure 2: Free body diagram showing forces on the tibia when mounted in the test apparatus. 10

Figure 3: Decreased ACL modulus causes a right shift resulting in a delay in the onset of the opposing impulse (area under the tension versus time curve) supplied by the ACL. 13

Figure 4: Anatomy of the knee joint 16

Figure 5: MRI showing the medial femoral condyle in the sagittal plane 17

Figure 6: Lateral and Medial Tibial Slopes (Hashemi et al, 2010) 18

Figure 7: Internal factors contributing to ACL injury risk 30

Figure 8: Panel 1 – The drop land test apparatus used to measure relative strain in ACL (Withrow et al, 2006); Panel 2 – The 2-D FE model used to test the hypotheses 37

Figure 9: Average ACL strain profiles obtained for different ACL laxity values 40

Figure 10: Peak average ACL strains and peak anterior tibiofemoral accelerations obtained for different ACL modulus values 41

Figure 11: Average ACL strain profiles obtained for different lateral tibial slopes. A 7^{o} slope was normal, 10.1^{o} was high slope and 3.9^{o} slope was low. 42

Figure 12: Segmented solid model of the knee joint 49

Figure 13: Meshed (discretized) 3-D knee joint model 50

Figure 14: Fitting coefficients C10 and C01 on the experimental data. The solid line is the fit and the red data markers indicate the stress-strain data. 52

Figure 15: 3-D FE model of knee joint in LS-Dyna 54

Figure 16: Impulsive load applied to distal tibia (Oh et al. 2011). Tibia_AP denotes the anterior-posterior force, Tibia_ML denotes the medial-lateral force and Tibia_Vert denotes the vertical force. 55

Figure 17: Arrow indicates the region from which strain was measured 55

Figure 18: Kinematic and ACL strain results from the cadaveric experiments (Oh et al. 2011). Flexion angle, Internal rotation angle and Valgus angle are all positive on the Y-axis. 56

Figure 19: Kinematic and ACL strain results predicted by the FE model. The Flexion angle, Internal rotation angle, Valgus angle are all positive on the Y-axis 57

Figure 20: Uniaxial stress-strain data used to determine mechanical behavior of ACL 61

Figure 21: Non-linear (toe) region of the uniaxial stress-strain data used to determine mechanical behavior of ACL 61

Figure 22: Variation in change in ACL strain with respect to ACL modulus 63

Figure 23: Variation in relative tibiofemoral acceleration with respect to ACL modulus [-y → anterior acceleration] 63

Figure 24: Variation in peak change in ACL strain and peak anterior tibiofemoral acceleration with respect to ACL modulus 64

Figure 25: Variation in change in ACL strain with respect to different tibial surface geometries. 70

Figure 26: Variability in valgus(+) angle with change in tibial surface geometry 71

Figure 27: Variability in internal rotation (+) with change in tibial surface geometry 72

Figure 28: Comparison of distribution of residuals to normal distribution 73

Figure 29: Change in ACL strain profiles for the 25 cases simulated 79

Figure 30 (a-e): Variation of peak ACL strain graphed with variation in peak anterior tibiofemoral acceleration, peak valgus angle and peak internal rotation angle for each of the five cases 82

Figure 31: Comparison of distribution of residuals to normal distribution 84

LIST OF TABLES

Table 1: Material property definitions for bone, cartilage, meniscus and tendons 51

Table 2: Force-length definitions for the spring elements representing muscles (Oh et al. 2011) 53

Table 3: Values of MTD, MTS and LTS applied to test the hypotheses (Hashemi et al. 2011) 69

Table 4: Different combinations of MTD, MTS and LTS tested 69

Table 5: List of simulations run to test the effect of ACL modulus and tibial surface geometry .. 78

Table 6: Summary of results from Chapter IV 90

Table 7: Summary of results from Chapter V 90

Table 8: Summary of results from Chapter VI 90

Table 9: Summary of results from Chapter VII 91

ABSTRACT

Using Finite Element Methods to study Anterior Cruciate Ligament Injuries: Understanding the role of ACL modulus and Tibial Surface Geometry on ACL loading

By

Jesal N. Parekh

Chair: Mark Palmer

ACL injury is frequently encountered in sports resulting in impaired gameplay, accruement of medical expenses and potential for long-term degenerative disease of the knee joint. More than 200,000 ACL injuries occur annually with the injury rate disproportionately higher in females. Many factors are implicated in this gender dimorphic behavior including ACL modulus and tibial surface geometry. The main objective was to determine if the effects of knee geometry and ligament properties manifest as externally measurable variables such as anterior tibiofemoral acceleration or 3-D tibiofemoral rotations. This would provide us with much needed insight into the mechanism of ACL loading and also inform the potential for surveillance monitoring of knee kinematics to identify injury risk in real-time. To achieve this goal, a finite element model was developed to simulate a single-leg landing by applying an impulsive load to the distal tibia recreating an experiment using cadaver knees by Oh et al. (2011). A significant correlation (Pearson's $R = 0.861$, $p < 0.01$) was found for the peak in ACL strain between 40ms and 70ms. The model was then used to predict knee kinematics and ACL strain resulting from a variation in ACL modulus and tibial surface geometry during simulated single-limb landing. The results

indicate that ACL modulus had a significant effect on ACL strain. Additionally, a significant correlation (0.999) was observed between the peak ACL strain and peak anterior tibiofemoral acceleration. Tibial surface geometry examined through the effect of lateral tibial slope, medial tibial slope, and medial tibial depth had a significant effect on ACL strain. However, it was interesting to note that none of these parameters individually influenced the ACL strain. Additionally, peak ACL strain correlated with peak anterior acceleration (0.483), peak valgus angle (0.779) and peak internal rotation angle (0.678). Simulations examining the effect of ACL modulus and tibial surface geometry indicated a significant main effect of both the factors. However no interaction effect was observed. A significant correlation was observed between the peak ACL strain with peak anterior tibiofemoral acceleration (0.979), peak valgus angle (0.458) and peak internal rotation angle (0.853). These findings support our hypothesis that differences in morphometric and ligament properties manifest as altered kinematics of the knee joint that correlate with ACL strain.

CHAPTER I

Introduction

An estimated 80,000 to 250,000 ACL injuries occur each year afflicting, for the most part, people in the range of 15-24 years of age (Griffin et al. 2006). Approximately 100,000 of these patients will undergo ACL reconstruction and rehabilitation each year resulting in total medical expenses exceeding 2 billion dollars (American Academy of Orthopedic Surgeons, 2000; Griffin et al. 2000; Huston et al. 2000). With a steadily increasing number of participants in sports, at both the high school and collegiate level, the number of ACL injuries has also dramatically risen (NCAA, 2002; NFHS, 2004). Although male participation in sport activities is greater, the rate of ACL injuries in females is disproportionately higher. Female athletes have an increased proclivity for ACL injuries with a rate of incidence of non-contact ACL injuries 4 to 8 times greater in females than in males for the same sport (Ireland et al. 1990; Arendt et al. 1999; Gwinn et al. 2000; Ford et al. 2003; Hewett et al. 2005). ACL injuries not only impede immediate physical activity and participation in sports but also result in long term debilitative effects. Degenerative diseases like osteoarthritis (OA) are evident in the affected knee shortly after reconstructive surgery (Daniel et al. 1994; Lohmander et al. 2004). Long term studies report an estimated 45% of individuals who sustain ACL rupture experienced premature knee OA within 10 years of the injury to a degree most

frequently observed in people aged 65 years and above (Brandt et al. 1991; Roos et al. 2005). Moreover, current research suggests that an increased number of individuals will exhibit premature knee OA when in their 30s and 40s as a consequence of knee injuries sustained at a young age, making the knee five times more likely to develop OA with rapid degeneration and "wear-and-tear" of soft tissues (Englund et al. 2003; Gelber et al. 2000; Lohmander et al. 2004; von Porat et al. 2004). Taking into consideration the number of players being injured, it is likely that a cohort of a large number of young athletes, particularly females, will be afflicted with degenerative joint disease permanently impacting physical activity and health across the remainder of the lifespan.

ACL injuries occur when the ACL is stretched beyond the normal physiological range resulting in weakening or rupture of the tissue. Approximately 70% to 90% of all ACL injuries are attributed to a non-contact mechanism during dynamic activities such as single leg landing from a jump, pivoting, or decelerating abruptly (Hughes et al. 2006). **While there is no direct, non-invasive way to measure stretch of the ACL, we propose that it can be assessed indirectly by means of anterior tibiofemoral acceleration and knee rotation in frontal and transverse planes. Specifically, we propose that 3-D knee kinematics (anterior tibiofemoral acceleration, varus-valgus angle and internal-external rotation angle) can be potentially used as a non-invasive, surrogate measure to determine when the ACL is at risk of injury.**

Gender disparity in ACL injury rates and the existing gender dimorphism has led to delineation of biomechanical, neuromuscular, and anatomical factors specifically

observed in female athletes. For instance, knee abduction (valgus) angle and torques (Ford et al. 2003; Griffin et al. 2006; McLean et al. 2004); lower limb muscle strength (Withrow et al. 2006), quadriceps and/or hamstrings strength and activation (Beynnon et al. 1998; Hewett et al. 2005; Shultz et al. 1999); joint laxity (Uhorchak et al. 2003), ACL laxity, and tibial slope (Hashemi et al. 2010) are considered especially strong predictors of ACL injury risk in female athletes. Therefore, in recent years, a pivotal issue has been the development of suitable training and exercise regimens to counter the effect of these risk factors and prevent ACL injuries (Cochrane et al. 2010; Hashemi et al. 2010; Hewett et al. 2005). While these training programs have successfully demonstrated short-term modification in athletes' biomechanics and neuromechanics, long-term retention has not been observed. Additionally, not all of these learned skills get transferred to the field where conditions of stress and fatigue further increase risk of ACL injury (Smith et al. 2009). Epidemiology suggests that despite these efforts, the rate of ACL injuries remains high (Arendt et al. 1999), approximately 1,184 per 100,000 (Gianotti et al. 2009). An effective training protocol especially for female athletes is challenging to design in view of the fact that a female athlete's biomechanical and neuromuscular response change depending on the current phase of the menstrual cycle of the athlete (Shultz et al. 2005). **Thus, an immediate critical need is to develop an alternative strategy for effective, long-term reduction in ACL injuries. This can be achieved by expanding our study to understand other risk factors and mechanisms and use that knowledge to gain insight into the loading mechanism of ACL during the course of dynamic activity.**

This dissertation serves to address a void in the existing research pertaining to non-contact ACL injuries. Majority of non-contact ACL injuries occur during dynamic landing or pivoting activities when the knee joint experiences impulsive loading with acceleration of the segments followed by rapid deceleration. Certain knee kinematics and kinetics were consistently observed in video analysis immediately prior to an ACL injury. These biomechanics collectively identified as the 'point of no return' are as follows: the athlete comes to an abrupt halt, the shank rapidly decelerates, foot is planted to the ground, the knee is in extension or locked with valgus collapse and internal rotation of the tibia and the body experiences 4-12 body weights of ground reaction force. A critical aspect to the non-contact injury mechanism is the acceleration response of the segments. Knee anatomy, specifically ACL modulus and tibial surface geometry (slopes and depth) could have a profound effect on segmental accelerations and subsequently on ACL loading. Dynamic loading conditions especially those tending towards injuries, however, are difficult to recreate with human subjects and ACL strain is impossible to study without employing invasive measures. Even though *in vitro* studies make it easier to determine ACL strain under such loads, effect of specific factors cannot be studied in isolation. Finite element modeling (FEM) and finite element analysis (FEA) provide alternatives to both human and cadaveric experiments. In particular, modeling enables the study of risk factors in isolation. By employing modeling methods, very specific changes in the anatomy of the knee joint and ACL can be introduced and the sensitivity of ACL strain to these changes can be subsequently monitored. This dissertation therefore draws from the advantages offered by the

methods of FEM and FEA to first develop and validate a 3-D FE model and then use the validated model to determine sensitivity of ACL strain and frontal and transverse plane rotations and sagittal plane tibiofemoral acceleration to ACL modulus and tibial surface geometry.

Thesis Statement

The ultimate goal of this thesis is to test the hypothesis that externally observable knee kinematics predict the strain in the ACL during the course of a dynamic activity.

Specific Aims and Hypotheses

Aim 1: Validate the results from 3-D FE Model against data from a cadaveric model.

A 3-D computational knee model derived from noninvasive imaging was created to simulate the ACL tissue response to impulsive loads. The computational model was configured to replicate conditions of an impact loading experiment initially developed by Withrow et al (2006) and later modified by Oh et al (2011) (Figure 1). ACL strain and knee kinematic data from the cadaveric experiment carried out by Oh et al (2011) were used to validate ACL strain and knee kinematics predictions from the computational model. Once validated, the model then served to drive the following aims.

Hypothesis 1: Compared with a cadaveric model, a 3D finite element model can predict the kinematics (and/or kinetics) of impact loading with a Pearson's correlation greater than 0.80.

Rationale: Validating the model by using both kinematic and strain measures would provide a more comprehensive validation adding confidence to the predictive capacity of the FEM especially considering the objective of this thesis relies largely on the kinematic as well as ACL strain prediction by the FEM. In view of the fact that only the mounting and impact conditions from the experiment were recreated in the FEM and that the rest of the parameters critical to the definition of the FEM were obtained from literature, a Pearson's correlation greater than 0.80 would provide the statistical evidence that the FEM behavior closely mirrors a cadaveric knee under similar conditions of loading and boundary conditions.

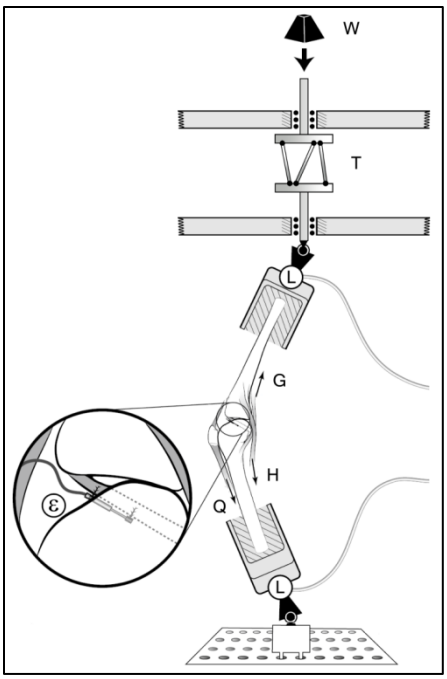

Figure 1: Schematic representation of cadaveric test device used by Oh et al (2011). Note the inverted limb for distal-to-proximal impact.

Aim 2: Determine the effect of ACL Modulus on ACL Strain and understand how it implicates in an ACL loading mechanism.

The effect of ACL modulus on ACL strain was tested using the validated 3-D FE model. Investigating the role of ACL modulus elucidates the relationship between model predicted ACL strain and model predicted relative anterior tibial acceleration over a range of ACL moduli. This knowledge would be useful in gaining insight into the role that ACL modulus plays in ACL loading during the execution of a dynamic motion. Ultimately, this understanding could potentially provide the necessary insight to design an effective screening and surveillance protocol that can pre-emptively mitigate the conditions that increase risk for ACL injury.

Hypothesis 2: An ACL with low modulus will (i) experience greater strain and (ii) develop higher anterior tibiofemoral acceleration during the course of impact.

Rationale: Low ACL modulus (high laxity) would cause the ligament to have poor restraining capabilities, resulting in an inability to provide the necessary force to sufficiently oppose anterior translation of the tibia relative to femur. This would result in high anterior tibiofemoral acceleration which would manifest as greater stretch in the ACL and therefore, as greater strain.

Aim 3: Determine the effect of tibial surface geometry (medial tibial slope, lateral tibial slope and medial tibial depth) on ACL strain and understand how it implicates in an ACL loading mechanism.

The effects of tibial surface geometry including medial tibial slope (MTS), lateral tibial slope (LTS) and medial tibial depth (MTD) on ACL strain were simulated using the validated 3-D FE model. Investigating the influence of tibial surface geometry will enable us to quantify the effect of tibial plateaus and concavity on model predicted ACL strain and model predicted relative anterior tibial acceleration, varus-valgus angle and internal-external rotation angle over a range of MTS, LTS and MTD. Tests were performed to elucidate both the main effect and interaction effect of each of these three parameters. The best combination and the worst combination with respect to ACL strain manifestation were identified and used to drive the following aim.

Hypothesis 3a: A high lateral tibial slope, high medial tibial slope and a shallow concavity will result in (i) the highest ACL strain and (ii) higher anterior tibiofemoral acceleration.

Rationale: High lateral tibial slope would exacerbate relative anterior tibial translation by promoting posterior slide of femoral condyles on the tibial surface which would undermine the restraining functions of ACL. Additionally, valgus and internal rotation could further stretch the ACL resulting in development of greater ACL strain.

Hypothesis 3b: A lateral tibial slope higher than the medial tibial slope and a shallow concavity will result in (i) the highest ACL strain (ii) higher internal rotation of the tibia and (iii) higher valgus angle

Rationale: A lateral tibial slope higher than the medial tibial slope would promote valgus and internal rotation at the tibiofemoral joint. High lateral tibial slope and a shallow medial concavity would encourage posterior slide of femoral condyles on tibial surface resulting in development of high anterior tibial acceleration. These kinematic conditions would load the ACL cause high strains to manifest in the structure.

Hypothesis 3c: A knee with a medial tibial slope higher than the lateral tibial slope and a deep concavity will result in the least ACL strain and more stable knee kinematics.

Rationale: A medial tibial slope higher than the lateral tibial slope would discourage valgus and internal rotation at the tibiofemoral joint. Additionally, low lateral tibial slope and a deep medial tibial depth would result in increased congruity between the tibial-femoral articular surfaces, minimizing the development of the anterior tibiofemoral acceleration. These kinematic factors will lead to least strain manifesting in the ACL.

Aim 4: Explore the interaction effect of ACL modulus and tibial surface geometry on ACL strain and understand the sensitivity of ACL strain to these parameters.

The interaction of ACL modulus and tibial surface geometry was tested to explore its combined effect on ACL strain.

The results from these aims will provide much needed insight into the role of knee physiology and anatomy on ACL loading mechanism. Because these factors result in interplay of complex, three dimensional mechanics, their study is greatly facilitated by using computational modeling. In addition, these factors have been identified as crucial for determining the proclivity for ACL injury particularly in female athletes but the mechanism by which these implicate in an injury is unknown (Griffin et al. 2006).

Theoretical Basis

The theoretical basis for the influence of ACL modulus, tibial slopes and tibial depth on anterior-posterior tibiofemoral acceleration can be laid out using equilibrium equations derived from segmental analysis in the *sagittal plane* of the tibia. The free body diagram shown in Figure 2 depicts tibia mounted on the experimental apparatus used by

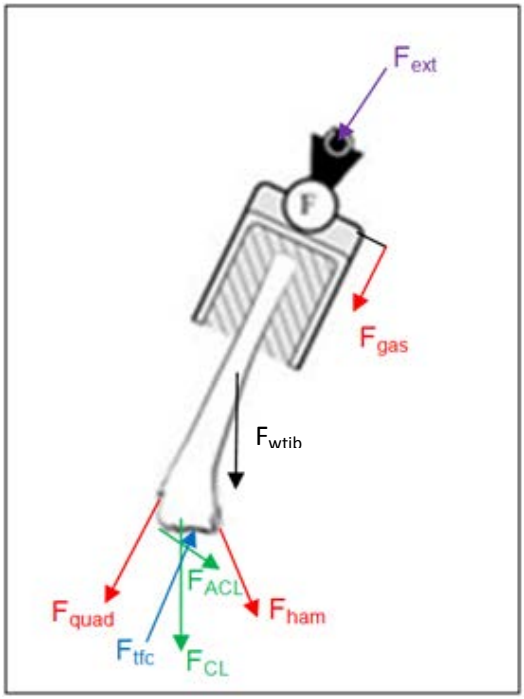

Figure 2: Free body diagram showing forces on the tibia when mounted in the test apparatus.

Withrow et al (2006) (Figure 1). The arrows indicate the forces acting on the tibia as the external load ($F_{ext,x}$, $F_{ext,y}$), the weight of the tibia mounted in the pot (F_{wtib}), the net muscle forces ($\Sigma F_{muscles}$), the tibiofemoral contact force (F_{tfc}), and the net ligamentous forces, ΣF_{lig} (sum of forces due to the cruciate and collateral ligaments: F_{acl}, F_{cl} = $F_{pcl}+F_{lcl}+F_{mcl}$). The positive x-direction corresponds to posterior direction, the positive y-direction corresponds to the inferior direction, and positive torque corresponds to extension at the knee joint. This loading configuration results in increased anterior tibial translation of the tibia with respect to the femur (Withrow et al. 2006, 2008). The load frame in the protocol limits the motion of the distal tibia to superior translation while preventing anterior-posterior and medial-lateral translations. This indicates that the load frame imposes a superior (-y) and anterior (-x) load on the tibia.

The resulting set of equilibrium equations are as follows:

$$\Sigma F_x = ma_x$$
$$-F_{ext,x} + \Sigma F_{lig,x} + F_{tfc,x} + \Sigma F_{muscles,x} = ma_x$$

$$\Sigma F_y = ma_y$$
$$-F_{ext,y} - F_{wtib} - \Sigma F_{lig,y} + F_{tfc,y} + \Sigma F_{muscles,y} = ma_y$$

$$\Sigma \tau_k = I_g\alpha - \left(ma_x R_x\right) + \left(ma_y R_y\right)$$
$$-\tau_{ext} + \Sigma \tau_{lig} - \tau_{wshank} + \Sigma \tau_{muscles} = I_g\alpha - \left(ma_x R_x\right) + \left(ma_y R_y\right)$$

where $\Sigma F_{muscles}$ denotes the sum of muscle forces (F_{gas}, F_{ham}, F_{quad}) and ΣF_{lig} denotes the sum of forces due to the cruciate and collateral ligaments (F_{acl}, $F_{cl} = F_{pcl}+F_{lcl}+F_{mcl}$); $\Sigma\tau_k$ denotes the sum of torques about the tibiofemoral joint at the intersection of the mechanical axes of the femur and tibia, I_g is the mass moment of inertia about the axis perpendicular to the long axis of the tibia, α is the angular acceleration and R_x and R_y are the moment arms with respect to the x and y axes respectively. The equilibrium expressions are integrated with respect to time, transforming them to a set of impulse momentum equations corresponding to the loading conditions for the experiment:

$$-\int_0^t F_{ext,x}dt + \int_0^t \Sigma F_{lig,x}dt + \int_0^t F_{tfc,x}dt + \int_0^t \Sigma F_{muscles,x} = m\int_0^t a_x dt$$

$$-\int_0^t F_{ext,y}dt + \int_0^t \Sigma F_{lig,y}dt + \int_0^t F_{tfc,y}dt - \int_0^t F_{wshank}dt + \int_0^t \Sigma F_{muscles,y} = m\int_0^t a_y dt$$

$$-\int_0^t \tau_{ext}dt + \int_0^t \Sigma\tau_{lig}dt - \int_0^t \tau_{wshank}dt + \int_0^t \Sigma\tau_{muscles}dt = I_g\int_0^t \alpha dt - m\int_0^t a_x R_x dt + m\int_0^t a_y R_y dt$$

The main contributors to ΣF_{lig} are the ACL, MCL, and PCL. At 15 degrees of flexion in the loading frame, the MCL and PCL are primarily vertically oriented. Tension in these ligaments will result in an increase in (F_{tfc}) as the tension from the ligaments pull the femur and tibia close together. By the virtue of its orientation, the line of action through which ACL exerts a force on the tibia is directed primarily in the posterior (+x) direction with a smaller superior (-y) component. The ACL, therefore, serves primarily as a restraint against anterior motion of the tibia opposing the effects of the externally

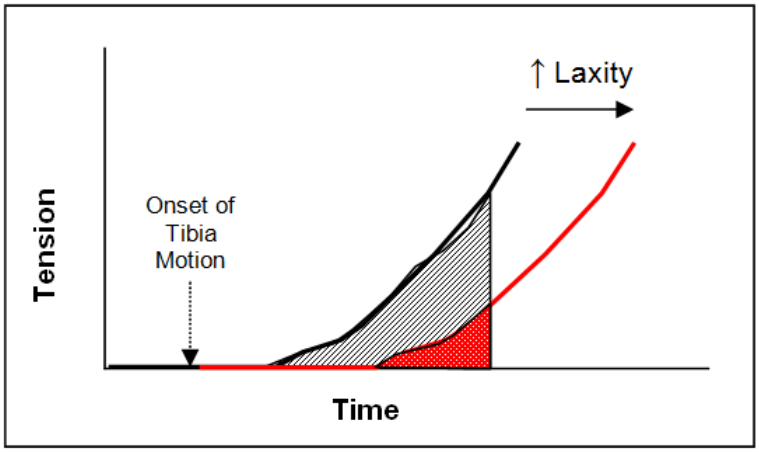

Figure 3: Decreased ACL modulus causes a right shift resulting in a delay in the onset of the opposing impulse (area under the tension versus time curve) supplied by the ACL.

applied loads in the negative x-direction, adding to the resultant vector between the ACL force and tibiofemoral force thereby increasing the force of contact (F_{tfc}) between the tibia and femur. Figure 3 shows that at each time point following the onset of anterior tibial motion, the tension versus time curve is shifted to the right in the ACL with low modulus. This results in an increase in the anteriorly directed ACL impulse with decreasing modulus. *Therefore the impulse momentum equation predicts that decreased ACL modulus results in increased anterior tibiofemoral accelerations.*

The equilibrium and impulse-momentum expressions presented above are defined in terms of the motion of the center of mass of the system. The axes are defined according to a global coordinate system. To determine the effect of tibial surface, in terms of medial tibial slope, lateral tibial slope or medial tibial depth, we focus on the forces acting on the tibial plateau. At 15^{o} of flexion with the distal tibia above the proximal femur, the average female tibia will be mounted at an angle of approximately 11.5^{o} from the vertical (Yoshioka et al., 1987; Yoshioka et al., 1989; Yoo et al., 2008).

An average lateral or medial tibial slopes of approximately 7 ± 3.1^{o} and 5.9 ± 3.0^{o} respectively (Hashemi et al. 2008) in the apparatus would result in a plateau angle approximately 5.5^{o} below the horizontal. The forces shown in the equations above acting in the inferior-superior directions (y-axis) are directed primarily perpendicular to the tibial plateau minimizing the contribution to the accelerations in the A-P directions (x-axis). An increase in the posterior slope of the tibia, either medial or lateral, increases the angle of the tibial plateau in the apparatus above the horizontal thereby improving the alignment with the anterior-superior directed external force and increasing the contribution of I-S directed loads to the motion of the tibia relative to the femur. The same effect is replicated when the concavity of the tibial surface is decreased i.e. medial tibial depth is shallower. *Therefore increased tibial slopes or shallower tibial depth will improve the alignment of the tibial plateau with the externally applied load resulting in an increase in anterior tibiofemoral translation.* This conclusion, however, assumes constant frontal and transverse plane kinematics. A change in the concavity and slopes would significantly impact the varus-valgus and internal-external rotation angles of the knee during the course of impact. These rotations play a crucial role in the loading of ACL and could have a significant effect on the manifestation of ACL strain.

The effect of ACL modulus can be either aggravated or mitigated by the tibial surface geometry. We speculate that certain combinations of knee morphometric parameters will amplify the effects of a low ACL modulus on ACL strain and joint kinematics. Likewise, a different geometric configuration would minimize the strain that manifests in the ACL.

Therefore, the equilibrium and impulse-momentum equations suggest that an in-depth investigation of the role of ACL modulus, medial tibial slope, lateral tibial slope and medial tibial depth within a 3D model is warranted.

CHAPTER II

Literature Review

The Knee

The knee joint is generally considered to be the largest and the most complex diarthrosis of the human body (Figure 4). Although its behavior is characteristic of a hinge joint, when flexed the knee joint is also capable of modest rotation and lateral

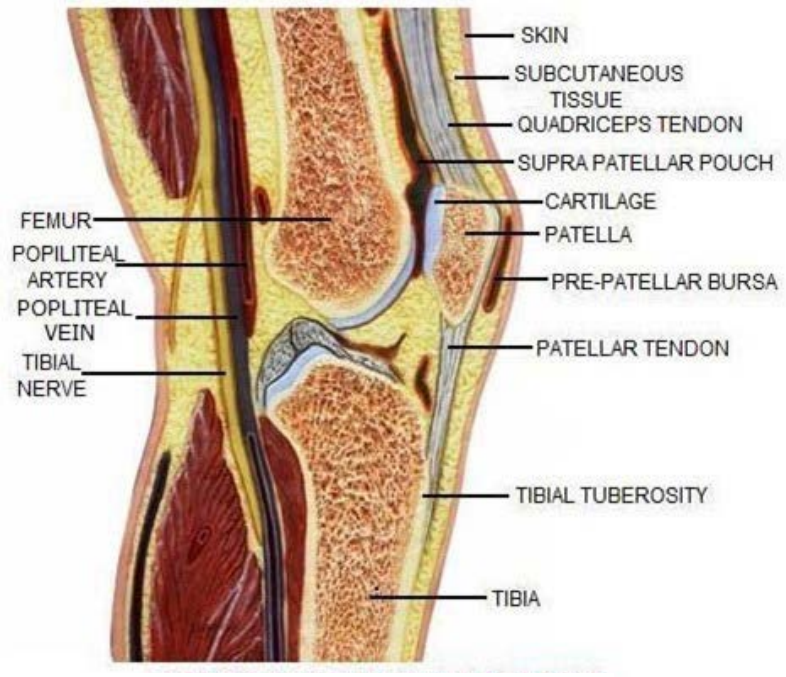

Figure 4: Anatomy of the knee joint

(http://www.joint-pain-expert.net/knee-joint.html)

gliding. The knee joint is formed where the distal end of the femur and proximal end of tibia meet. The femur, tibia and patella constitute the knee joint and result in two

separate articulations – the tibiofemoral joint between the condyles of the femur and the tibial plateau and the patellofemoral joint between the patella and the patellar surface of the femur.

Femoral Condyles (Evans, 1986; Al-Turaiki, 1986; Gray, 1993)

Along the femoral longitudinal axis, the lateral condyle protrudes less than the medial condyle but is wider in the sagittal and axial planes. When observing in sagittal plane, the condyles become more curved posteriorly (Figure 5). The curvature of lateral condyle increases from anterior to posterior more quickly than that of the medial condyle. The anterior surface between the femoral condyles forms a slight groove, extending down into the intercondylar notch and articulates with the patella.

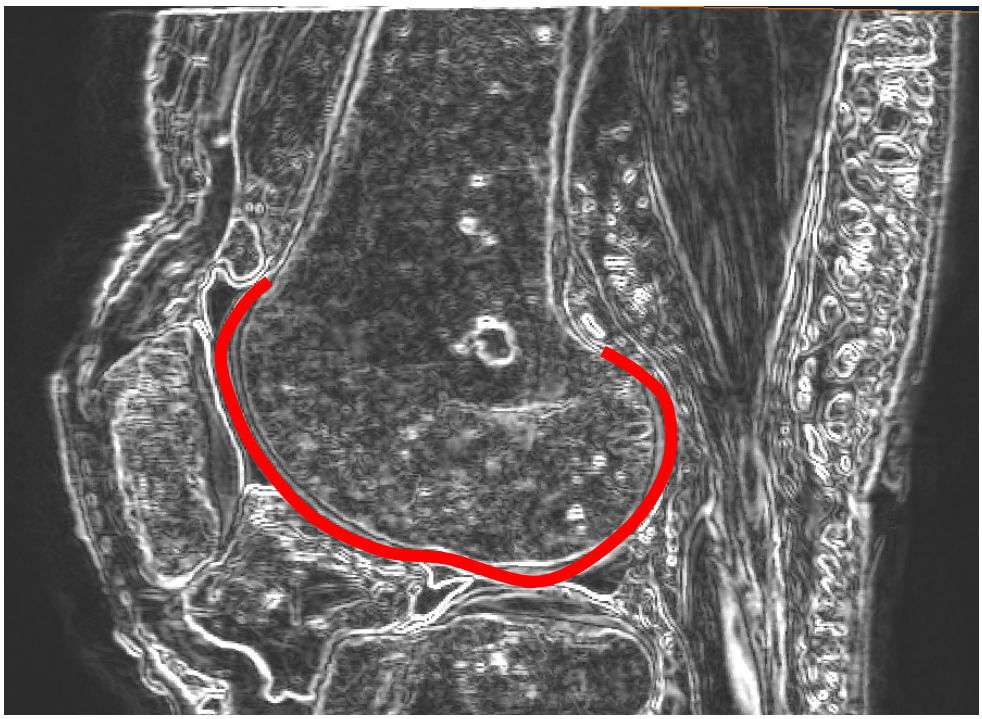

Figure 5: MRI showing the medial femoral condyle in the sagittal plane

Tibial Plateaus (Evans, 1986; Al-Turaiki, 1986; Gray, 1993; Hashemi et al. 2010)

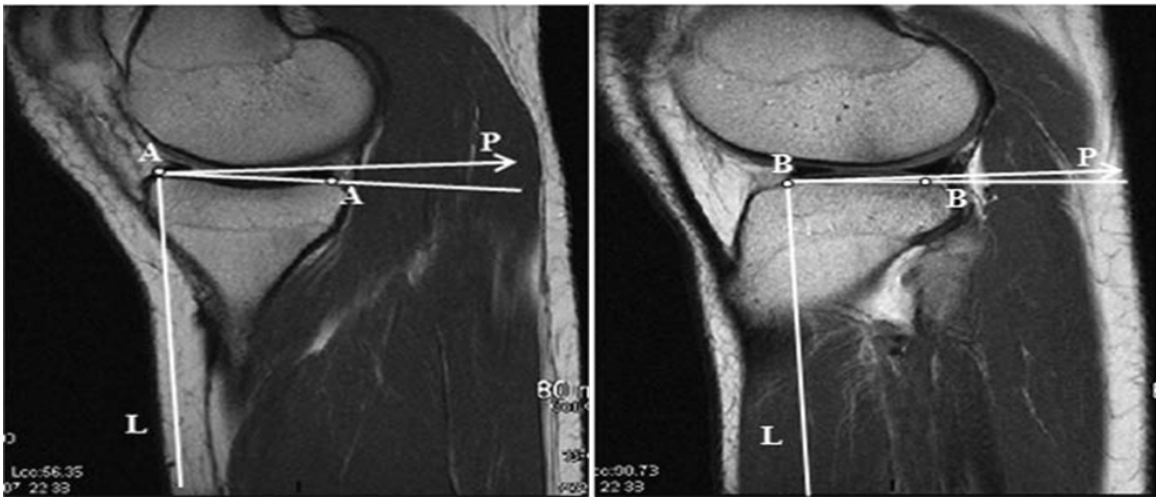

Figure 6: Lateral and Medial Tibial Slopes (Hashemi et al, 2010)

The tibial plateaus are defined by three slopes including the medial tibial slope (MTS), lateral tibial slope (LTS) (Figure 6) and coronal tibial slope (CTS). Compared to LTS, the MTS is bi-concave in shape and longer in the sagittal direction. In contrast, the LTS is more circular and broader than the MTS. In general, MTS is larger than LTS and consequently is thought to bear more of the weight. The depth of concavity of medial plateau in the middle of the articular region is defined as the medial tibial depth (MTD).

Patella (Nordin and Frankel, 1989)

The patella is a flat triangular bone situated in the anterior aspect of knee within the tendon of quadriceps extensor muscle. Its posterior surface is oblong and smooth with a vertically running ridge dividing the medial and lateral facets. Articulation with the femur occurs with this ridge moving along the groove on the *trochlear* surface of the femur forming the *patellofemoral joint*. The function of the patella is two-fold, first it

lengthens the lever arm of the quadriceps muscle force by displacing the quadriceps tendon anteriorly and second, it offers a larger contact area between the patellar tendon and femur thus reducing contact stress between the two.

Articular Cartilage

All articulating surfaces in the knee joint are covered by a protective layer of tissue known as hyaline articular cartilage. Hyaline articular cartilage covers the femoral condyles, tibial plateaus and posterior surface of patella. The articular cartilage is typically thicker on the tibial plateau particularly in regions where menisci are not effective and the bones are in direct contact. Additionally, thickness is pronounced on the medial aspect of tibia (Nordin and Frankel, 1989), further suggesting greater loading on medial surface of tibia. The main functions of the cartilage are to protect the subchondral bone from mechanical damage, to prevent abrasive wear between bone extremities and to lower the friction of the bearing surfaces. These functions are achieved by (i) reducing contact stresses at the joint by increasing the contact area and redistribution of contact forces (Kempson, 1980; Freeman et al. 1975; Weightman and Kempson, 1979; Todd et al. 1972) (ii) reducing maximum dynamic forces across the joint (Kempson, 1980) (iii) reducing energy transmitted across the joint (Kempson, 1980).

Menisci

The menisci are fibrocartilaginous semilunar structures wedge-shaped in cross-section formed by collagen fibers arranged circumferentially making them highly resistant to lateral shear forces (Bullough et al., 1970; Aspden et al., 1985). These are attached to

the tibial plateau along the central sagittal line by their anterior and posterior horns and are held sandwiched between femur and tibia via the joint capsule at their outer peripheries. The flexibility of menisci enables them to move anteriorly and posteriorly across the plateaus about their horn attachments to serve these functions (MacConail, 1950; Barnett et al. 1961; Nordin and Frankel, 1989; Evans 1986) (i) shock absorption to protect the articular surface; (ii) increase surface contact area reducing contact stresses; (iii) improve stability and increase range of flexion; (iv) act as load bearing ligaments by restricting lateral sliding of femoral condyles.

Ligaments

Ligaments in the knee joint are categorized based on location. There are four categories – patellar, capsular, extra-capsular and cruciates.

Patellar Ligaments (Evans, 1986): Patellar ligaments are comprised of layers of vertical fibers from the quadriceps interleaved with oblique fibers between patella and femur. The primary function of this group of ligaments is to stabilize the patella.

Capsular and Extra-capsular Ligaments: The ligaments of the capsule can be divided into the *deep layer ligaments* and the *major capsular ligaments*. The meniscal-femoral ligament and coronary ligament constitute deep layer ligaments. The major capsular ligaments include the medial collateral ligament (MCL), posterior-medial complex, oblique popliteal ligament, arcuate complex

and posterior-lateral complex. Finally, the lateral collateral ligament (LCL), iliotibial tract and fabello-fibular ligament form the extra-capsular ligaments.

Cruciate Ligaments: Two ligaments originating in the inter-condylar notch of femur are categorized as cruciate ligaments. The anterior cruciate ligament (ACL) originates on the posterior aspect of the medial surface of lateral femoral condyle, passes forward, medially and downward to its insertion on the anterior area of medial tibial spine (Evans, 1980; Girgis et al. 1975). The posterior cruciate ligament (PCL) originates on the posterior aspect of the lateral surface of medial femoral condyle, passes posteriorly, downwards and laterally to the ACL and inserts between the articular upper surfaces of the tibia. The primary function of the cruciate ligaments is to provide translational and rotational stability to the knee joint.

Function of Ligaments

Integrity of the knee joint is determined by the joint action of the surrounding muscles and tendons, articular joint capsule, intrinsic ligaments and bone architecture of the osseous structures (Brantigan and Voshel, 1941). Ligaments contribute in large part to the overall stability of the knee joint. They serve the following functions –

- Knee adduction during extension is restrained by the LCL, ACL, PCL and joint capsule. During flexion, knee adduction is regulated by the ACL, PCL and joint capsule (Grood et al. 1981; Seering et al. 1980).

- Knee abduction during extension is controlled by the MCL and joint capsule. During flexion, knee abduction is controlled by the ACL, PCL and joint capsule. (Warren et al. 1974; Seering et al. 1980; Grood et al. 1981; Crowninshield et al. 1976; Kennedy and Fowler, 1971).
- Knee rotation during extension is regulated by the joint capsule, MCL, LCL, ACL and PCL. In flexion, knee rotation is controlled by the capsule, MCL, ACL and PCL (Girgis et al. 1975; Seering et al. 1980; Wang and Walker 1974).
- Anterior translation of tibia with respect to the femur is restrained by the ACL (Girgis et al. 1975; Piziali et al. 1980).
- Posterior translation of tibia with respect to femur is restrained by the PCL (Kennedy and Grainger, 1967; Girgis et al. 1975; Piziali et al. 1980).
- Medial and lateral gliding of tibia is restricted by the tibial intercondylar eminence, femoral condyles and all ligaments (Piziali et al. 1980).
- Hyperextension of knee is controlled by the MCL, LCL, ACL, PCL, menisci, anterior aspect of posterior joint capsule, oblique popliteal and curvature of femoral condyles (Kennedy and Grainger, 1967; Girgis et al. 1975; Hughston and Eilers, 1965).

Knee Joint Movement

Knee joint motion can be categorized as active, conjunct or passive (Evans, 1986). Any voluntary movement of knee joint is an active motion. This includes knee flexion, extension and slight internal and external rotation. Conjunct motions occur as a

consequence of other movements and are often dictated by morphology of the articulating surfaces and behavior of menisci and ligamentous structures. The associated musculature does not influence conjunct motions. For instance, if the foot is unconstrained and the knee was to rotate in sagittal plane, slight rotation of tibia would be observed. Passive motions are typically those that an examiner would perform to evaluate joint biomechanics. Some examples of such motions include knee abduction-adduction, anterior-posterior drawers (tibial translation), medial-lateral gliding and compression-distraction. These are not too frequently observed under normal physiological loading conditions. However, motions of the knee joint during a contact injury can be classified as passive motions.

Flexion-Extension: Normal range for sagittal plane motion is typically 140^{o}-0^{o}; 140^{o} being the upper limit for flexion and 0^{o} being the upper limit for extension. The knee however may extend about 5^{o} beyond 0^{o}, a motion recognized as hyperextension. During full flexion, the posterior aspect of the femoral condyles rest on posterior periphery of the tibial plateau. As the joint rotates to extension, femoral condyles roll forward or slide in the menisci. At full extension, the flats of femoral condyles are located at the anterior edge of the tibial plateau. Rotating from full flexion to extension, the tibial contact locations experience large displacements. These displacements are larger on the lateral side than the medial side.

Internal-External Rotation: The knee joint is not a perfect hinge and is capable of transverse plane motion. Both internal and external rotations are observed at the knee. With increasing flexion angles, rotation in transverse plane diminishes due to the restricting action of surrounding soft tissues. At full extension no external or internal rotation can occur due to the alignment of articulating surfaces (close-pack condition). Rotation in transverse plane is typically largest at 90^{o} flexion, with range of motion for internal rotation 0-30^{o} and that for external rotation 0-45^{o}.

Abduction-Adduction: In the coronal plane, the knee joint can move which results in excessive compression of either the lateral compartment (knee abduction or valgus) or the medial compartment (knee adduction or varus) of knee. This is typically a conjunct rotation and is dictated by a variety of factors including geometry of articulating surfaces, biomechanics of hip or ankle joint etc.

Anterior Cruciate Ligament (ACL)

ACL microstructure and behavior: Cadaveric studies have determined the existence of three fiber bundles in ACL when viewed within the intercondylar notch (Norwood and Cross, 1979; Amis et al. 1991) – anterior-medial bundle; intermediate bundle; posterior-lateral bundle. Each bundle is formed of a hierarchy of collagenous structures bundled together into fascicular units 0.25 to 3 mm in diameter (Danylchuk et al. 1978) passing directly from femur to tibia or taking a spiral path around the axis of the ligament (Amis et al. 1991). These fiber bundles twist upon themselves to a varying degree as the knee

flexes due to relative rotations of the attachments (Hefzy and Grood, 1986). Amis et al (1991) demonstrated that all fiber bundles experience tension during final 30^{o} of extension. Typically, during flexion anterior-medial band tightens and the posterior-lateral band slackens. Internal rotation caused greater lengthening of ACL fibers compared to external rotation. The most severe lengthening effect of tibial rotation was observed at about 30^{o} flexion.

ACL Injuries

Epidemiology and Impact of ACL Injuries

An estimated 80,000 to 250,000 ACL injuries occur each year (Griffin et al. 2006). Of these, 70% to 90% are attributed to a non-contact mechanism (Hughes et al. 2006), afflicting, for the most part, people in the 15-24 years of age (Griffin et al. 2006). Approximately 100,000 ACL reconstruction surgeries are performed each year (American Academy of Orthopedic Surgeons, 2000) resulting in total medical costs greater than USD 2 Billion (Griffin et al 2000, Huston et al. 2000). With steadily increasing number of participants in sports, at both the high school and collegiate level (NFHS, 2004; NCAA, 2004), the number of ACL injuries have also dramatically risen. Even though male participation in sport activities is greater, the rate of ACL injuries in females is disproportionally much higher. The rate of incidence of non-contact ACL injuries has been observed to be 4 to 8 times greater in females than in males for the same sport (Gwinn et al. 2000). Several studies have shown that female athletes have an increased proclivity for ACL injuries (Ireland, 1990; Arendt, 1999; Ford et al. 2003; Hewett et al. 2005). Females, for instance, demonstrate greater total valgus knee motion than males

do (Ford et al. 2003; McLean et al. 2004) and increased knee valgus angle was identified to be predictive of ACL injuries (Hewett et al. 2005). Additionally, various attributes of the female knee and ACL anatomy have been demonstrated to be a risk factor for ACL injury (Anderson et al. 2001; Shelbourne et al. 2001; Chandrashekar et al. 2005). Similarly, hormonal influence has been shown to contribute to joint and ligament laxity, increasing risk of ACL injury in females (Shultz et al. 2005; Uhorchak et al. 2003).

ACL injuries not only cause intense trauma and impede immediate game and sport participation of the athlete but also result in long term debilitative effects. Degenerative diseases like osteoarthritis (OA), for example, are observed in the affected knee in a relatively short time even after reconstructive surgery (Daniel et al. 1994; Lohmander et al. 2004). Long term follow-up studies have reported that an estimated 45% of individuals who sustain ACL rupture experience premature knee OA within 10 years of the injury (Roos, 2005). Knee OA is seen most frequently in people aged 65 years and above and is diagnosed using radiographic methods (Brandt, 1991). However, current research suggests that an increased number of individuals will exhibit premature knee OA when in their 30s and 40s as a consequence of knee injuries sustained at a young age (Englund et al. 2003; von Porat et al. 2004). Studies have reported that an ACL tear ages the knee by 30 years (Lohmander et al. 2004), making the knee 5 times more likely to develop OA with rapid degeneration and “wear-and-tear” of soft tissues (Gelber et al. 2000). Taking into consideration the number of players being injured, it is likely that a cohort of a large number of young athletes, particularly females, will be afflicted with degenerative joint disease.

ACL Injury Risk Factors

Several factors have been identified to contribute to risk of ACL injury. These factors are broadly classified as "modifiable" and "non-modifiable" (Griffin et al. 2006) (Figure 5). Modifiable factors include those that are amenable to change by training, for instance internal factors like neuromechanics, postural stability or external factors like shoe interaction with floor and turf etc. Non-modifiable factors include gender, anatomy, hormonal influence, laxity, anthropometry etc. The internal factors have been summarized in Figure 7.

ACL injury risk and mechanisms are largely dictated by how these factors interact with each other. Gender disparity in ACL injury rates and the existing gender dimorphism has led to delineation of biomechanical, neuromuscular and anatomical factors specifically observed in female athletes. Thus, some factors have been specifically identified to be stronger predictors of ACL injury risk. For instance, knee abduction (valgus) angle and torques (Ford et al. 2003; McLean et al. 2004; Griffin et al. 2006); lower limb muscle strength (Withrow et al. 2005), quadriceps and/or hamstrings strength and activation (Beynon et al. 1998, Shultz et al. 1999, Hewett et al. 2005); joint laxity (Uhorchak et al. 2003), ACL laxity, tibial slope (Hashemi et al. 2010) are suggested to indicate ACL injury risk. In recent years, therefore, a pivotal issue has been development of suitable training and exercise regimen to counter the effect of these risk factors and prevent ACL injuries (Hewett et al. 2005; Cochrane et al. 2010; Hashemi et al. 2010). While these training programs have successfully demonstrated short-term modification in athletes'

biomechanics and neuromechanics, long-term retention of those has not been observed. Additionally, not all of these learned skills get transferred to the field where conditions of stress and fatigue further increase risk of ACL injury (Thomas et al. 2010). Epidemiology suggests that despite these efforts, rate of ACL injuries remains high (Arendt et al. 1999), approximately 1184 per 100,000 (Gianotti et al. 2009). An effective training protocol especially for female athletes is challenging to design in view of the fact that the athletes' biomechanical and neuromuscular response change depending on which phase of menstrual cycle the athlete is currently in (Shultz et al. 2005). **Thus, an immediate critical need is to expand our study and understanding to other risk factors and mechanisms and use that knowledge to develop sophisticated screening and surveillance protocols to identify athletes predisposed to risk of ACL injuries.**

Over recent years, a shift in research regarding ACL injuries has been observed with focus being given to "non-modifiable" factors. Various structural, anatomical, physiological and hormonal factors are being studied and their roles in ACL injury investigated. Q angle, the angle between the quadriceps (usually rectus femoris) and the patellar tendon, is an indicator of the knee joint alignment which if outside of normal ranges, can be a precursor for injuries. A large Q angle typically observed in females, for example, has been suggested as a contributing factor to the risk for ACL injuries (Heiderscheit et al. 2000; Mizuno et al. 2001). Smaller inter-condylar notch size has also been found to compound the proclivity for ACL injuries (Souryal et al. 1993; LaPrade et al. 1994; Arendt, 2001). Yet another significant factor identified is the geometry of the tibial plateau. A greater lateral tibial slope, medial tibial slope and shallower medial

tibial depth are considered to increase the risk of ACL injury (Hashemi et al. 2008, 2010). Other studies have indicated that risk for ACL injuries is also dictated by ACL geometry and material properties of the soft tissue. Females have ACLs smaller in size (Anderson et al. 2001) which has been found to have a strong correlation with ACL injury (Shelbourne et al. 2001; Uhorchak et al. 2003). Specifically, the average length, cross-sectional area, volume and mass of ACL were determined to be much smaller in females making them prone to injuries (Chandrashekar et al. 2005). Some studies also indicate that female ACL material properties are significantly different from that of males. This results in varying mechanical response that may also contribute to ACL injuries (Chandrashekar et al. 2005).

Hormonal risk factors are also of concern especially considering their influence on ACL mechanical properties (Liu et al. 1996). Several studies have indicated that changes in sex hormone concentrations, particularly associated with female menstrual cycle, affect knee joint laxity (Deie et al. 2002; Heitz, 1999; Slauterbeck et al. 1999; Shultz et al. 2005; Zazulak et al. 2006). This is significant because knee joint laxity is also considered as a potential risk factor. Prospective studies reveal that anterior knee laxity is a common characteristic of athletes with ACL injuries (Woodford-Rogers et al. 1994; Uhorchak et al. 2003; Myer et al. 2008). However, exact implication of the hormonal risk factors on knee laxity and subsequently on ACL injury risk is yet to be determined. Additionally, most of the research focuses on knee joint laxity as opposed to ACL laxity. ACL laxity determines a significant component of the knee joint laxity and therefore we would like to elicit the effects of ACL laxity (modulus) as a risk factor.

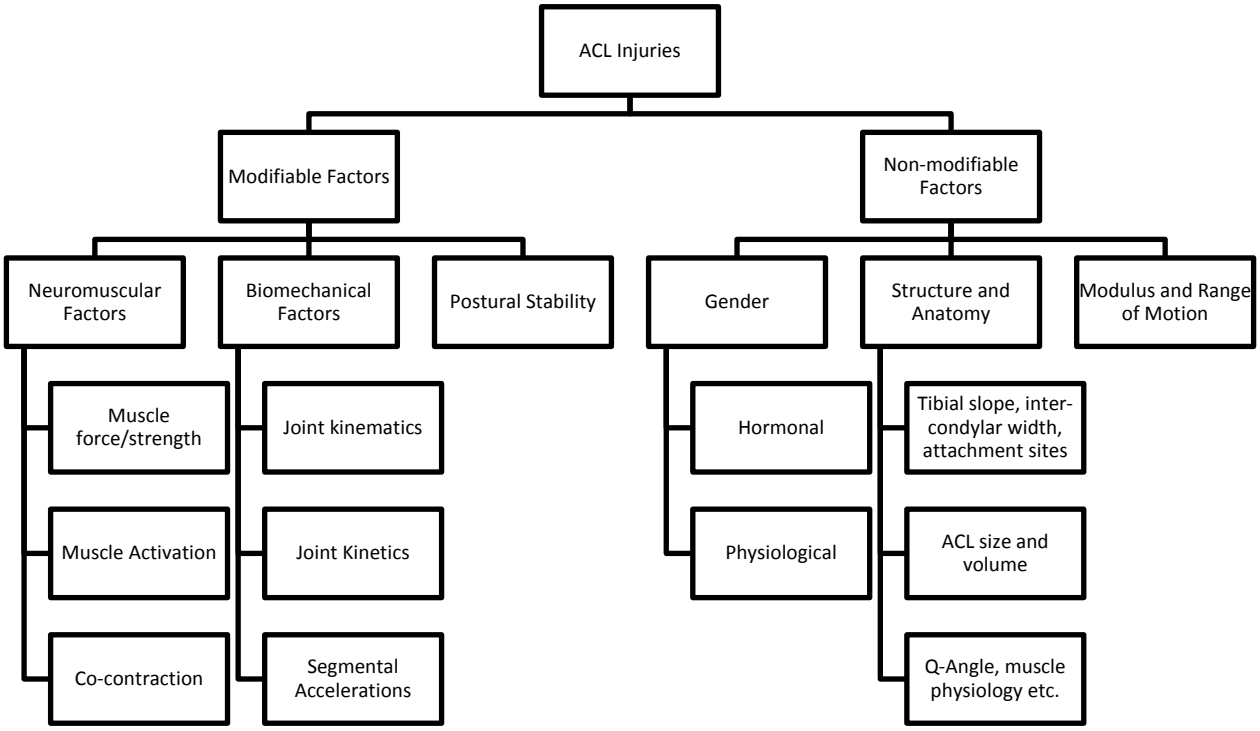

Figure 7: Internal factors contributing to ACL injury risk

ACL Modulus

While a number of studies have examined the ACL at both macroscopic and microscopic levels, very few studies have attempted to elucidate ACL mechanical properties as a potential risk factor. ACL mechanical structure, properties and geometric characteristics were found to be dependent on sex (Chandrashekar et al. 2005, 2006). Differences ranged from the physical construct of ACL (size, volume, diameter, length) to its mechanical response under tensile loading conditions. Female ACLs were found to be smaller in size (Chandrashekar et al. 2006) with weaker mechanical properties under tensile loading (Chandrashekar et al. 2005). In yet another study, sex dimorphism was observed at the molecular level in the ACL (Slauterbeck et al. 2006). They determined

that the expression of collagen and matrix metalloproteinase genes that influence remodeling and turnover of structural elements in ACL is dependent on sex. Moreover, differences were also observed in the fibril characteristics of ACL and significant correlations were found with risk of ACL injuries (Hashemi et al. 2007). They determined that the average number of fibrils per unit area was significantly larger in males than in females. They proceeded to reveal that 92% of the stiffness of female ACL was determined by this factor. The number of fibrils per unit area also determines failure load and failure stress for the ACL. Taking into account the observation that female ACLs have fewer fibrils per unit area, it can be inferred that the female ACLs are relatively less stiff (have low modulus) with weaker mechanical properties (Chandrashekar et al 2006, Hashemi et al. 2007). Thus, considering that female ACLs are less stiff (more lax) we propose to determine how this characteristic implicates itself within an injury.

Tibial Slopes and Tibial Depth (concavity of tibial surface)

The articulation between femur and tibia dictates the manner in which the bones rotate and the subsequent loading of ACL. The tibial surface is complex and necessitates definition of multiple slopes and plateaus (Hashemi et al. 2008, 2010; Stijak et al. 2008). In an article by Hashemi et al (2008), tibial plateau geometry was defined by 3 slopes, including the medial tibial slope (MTS), lateral tibial slope (LTS), and coronal tibial slope (CTS), and the depth of concavity of the medial plateau in the middle of the articular region, defined as the medial tibial depth (MTD). Lateral tibial slope has been reported to be larger in athletes with ACL injury compared to control groups (Brandon et al. 2006;

Stijak et al. 2008; Hashemi et al. 2010). The medial tibial slope was shown to be larger in patients with patellar-femoral pain (Stijak et al. 2008).

In a blind study, Hashemi et al (2010) demonstrated that males with increased MTS and LTS combined with a decreased MTD are at increased risk of suffering an ACL injury, while females with increased LTS combined with decreased MTD are at increased risk of suffering ACL injury. They further suggest that MTD is an important risk factor for ACL injury, followed by LTS and MTS. These tibial plateau measurements could all be considered as robust risk factors for ACL injury in the development of injury risk models. Their study implies that articulating tibial surface implicates in an ACL injury differently between genders. Additionally, the tibial surface could compound the effect of other factors such as ACL laxity further increasing risk for ACL injury.

Non-contact Injury Mechanism

A non-contact injury is defined as an injury that occurs in the absence of player-to-player or body-to-body contact (Myklebust et al. 2003). Thus, a non-contact injury occurs when the only external force acting on the body is ground reaction force. The mechanism, however, is multi-factorial and often, idiosyncratic. Various studies have attempted to identify the position of lower extremity just before or during incurrence of a non-contact ACL injury. Boden et al (2000), for instance, collected video data, which, on analyses revealed that most of the non-contact injuries occurred with the knee almost fully extended during a sharp deceleration maneuver. Another study also using video data on female athletes showed that the injury mechanism involved a forceful

valgus collapse of knee accompanied by internal tibial rotation and knee joint close to full extension (Olsen et al. 2004). In a review paper, Hewett et al (2006) stated that a consistent mechanism including valgus, extended knee and widened stance were associated with non-contact ACL injuries. However, a more suitable dynamic injury mechanism was outlined by Myer et al (2005). They described it as follows – "The tibia is fully rotated, knee close to full extension, foot is planted and as the limb decelerates, it (knee) collapses into valgus". We consider this to be a more apt description as it is inclusive of all the externally observed biomechanical variables associated with non-contact ACL injuries. Yet another feature of dynamic ACL injuries is that the knee joint experiences an impulsive load associated with stance phase and not a constant load. Thus the magnitude and time to peak loading of the joints vary depending on the maneuver being implemented.

Computational Modeling

Various methods have been employed to directly assess the response of ACL under dynamic conditions. One category involves use of cadavers to study the dynamic ACL response. This scenario typically involves a cadaveric knee or ACL being subject to external loads and ACL response measured. These studies generally predict static behavior of the knee joint and ACL under low levels of loading. However, these loads are not truly representative of the large loading magnitudes and loading rates experienced during sport activities. Additionally, the physiological response of a cadaveric knee varies vastly from that of a live knee. On the other hand, *in vivo* studies of ACL response under dynamic injury-causing events on human subjects are not feasible. Thus, dynamic

3-D computational modeling and simulation techniques evolved as a very attractive alternative for studying ACL response. This method offers a number of advantages including modeling of a complex knee joint and associated soft tissue, allowing unconstrained motion, allowing modulation of anatomical and structural features, subjecting the model to actual physiological loads and testing the model response under injury-inducing external loads.

The complexity and characterization of computational models of the knee and associated soft structures have progressed significantly over the years. Most of the initial work was concentrated on developing 3-D models with functionality for all structural components being defined (Piziali et al. 1977; Wismans et al. 1980; Grood et al. 1982; Andriacchi et al. 1983; Loch et al. 1992). Concurrently, intense research was also aimed at revealing the structural and mechanical properties of the bone and ACL (Alm et al. 1974; Noyes et al. 1976; Dorlot et al. 1980; Woo et al. 1981; Kwan et al. 1993; Hirokawa et al. 1997; Pioletti et al. 1997). With the advent of technology and sophisticated computing resources being available, application of knowledge was profound with development of more comprehensive and complex models incorporating wider realm of physiological parameters (Pioletti et al. 1995; Shelburne et al. 1997, 1998; Pandy et al. 1997; Li et al. 1999; Hirokawa et al. 2000). This field has now evolved with dynamic physical activities being simulated and model response being tested under those conditions. Complex and interactive models now exist that computationally replicate knee joint and ACL functionality under simulated knee joint kinematics (Darcy et al. 2006), under simulated muscle load (Li et al. 2002), during walking (Shelburne et

al. 2004), squats (Escamilla et al. 2009), or even single legged landing (Shin et al. 2007, 2009). No model or simulation exists that has accounted for the effects of ACL laxity or tibial surface geometry on knee biomechanics and subsequently on ACL loading. The aims outlined in this proposal will be tested using a 3-D computational model of the knee joint.

Computational Analyses involving Dynamic and Impulse Loading

Very few studies have examined the influence of dynamic or impulsive loads on knee joint and ACL mechanics. Shin et al (2007) created a 3-D finite element model (FEM) to recreate the experiment designed by Withrow et al (2006). They successfully validated the model and used it to predict ACL strain in response to impulsive loads. They used the model to predict ACL loading response to posteriorly applied tibial force simulating run-and-stop movements (Shin et al. 2007) and to isolated valgus moments simulating single leg landing (Shin et al. 2009). This model, however, does not include the stabilizing effect of menisci and employs spring-line elements to simulate all the ligaments. More recently, Taylor et al (2010) applied a combination of marker-based motion analysis, fluoroscopic and magnetic resonance (MR) imaging techniques to determine ACL strain in vivo during dynamic jump landing. They determined ACL strain by superimposing kinematics obtained via motion-markers and fluoroscopy onto a solid computational model reconstructed from MR images. Although this techqnique is useful for estimating ACL strain *in* vivo, it cannot be used as a tool to predict ACL strains in conditions where it is unethical to use human subjects. Other studies investigating the

effect of impulsive load on lower limb injuries have been found in vehicle-pedestrian crash literature. Soni et al (2009) created a FE model of the whole body including muscles in the lower limbs. They applied an impulsive load equivalent to force from the impact of a moving vehicle and determined that muscle contraction results in reduced force transmission through the ligaments. Their work, however, was specific to contact injuries to the bones and ligaments in the lower limb and cannot be translated to the realm of sport injuries that involve non-contact injuries. In this proposal, we intend to create a fully functional 3-D computational model of the knee joint including 3-D ACL capable of predicting ACL strain under conditions of non-contact impulsive loads.

CHAPTER III

Preliminary Tests

A patient-specific 2-D finite element (FE) knee model was initially developed to examine relations between joint morphology, anterior-posterior tibiofemoral accelerations and ACL strain in the sagittal plane (Figure 8). This model served to provide the proof-of-concept necessary to establish the relationship between peak ACL strain and relative anterior tibial acceleration and justify the development of a more complex 3-D FE model. Females typically are known to have an ACL with low modulus. Low modulus ACL

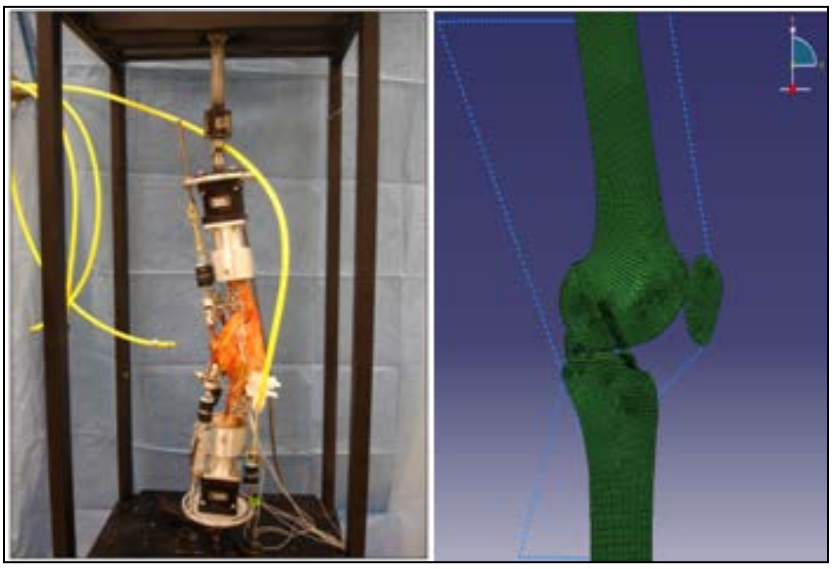

Figure 8: Panel 1 – The drop land test apparatus used to measure relative strain in ACL (Withrow et al, 2006); Panel 2 – The 2-D FE model used to test the hypotheses

can also be a consequence of partial tear or micro damage to the ligamentous tissue. Under such circumstances, the ligament, functionally compromised, fails to restrain the

tibia resulting in the development of high anterior tibiofemoral acceleration manifesting as greater stretch in the ACL and subsequently higher ACL strain.

Lateral tibial slope is also notably higher in female athletes and in males who have sustained an ACL injury. A higher posterior slope would cause the femur to roll back on the tibial surface resulting in higher anterior tibiofemoral acceleration and subsequently higher ACL strain.

The 2-D computational model of the femur, tibia, patella, femoral cartilage, tibial cartilage and meniscus was rendered from a single sagittal MR slice through the mid-medial condyle using Mimics® (Materialise). The rendered 2-D model was then discretized using 4-noded quad shells using the meshing tool Hypermesh® (Altair Hyperworks). The ACL was superimposed on these structures by identifying from the MR images, the ACL attachment sites. Elastic material models were used to define the behavior of bone (E=15GPa, nu=0.3), cartilage (E=5MPa, nu=0.475) and meniscus (1MPa, nu=0.25) (Wirtz et al. 2000, Donahue et al. 2003). ACL behavior was dictated by a hyper-elastic, neo-Hookean material law (Bischoff et al. 2008) the coefficients of which were derived ($C1 = 33.557 \times 10^{6}$, $D1 = 1.2 \times 10^{-9}$) so that the modulus of the ligament was 100 MPa (Chandrashekar et al. 2006) and Poisson's ratio 0.49. ACL stiffness was determined by stiffness parameter, C1, a higher C1 implying a stiffer ACL.

Impact load, muscle loads and boundary conditions analogous to that in the Withrow et al. (2006) experiment were applied. In the experiment, Withrow used pre-tensioned linear axial cables to simulate functions of quadriceps, hamstrings and gastrocnemius

muscles to initially set the knee joint flexion angle to 15^{o} before loading with an impulsive impact load. We used similar constraints computationally and simulated muscle functions using linear axial connectors with appropriate stiffnesses to hold the initial knee flexion angle at 15^{o} before external loading was applied. Attachment sites of these muscles were also determined from segmentation data.

Boundary conditions, also consistent with the experimental setup, were then applied. Translational motion was constrained at the central node of the distal end of the femur allowing only rotation in sagittal plane. The central node on the distal tibia was allowed to rotate in sagittal plane and translate along the vertical axis. Horizontal translation for the distal tibia was restrained. In the physical experimental apparatus, the impact force simulating single-limb landing was applied at the distal tibia by dropping a weight. The measured force versus time response was used as the boundary condition applied at the central node of distal tibia with duration of 100ms and a peak load of 1200N at 35ms. Contact forces at the tibio-femoral and patella-femoral articulations were defined using the frictionless, hard-surface definitions in the Abaqus® solver.

For the first phase of the study, ACL modulus was modified to account for a range encompassing 50% to 150% of the normal values. This range was chosen to encompass the variation of ACL modulus from 50MPa to 150MPa. This was based on the reported

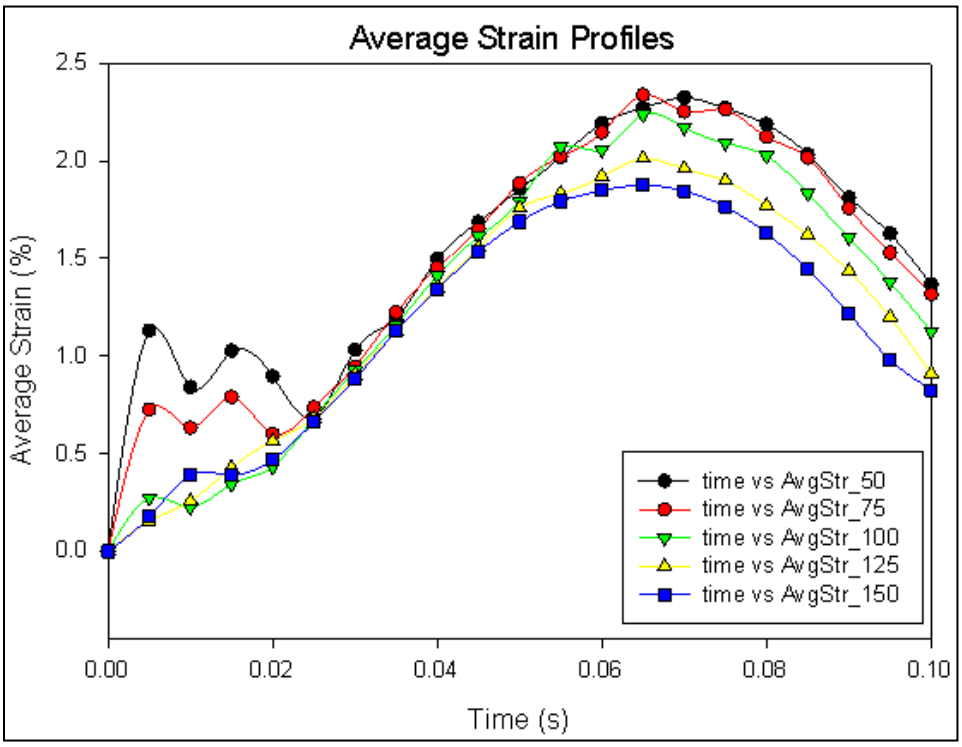

Figure 9: Average ACL strain profiles obtained for different ACL laxity values

ACL modulus for females to be about 100MPa (Chandrashekar et al. 2005). For the purposes of this study, we believe that this range of ACL moduli would be sufficiently informative on the effect of ACL modulus on ACL loading mechanism. For the second phase, the lateral tibial slope was modified to include –SD (3.9^{o}), mean (7.0^{o}) and +SD (10.1^{o}) values.

A decrease in modeled ACL modulus (increase in laxity) was shown to increase the peak ACL strain and to increase the anterior tibiofemoral acceleration (Figure 10). It was also established that an increase in the lateral tibial slope leads to higher strain manifesting

in the ACL (Figure 11). These results demonstrate that anatomical factors largely dictate the ACL strain response during a dynamic loading activity and justify the development of a 3-D FE model.

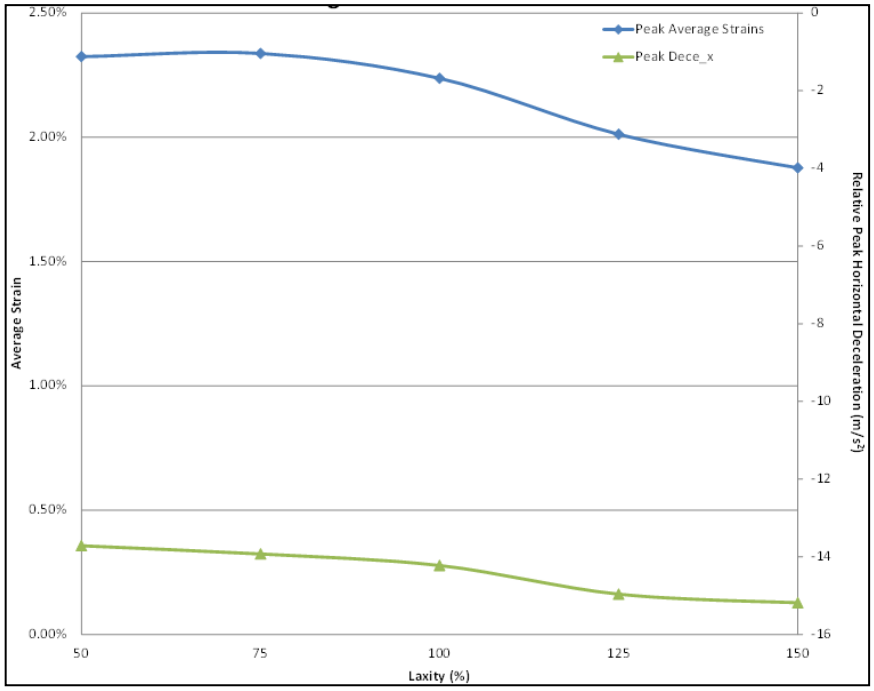

Figure 10: Peak average ACL strains and peak anterior tibiofemoral accelerations obtained for different ACL modulus values

In this study the effect of two factors, specifically, ACL modulus and tibial slopes were analyzed using a 2-D FE model. The results suggest that ACL strain largely depends on the anatomy and physiology of the knee joint. Additionally, the results suggest that ACL strain can be predicted by means of an externally assessable variable, in this case of sagittal plane analysis, anterior-posterior tibiofemoral acceleration. Acceleration can be quite easily measured on field by video analysis or by the use of tri-axial accelerometers. This provides a number of advantages including measurement of real time kinematic data without hindering athletic performance. This would also help us identify athletes as they become more vulnerable to injury in the course of a game due to changes in

biomechanics and neuromechanics associated with stress, fatigue or the variability observed in female biomechanical and neuromuscular response due to the effect of changes in hormones associated with their monthly menstrual cycle. Ultimately, these results justify the development of a complex 3-D knee joint FE model to verify the

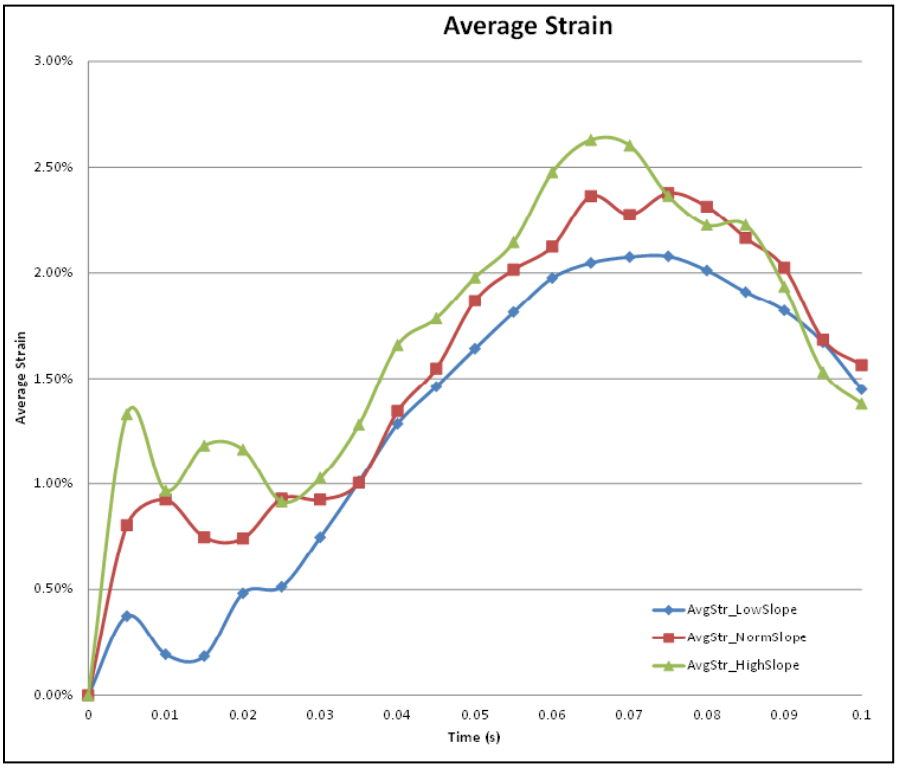

Figure 11: Average ACL strain profiles obtained for different lateral tibial slopes. A 7° slope was normal, 10.1° was high slope and 3.9° slope was low.

sensitivity of ACL strain and relative anaterior-posterior tibial acceleration to (i) ACL modulus and (ii) tibial surface geometry (lateral tibial slope, medial tibial slope and medial tibial depth).

CHAPTER IV

Development of a Finite Element Model of the Knee

Introduction

Difficulties remain in measuring in vivo or in vitro knee mechanics in tissues that mediate the articular response. To fill these knowledge gaps, numerous theoretical approaches have been developed. Unfortunately, exact analytical solutions can only be obtained using simplistic assumptions such as basic geometries and small displacements (Blankevoort et al. 1991; Han et al. 2005). FE modeling is a powerful and versatile tool that discretizes the solution space into analyzable elements to solve for system behaviors. Unlike other approaches, this method can accurately reproduce highly complex geometries and mechanical behaviors to estimate forces and displacements at discrete points (Baldwin et al. 2009; Kupper et al. 2007). FE models that analyze articular surface behaviors via dynamic time-dependent variables have been used to assess ACL structure (Zhang et al. 2008), knee mechanical changes due to ACL deficiency (Li et al. 2002), meniscus and articular cartilage property interactions (Yao et al. 2006), tibiofemoral contact and articulation (Blankevoort et al. 1991) and joint contact pressure (Papaioannou et al. 2008). None, however, have modeled the loading conditions associated with single limb landing to study the influence of physiological and anatomical parameters using FE models of this complexity. Building on these previous

studies, an explicit dynamic FE model was developed that recreated the mounting and loading techniques used in an experimental protocol (Oh et al. 2011) to simulate in vitro jump landings. Boundary and loading conditions applied in the simulation were similar to those in the experiment and constitutive laws governing the behavior of the model were obtained from literature. The model response was verified and its validity was determined by correlating model-predicted data with experimental data. The model was then simulated under different test conditions to elucidate the effect of ACL modulus and tibial surface geometry on ACL strain manifesting through the effect of sagittal plane tibiofemoral acceleration, frontal plane and transverse plane rotations.

Overview of the experiment by Oh et al. (2011)

In his experiment, Oh analyzed ACL behavior in dynamically loaded cadaver knees. An in-vitro impact testing apparatus was built to simulate single-limb landing in the presence of muscle forces (Figure 1). Each knee specimen was mounted in the testing apparatus to simulate the position of the lower limb as it strikes the ground while landing. The proximal end of the femur was translationally constrained and the distal end of the tibia had translation in the medial-lateral and anterior-posterior direction constrained. The quadriceps and the medial and lateral gastrocnemius were represented by linear elastic cords (tensile stiffness: 2kN/cm) pre-tensioned to 180N and 70N each respectively. Two constant force springs, pre-tensioned to 70N each, were used to represent the medial and lateral hamstring muscle forces. These pre-tensioned muscle forces maintained an initial knee flexion angle of 15^{o}. An impulsive impact load was simulated by releasing a weight so as to generate a 2*BW force peaking at

approximately 55ms. The load was applied to the distal tibia while recording 3-D knee loads and tibiofemoral kinematics. Strain in the anteromedial ACL bundle was measured using a DVRT. The FE model was set up with similarly defined muscle forces, boundary conditions and loading.

Essential features of a desired model

1. Three Dimensional Geometric Rendering: A 3-D solid model of the knee joint is required to accurately describe the layout of the entire structure and its spatial inter-relationships. An accurate 3-D structural representation of osseous structures (patella, tibia, fibula and femur), articular cartilage (femoral, tibial and patellar), meniscus and ligaments (ACL, PCL, MCL and LCL) was obtained from MR images by 3-D graphical reconstruction using Amira® (v 5.4.0, Visage Imaging, Inc.). This modality has been previously employed and its accuracy validated (Weiss et al. 2005).

2. Six Degrees of Freedom: Six degrees of freedom (three translational and three rotational) are necessary to accurately model knee joint motion in 3-D space and were accordingly attributed to the FE model.

3. Conjunct Motion: Conjunct motion, described as motion resulting from other motions and from the geometry of articulating surfaces or presence of surrounding ligamentous structures was also made to be physiologically viable. The FE model was therefore allowed to rotate about all the three axes of motion enabling frontal, sagittal and transverse plane rotations and translations.

4. Instantaneous Axes of Motion: Instantaneous axes are required to account for the six degrees of freedom conjunct motion inherent in the passive tibial-femoral joint because, fixing the axes of rotation may give rise to incorrect behavior from the model (Andriacchi et al. 1983).

5. Articulating Segments: Femur, tibia and patella form the osseous structures of the knee joint. The geometry of articulating surfaces especially the femoral condyles and tibial surface dictate to a large extent the biomechanics of the tibiofemoral joint and determine distribution and transmission of forces. Relative to the soft tissues, the bones are significantly stiffer and therefore, a linear elastic model was deemed sufficient to dictate the constitutive behavior of these structures.

Cartilage prevents mechanical damage to the subchondral bone by reducing contact stresses and reducing maximum dynamic forces and energy transmitted across the joint (Kempson, 1980). It is especially important to model the cartilage in a knee model subject to transmission of load across the joint (Shereppers et al. 1990). Menisci too play a significant role in absorbing energy transmitted across the joint (Krause et al., 1975) and eliminating majority of femoral-tibial contact while increasing surface contact area, thus reducing the contact stresses and distributing them more uniformly (MacConail, 1950; Barnett et al. 1961; Nordin and Frankel, 1980; Evans, 1986). The lateral meniscus is responsible for weight bearing while medial meniscus helps in stabilizing the joint (Fukubayashi and Kurosawa, 1980). These functions of the menisci are expected to implicitly occur by virtue of model definition and action of surrounding

ligamentous and muscle structures. These structures are known to exhibit viscoelastic behavior. However, under high velocity impact conditions simulated in our tests these structures tend to behave in a linearly elastic manner (Li et al. 2001, LeRoux and Selton, 2002).

6. Ligaments: Ligaments essential to a passive tibial-femoral joint motion are considered to be the primary ligaments (Brantigan and Voshell, 1941) and were all included in the model i.e. the posterior and anterior cruciate ligaments, and the medial and lateral collateral ligaments.

An isotropic, non-linear hyperelastic material model was used to characterize the constitutive law for the ligaments. Specifically, the Mooney-Rivlin strain energy hyperelastic function defined below was used.

$$W = C_{10}(I_1 - 3) + C_{01}(I_2 - 3)$$

This particular material model was used as it accurately recreated the non-linear and linear regions of the ligament stress-strain curve.

7. Muscles: Muscles play an important role in stabilizing the knee and dictate to a large extent its kinematic behavior. For the purposes of this study, the muscle behavior was modeled in a manner similar to that set up by Oh et al (2011). In his study, Oh used linear axial cables to simulate the function of the quadriceps and gastrocnemius. The hamstrings were simulated using constant force springs. The cables and springs were pre-tensioned (quadriceps: 180N, medial and lateral gastrocnemius: 70N each and

medial and lateral hamstrings: 70N each) to set the knee joint flexion angle at 15^{o}. Insertion sites for these muscles were obtained from the MR image data and were superimposed on the segmented 3-D solid model. The stiffness of hamstrings, gastrocnemius and quadriceps in the FE model at resting lengths were 140N, 140N and 180N respectively.

8. Dynamic Formulation – Loads and Boundary Conditions: Dynamic model formulation is an inherent requirement for the study given that its aims are predicated on the premise that ACL strain response is to be evaluated under conditions of external loading. A direct consequence of this is the development and transmission of forces and torques through the knee joint causing its motion.

Central to this study is evaluating ACL strain response under dynamic loading conditions. One characterization of such conditions is that the body experiences an impulsive load similar to that in a drop landing. Impulsive loads obtained from the experimental simulation by Oh et al (2011) were therefore applied at the distal end of tibia. The load was applied for 100ms with a peak load of approximately 1500N occurring at 55ms (Oh et al. 2011).

Methods

1. Segmentation: A 3-D solid model of the knee joint (Figure 12) was created from MR images using Amira®. The femur, tibia, patella, fibula, femoral cartilage, tibial cartilage, patellar cartilage, fibular cartilage, menisci, meniscal ligaments, ACL and PCL were segmented.

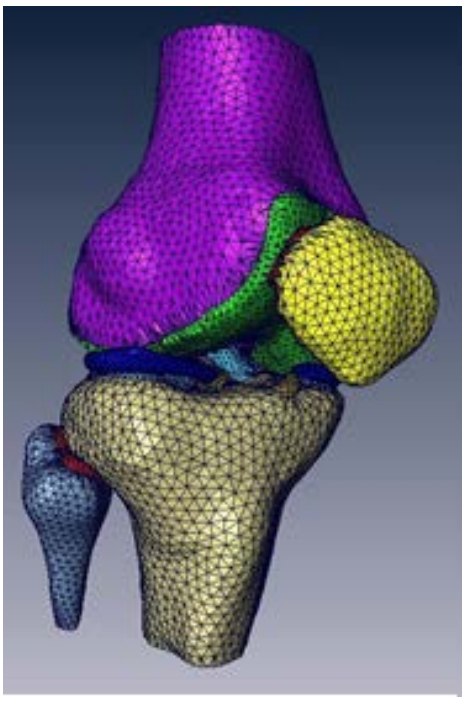

Figure 12: Segmented solid model of the knee joint

2. Meshing: To perform FEA, the solid model has to be discretized into elements (Figure 13). The solid model was meshed into solid, eight-noded hexahedral elements. The size of the elements is critical to the solution obtained and therefore an optimal size has to be determined at which the results converge. To do so, mesh sensitivity tests were performed and a mesh density was determined at which the strain in the antero-medial bundle of the ACL converged.

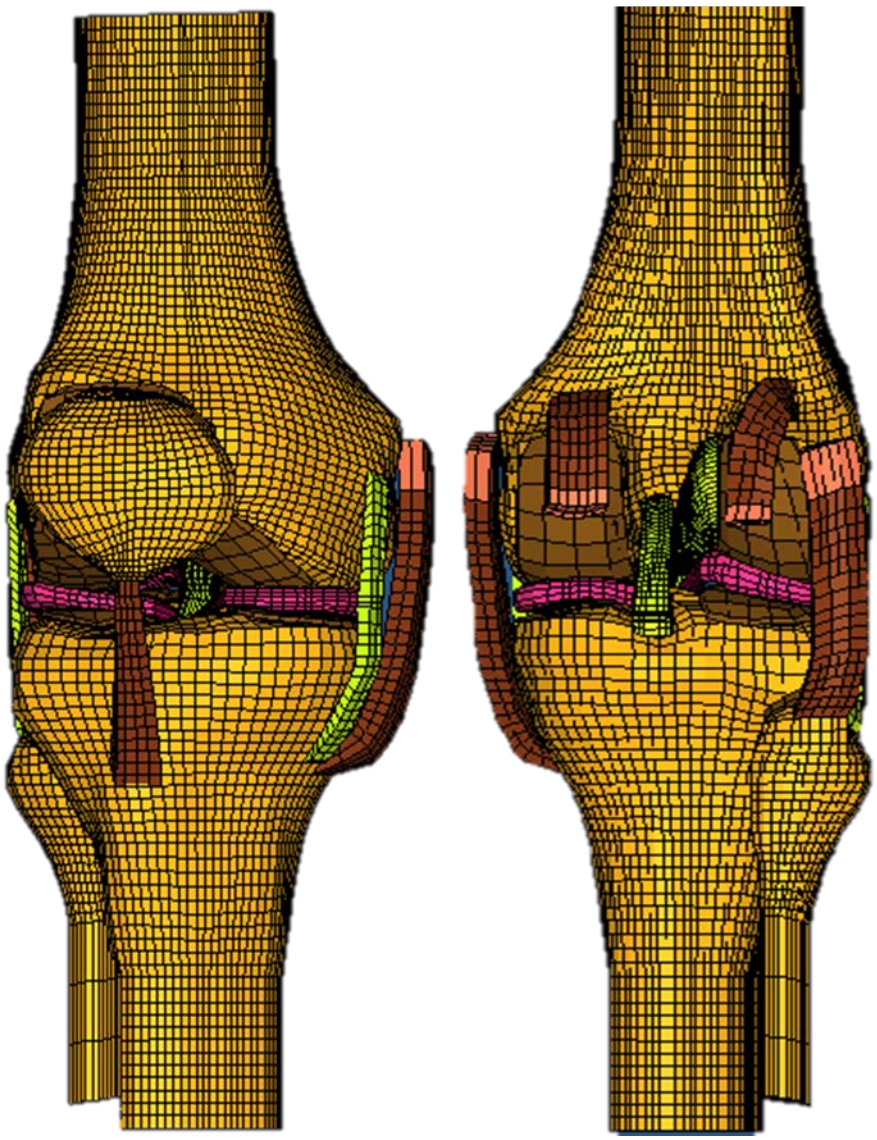

Figure 13: Meshed (discretized) 3-D knee joint model

During this stage, rigid rods and plates were added to the proximal end of the femur and the distal end of the tibia to recreate the mounting techniques used in the experimental protocol. The MCL, LCL and the tendons for the gastrocnemius and hamstrings were created based on the attachment sites identified from the MR images. Finally, spring elements were incorporated to simulate the muscles. Quadriceps, medial and lateral

gastrocnemius and medial and lateral hamstrings muscle pre-tension and stiffnesses were included in the model.

3. Constitutive Laws: The mechanical behavior of the bones, cartilage, menisci and tendons were governed by an isotropic, linear elastic homogeneous material model. The Young's modulus and Poisson's ratio were defined as shown in Table 01.

Table 1: Material property definitions for bone, cartilage, meniscus and tendons

	Young's Modulus (GPa)	Poisson's Ratio	Density (kg/m^3)
Bone (Wirtz et al. 2000)	15	0.3	2000
Cartilage (Li et al. 2001)	0.005	0.46	1150
Meniscus (LeRoux and Setton, 2002)	0.059	0.45	1000
Tendons (Nordin and Frankel, 1989)	2	0.3	1000

Modulus does not describe the non-linear behavior of the ligaments. Consequently, uniaxial-test data from the empirical formulae generated by Blankevoort were used. The load-elongation data from the Blankevoort formulation were normalized based on average specimen length and cross-sectional measures to generate the nominal stress-strain curves. Mooney-Rivlin strain energy function was then fit to the stress-strain data to determine the C10 and C01 coefficients. Mooney-Rivlin strain energy function was used as it satisfies the need for an isotropic, non-linear hyperelastic function.

Uniaxial load-elongation response for all the ligaments was derived from the piece-wise equations described by Blankevoort et al (1991):

$$f = 0, \qquad \varepsilon < 0$$

$$f = \frac{\frac{1}{4}k\varepsilon^2}{\varepsilon_l}, \qquad 0 \leq \varepsilon \leq 2\varepsilon_l$$

$$f = k(\varepsilon - \varepsilon_l), \quad \varepsilon > 2\varepsilon_l$$

where f is the tensile force, k is the ligament stiffness, ε is the strain in the ligament and ε_l is the non-linear strain level parameter assumed to be equal to 0.03 (Blankevoort et al. 1991). The ligament stiffness (k) was set at 5000 N, 9000 N, 3000 N and 2000 N for the ACL, PCL, MCL and LCL respectively (Blankevoort et al. 1991).

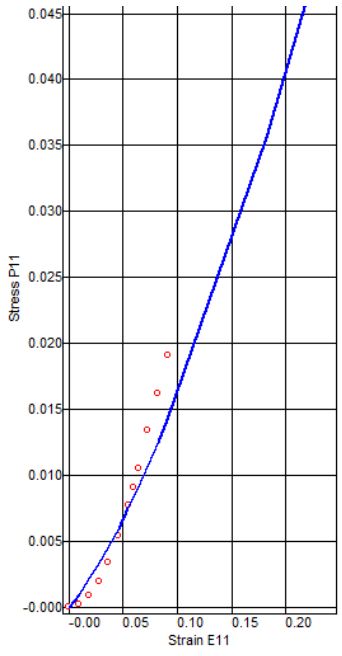

Figure 14: Fitting coefficients C10 and C01 on the experimental data. The solid line is the fit and the red data markers indicate the stress-strain data.

The ligaments were all pre-strained before the impact load was applied to include the effect of the tension in the ligaments at rest. The ACL was pre-strained at 3%, the MCL at LCL both at 4% (Shin et al. 2007).

The muscles were modeled as piecewise linear springs governed by the force-length relationship described in Table 2.

Table 2: Force-length definitions for the spring elements representing muscles (Oh et al. 2011)

Length (mm)	Quadriceps_Force (N)	Gastrocnemius_Force (N)	Hamstrings_Force (N)
-1000	0	0	70
-2	0	0	70
0	180	70	70
2	680	470	70
1000	250,180	200,070	70

4. Contact Surface Definitions: Tied contact definitions were imposed between the ligaments and the bones at the origin and insertion sites. The articulating surface interactions were defined to be frictionless and sliding type. Contact surface interactions were defined between all the interacting structures of the knee joint. Other than the joint articulations, the contacts between the ACL and PCL and the ligaments and the bones were defined. This allows the wrapping action of ligaments around the bone and around each other, replicating the anatomical behavior of the knee joint.

5. Boundary Conditions and Impulsive Load: Boundary conditions applied replicate those implemented by Oh et al (2011) (Figure 15). In his experiments, Oh positioned the knee joint at an initial flexion angle of 15^{o}. All translational degrees of freedom were constrained at the proximal end of femur. At the distal end of the tibia, anterior-posterior translation and medial-lateral translation were constrained allowing the tibiofemoral joint to execute flexion-extension, varus-valgus and internal-external rotation. The FE model implemented similar initial conditions and constraints on the femur and the tibia.

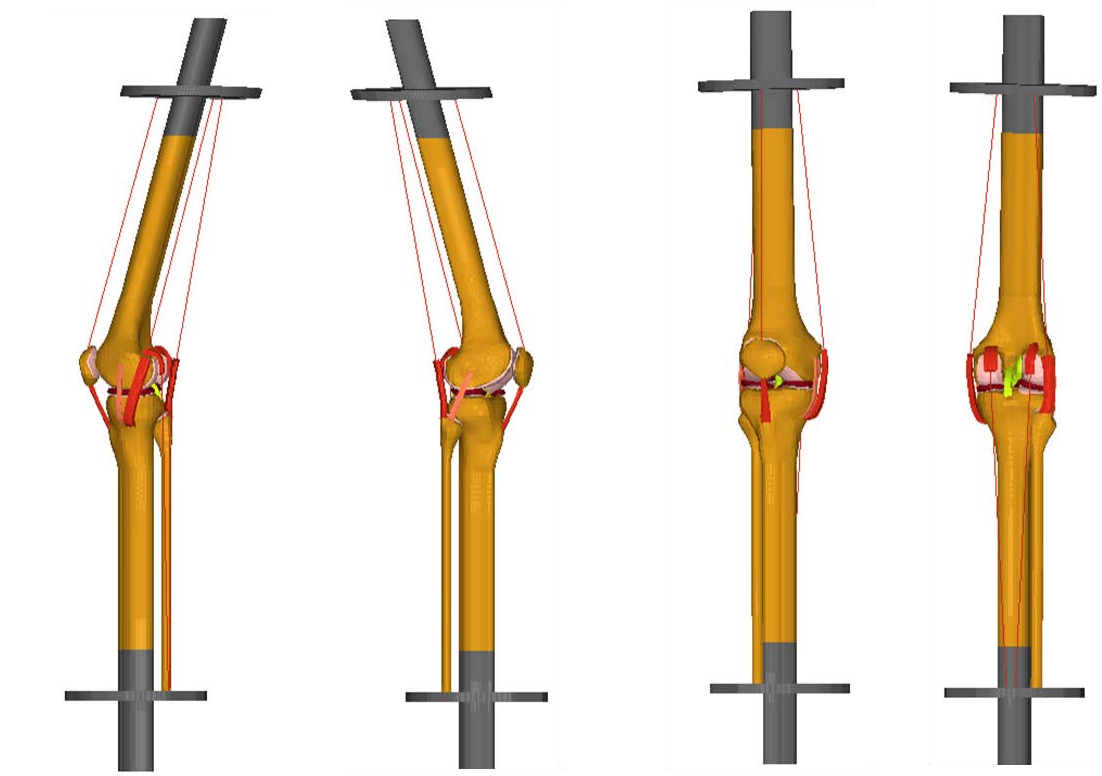

Figure 15: 3-D FE model of knee joint in LS-Dyna

In the physical experimental apparatus, the impact force simulating single-limb landing was applied at the distal tibia by dropping a weight. A 6-axis load cell placed at the distal

end of tibia measured the impact force. This impact force was applied to the distal end of the tibia in the FE model (Figure 16) to simulate single-limb landing.

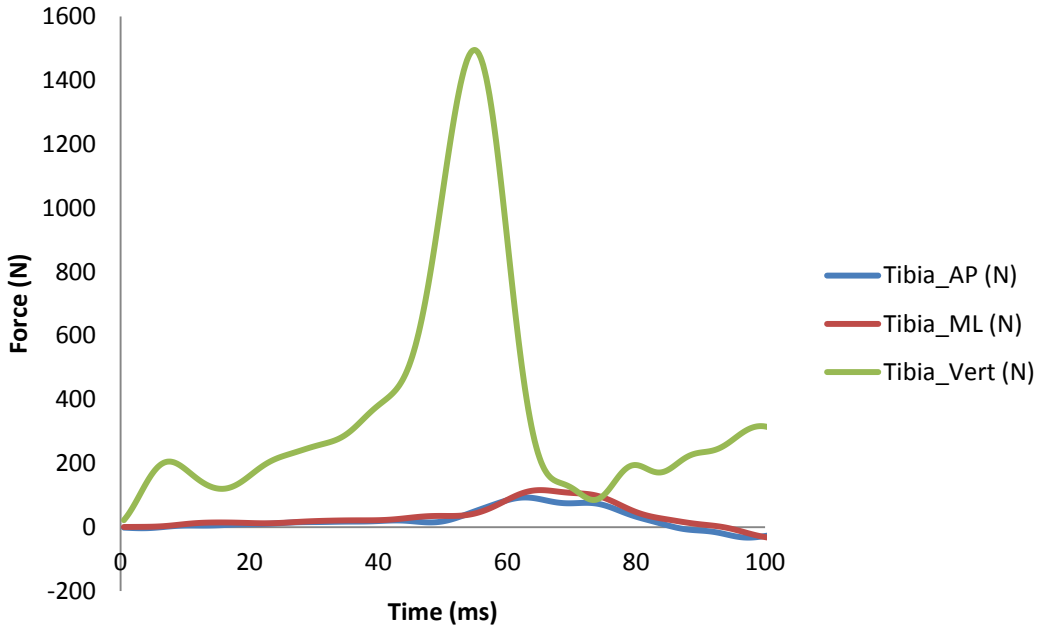

Figure 16: Impulsive load applied to distal tibia (Oh et al. 2011). Tibia_AP denotes the anterior-posterior force, Tibia_ML denotes the medial-lateral force and Tibia_Vert denotes the vertical force.

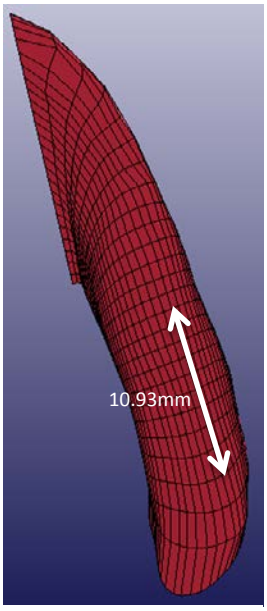

Figure 17: Arrow indicates the region from which strain was measured

6. Explicit analysis and solution: An explicit solution was obtained for the problem set up in LS Dyna®. From the solution, knee joint kinematics and ACL strain data were extracted for analysis. Specifically, anterior translation of tibia relative to femur, change in knee flexion-extension angle, knee varus-valgus angle and knee internal-external rotation angle were extracted. To obtain ACL strain, two nodes were identified approximately 11mm (initial length, L) apart along the antero-medial bundle of the ACL (Figure

17). These nodes correspond with the approximate placement of the DVRT on the cadaveric ACL during the experimental simulation. Change in length between these two nodes (ΔL) was used to calculate the percent strain using the following equation:

$$\varepsilon = \frac{\Delta L}{L} \times 100$$

Validation

To validate the model, knee rotation angles and ACL strain data from the experiment were compared to those predicted by the FE model. Figures 18 and 19 respectively show the data obtained from the experiment and that predicted by the FE model.

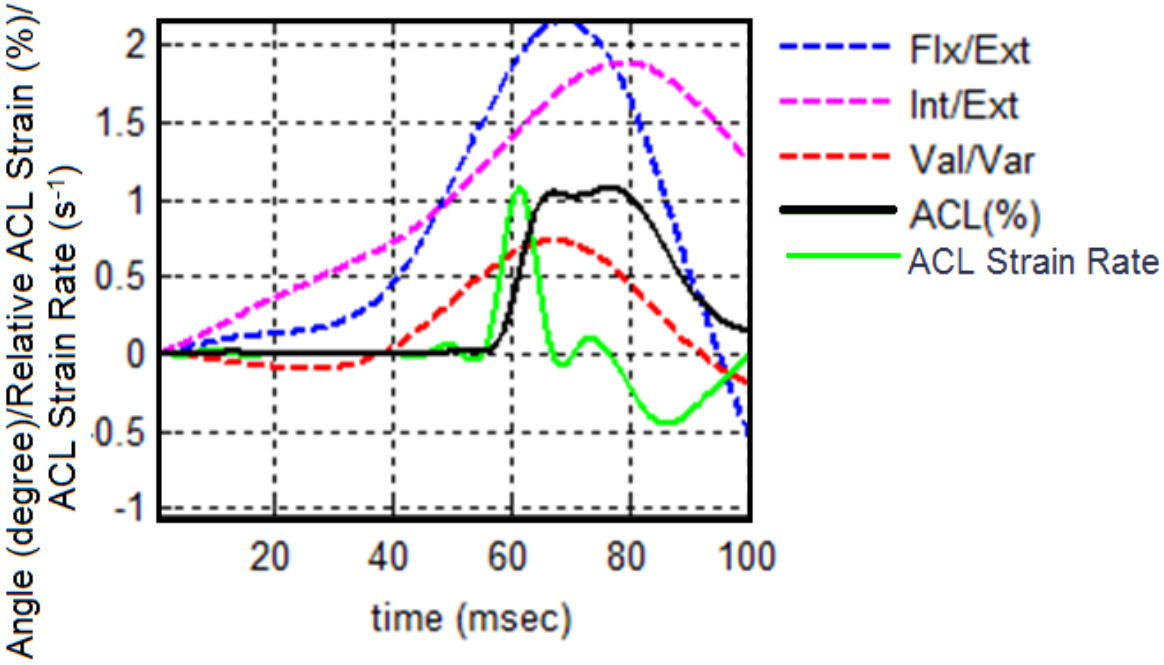

Figure 18: Kinematic and ACL strain results from the cadaveric experiments (Oh et al. 2011). Flexion angle, Internal rotation angle and Valgus angle are all positive on the Y-axis.

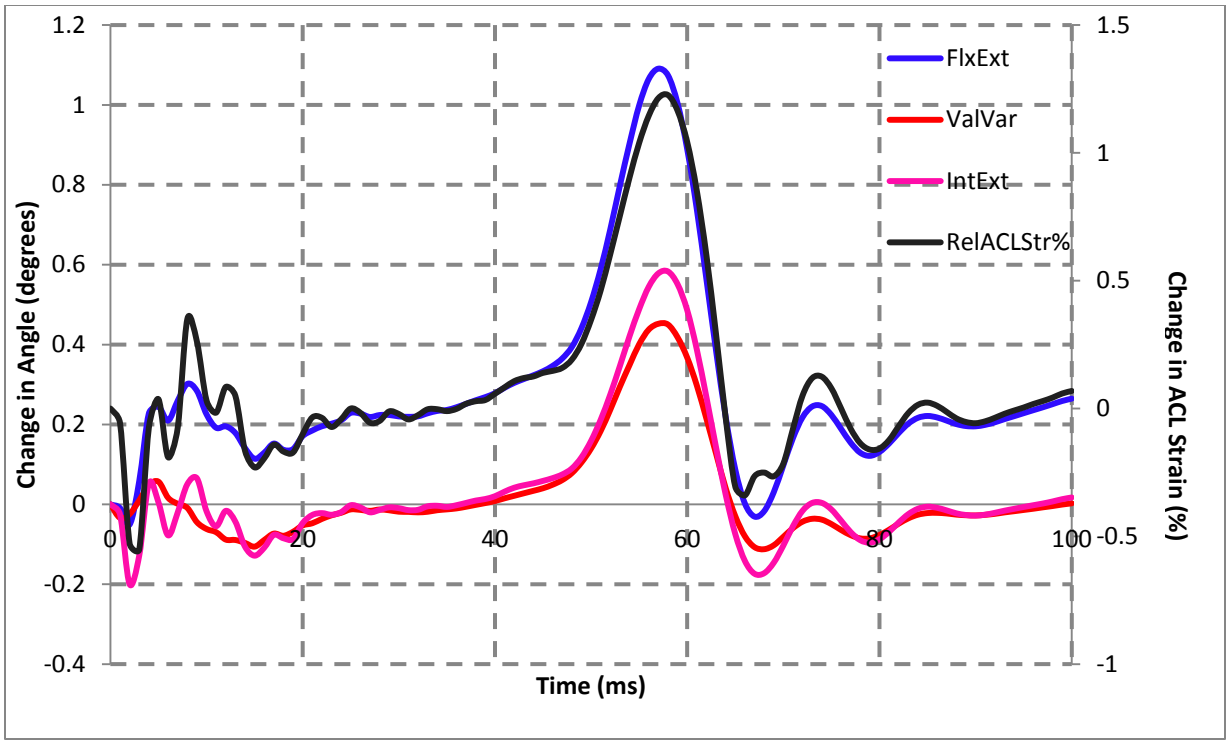

Figure 19: Kinematic and ACL strain results predicted by the FE model. The Flexion angle, Internal rotation angle, Valgus angle are all positive on the Y-axis

A statistical comparison of the data between Figures 18 and 19 was performed on the data in the window from 40ms to 70ms. A significant correlation (Pearson's R) of 0.861 ($p < 0.01$) was determined from correlation tests between the change in ACL strain from the cadaveric experiment and the change in ACL strain predicted by the FEA simulation in the window focused around the ACL peak (40ms to 70ms). A correlation of 0.80 ($p < 0.01$) was found between the change in flexion-extension angle predicted by the FE model and that observed in the cadaveric model within the same range (40ms to 70ms). Similarly, the anterior-posterior translation from the FE model and cadaveric simulation were found to have a correlation coefficient of 0.829 ($p < 0.01$). The differences observed between the results predicted by the FE model and that observed in the experimental simulation can be attributed to the difference in knee anatomy and the

inherent stiffness of the FE model. However, the similarities in the manifestation of sagittal plane motion viz. flexion-extension angle and anterior-posterior translation and ACL strain provide sufficient credence to the results predicted by the FE model. The range of flexion-extension and varus-valgus angles was observed to be similar as was the range for the ACL strain (peak ~1%).

In his review paper on 'Interpretation of Correlation Coefficient', Richard Taylor (1990) identified a correlation of 0.80 or greater as a very strong correlation. Based on these similarities observed in the results, the FE model can be considered as an experimentally-validated model. The FE model can, therefore, be used to predict sensitivity of the ACL strain response to changes in ACL modulus and to changes in tibial surface geometry. In the following chapters, the FE model was used to determine the effect that variation in ACL modulus and tibial surface geometry has on ACL loading.

Chapter V

Effect of ACL Modulus on ACL Strain during Impact Loading

Introduction

In this chapter a novel yet mechanically plausible mechanism to explain the role of ACL modulus in the kinematic behavior of the knee joint is introduced. Specifically, it is contended that for a single-limb landing, large anterior tibiofemoral accelerations are possible at impact that cannot be adequately countered by the neuromuscular strategy. In this instance, additional loads must be restrained by the ACL. The restraint offered by an ACL with low modulus (lax ACL) would be compromised resulting in unsustainable anterior tibiofemoral accelerations manifesting as greater stretch in ACL. The objective of this chapter is thus to demonstrate the influence of ACL modulus through a definitive link between impact-induced anterior tibiofemoral accelerations and ACL strain during a single leg landing. To achieve this objective, the hypothesis was tested that *anterior tibiofemoral acceleration during a simulated dynamic landing impact is proportional to peak relative anteromedial bundle ACL strain.* Further, it was hypothesized that an ACL with low modulus (high laxity) will experience greater peak relative anteromedial bundle ACL strain. The rationale for this goal is that establishing a link between impact-induced tibiofemoral accelerations and ACL strain provides immediate insights into the influence of ACL modulus and, therefore ACL injury causality. Statistical correlation between the

model-predicted anterior-posterior tibiofemoral acceleration and relative ACL strain during impact would provide the substantiation necessary to accept the hypothesis.

Methods

To test the hypotheses, the FE model of the knee joint validated against data from cadaveric simulation (Chapter IV) was employed. Mooney-Rivlin hyperelastic strain energy functions were used to fit the coefficients C10 and C01 to uniaxial stress-strain data for the ACL derived from the piece-wise equations described by Blankevoort et al (1991):

$$f = 0, \qquad \varepsilon < 0$$

$$f = \frac{\frac{1}{4}k\varepsilon^2}{\varepsilon_l}, \qquad 0 \leq \varepsilon \leq 2\varepsilon_l$$

$$f = k(\varepsilon - \varepsilon_l), \quad \varepsilon > 2\varepsilon_l$$

where f is the tensile force, k is the ligament stiffness, ε is the strain in the ligament and ε_l is the non-linear strain level parameter assumed to be equal to 0.03 (Blankevoort et al. 1991). The ligament stiffness parameter (k), determined to be 5000 N (Blankevoort et al. 1991) was considered the baseline modulus (100%) for the ACL. Variation in ACL stiffness was simulated without varying its geometry by modifying the value of 'k' in the above equations so that a range of 50% to 150% was obtained for the tests. Specifically, 5 single limb landing simulations were performed using k values of 2500 N (50%), 3750 N (75%), 5000 N (100%), 6250 (125%) and 7500 (150%) with 50% simulating lowest ACL

stiffness (high laxity) and 150% simulating highest ACL stiffness (low laxity). Figures 20 and 21 depict the uniaxial stress-strain test data corresponding to each of these simulations that was used to simulate the mechanical behavior of the ACL.

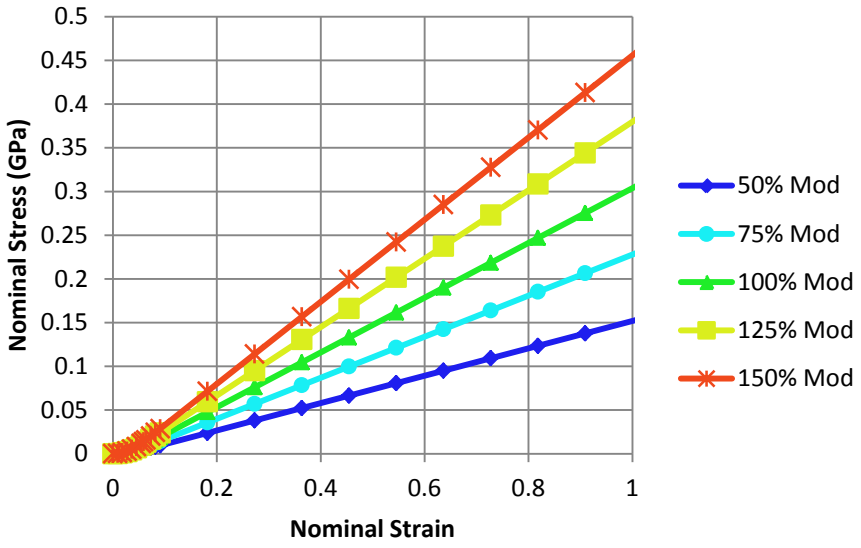

Figure 20: Uniaxial stress-strain data used to determine mechanical behavior of ACL

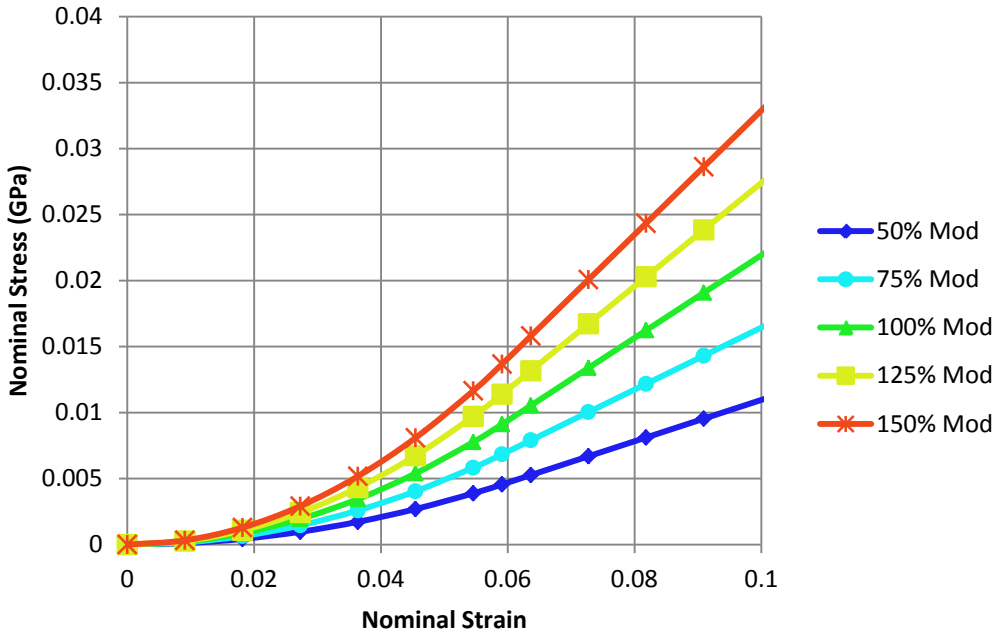

Figure 21: Non-linear (toe) region of the uniaxial stress-strain data used to determine mechanical behavior of ACL

An isotropic, non-linear, hyperelastic material model driven by Mooney-Rivlin strain energy functions was then implemented for each case using the coefficients C10 and C01 fit to the corresponding stress-strain data set. A pre-strain of 3% was imposed on the ACL as an initial condition in each case.

This range of 50% to 150% variation in stiffness was chosen to encompass the variation of ACL modulus from 150MPa to 470MPa. While the stiffer range of the ACL is higher than noted in the literature, Chandrashekar et al (2005) have observed ACL modulus in females to be as low as 100MPa. For the purposes of this study, we believe that this range of ACL moduli would be sufficiently informative on the effect of ACL modulus on ACL loading mechanism.

Results

Change in ACL strain and anterior-posterior tibiofemoral acceleration data were extracted for analysis from the solution of each simulation. ACL strain was measured based on the change in length between two fixed nodes on the anterior-medial bundle of the ACL identified in Figure 17. Tibiofemoral acceleration was obtained by differentiating twice the relative displacement of a node close to the ACL insertion site on the tibia with respect to a node close to the ACL origin site on the femur. Figure 22 shows the variation in the change in ACL strain with respect to change in ACL modulus.

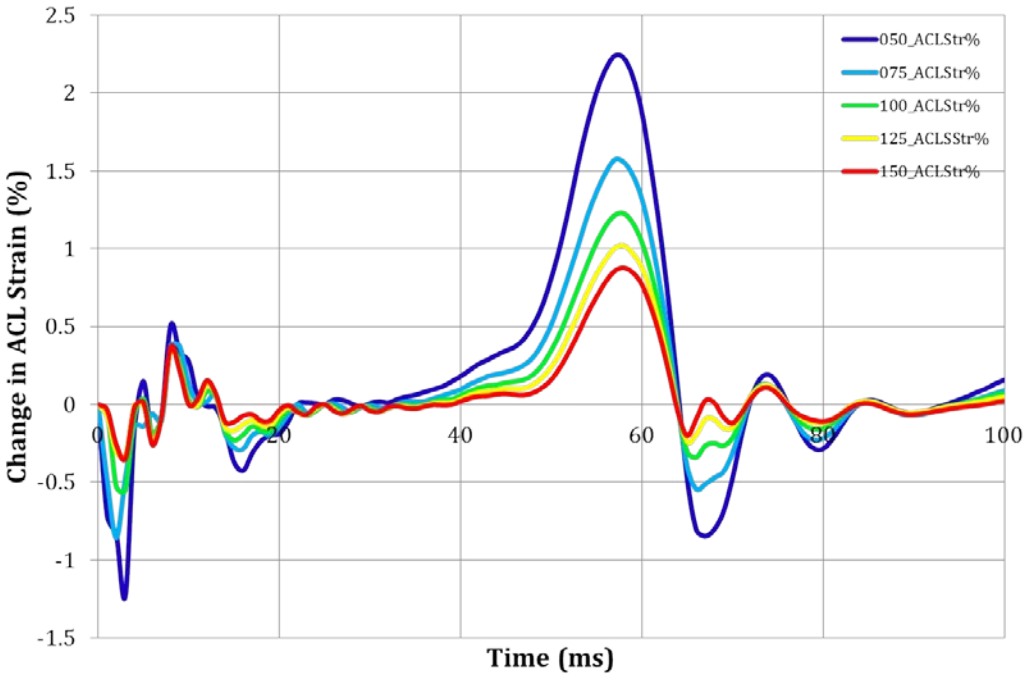

Figure 22: Variation in change in ACL strain with respect to ACL modulus

Variation in anterior tibiofemoral acceleration was also observed and is shown in Figure 23.

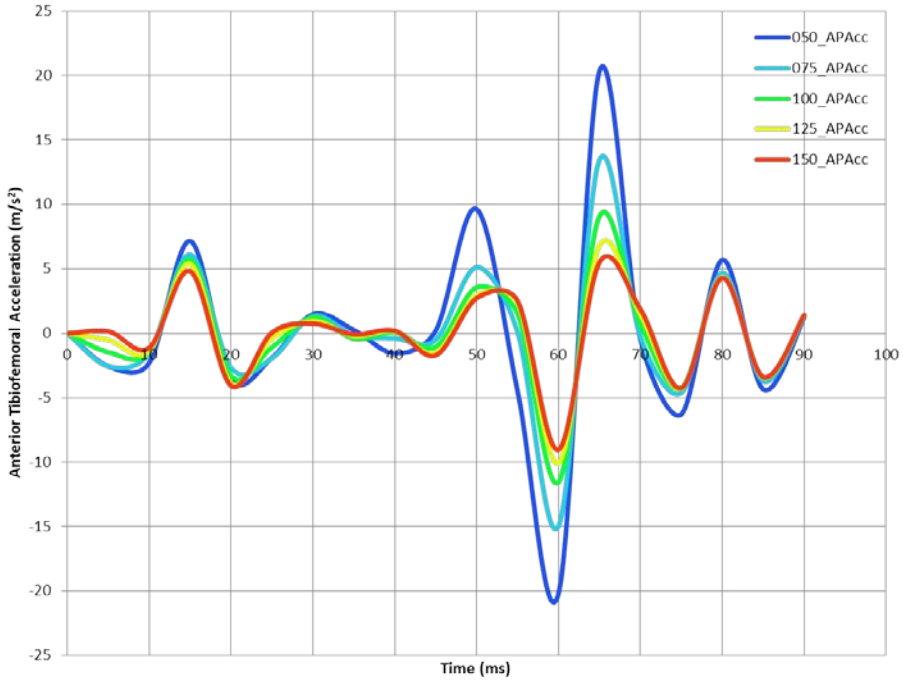

Figure 23: Variation in relative tibiofemoral acceleration with respect to ACL modulus [-y → anterior acceleration]

A test for model effects indicated a significant effect of ACL modulus on anterior tibiofemoral acceleration ($p < 0.01$). A correlation test between the anterior-posterior tibiofemoral acceleration and relative ACL strain resulted in a Pearson's correlation coefficient of 0.685 ($p < 0.01$).

Peak anterior tibiofemoral acceleration was observed to vary with respect to the peak relative ACL strain. Only anterior tibiofemoral accelerations were reported for this comparison as the ACL is stretched by the anterior motion of the tibia with respect to the femur and relaxes when the tibia displaces posterior relative to the femur. Figure 24 depicts the variation in both the peak change in ACL strain and peak anterior tibiofemoral acceleration with respect to ACL modulus. Variations in peak ACL strains and peak anterior tibiofemoral accelerations were highly correlated with a Pearson's coefficient of 0.999 ($p < 0.01$).

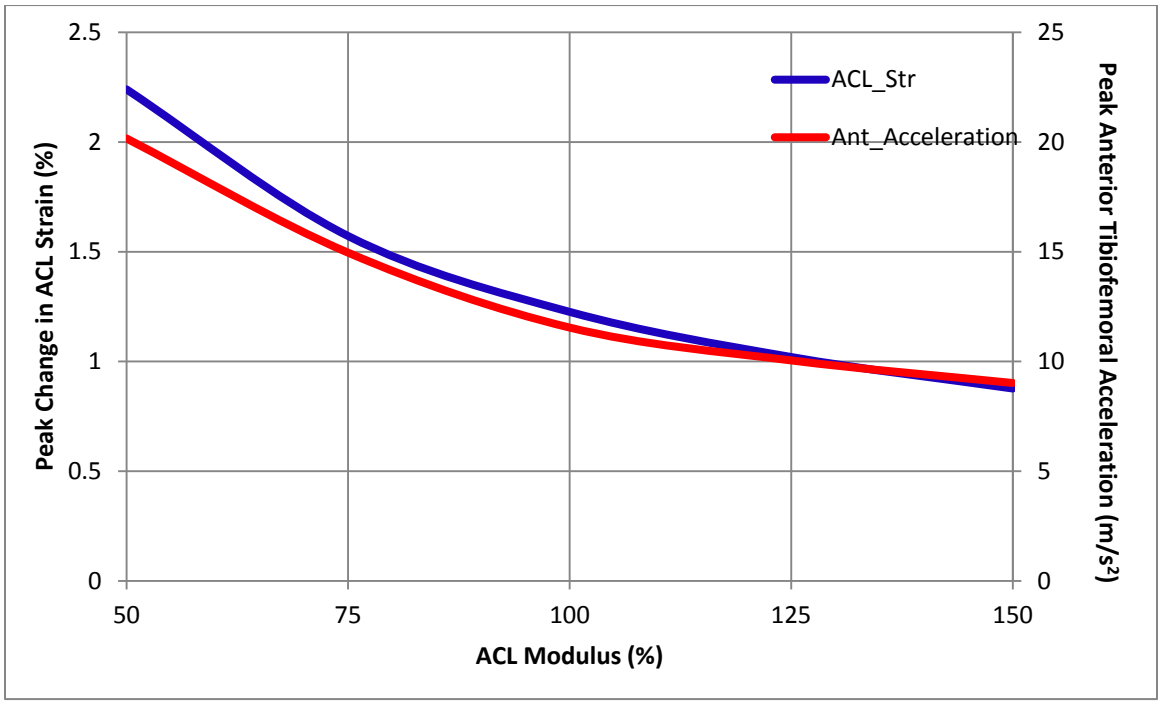

Figure 24: Variation in peak change in ACL strain and peak anterior tibiofemoral acceleration with respect to ACL modulus

Discussion

ACL modulus is considered a significant factor contributing to the risk of ACL injury. Previous work by Chandrashekar et al (2005) has characterized the tensile properties of the ACL and determined that the female ACL is in fact weaker and less stiff (low modulus) resulting in poor mechanical behavior. A structurally compromised ACL as observed after a partial tear would also have lower modulus and stiffness than a healthy ACL. The results presented from the analysis above support the notion that an ACL with low modulus leads to the development of potentially hazardous knee biomechanics during the course of dynamic impact. As indicated in figure 22, larger strains were observed in an ACL with low modulus. The ACL strains progressively decreased as the modulus of the ACL increased. Similar observations were made with respect to the sagittal plane tibiofemoral accelerations. A knee with a low modulus ACL was found to have larger anterior-posterior tibiofemoral acceleration compared to knees with higher moduli ACL. Furthermore, as figure 24 indicates, the change in peak ACL strain consistently varied in accordance with peak anterior tibiofemoral acceleration suggesting a highly coupled relationship between ACL strain and anterior tibiofemoral acceleration. These results lend credence to the theory that ACL modulus has an effect on the ACL strain manifesting in knee joint kinematics through tibiofemoral accelerations during the course of impact loading. Therefore, our hypothesis that low ACL modulus leads to high ACL strain and can potentially implicate itself in poor knee kinematics, specifically anterior tibiofemoral acceleration, and lead up to an injury is supported.

Implications

Considering that variations in anterior tibiofemoral accelerations predict variations in ACL strain, the potential for the development of a surveillance method to identify when during the course

of a game an athlete becomes susceptible to ACL injuries is evident. Properties of the ACL can change over time as a result of training, injury, fatigue or stress. These changes then manifest as a change in ACL stiffness or laxity. This is particularly true for female athletes as tissue stiffness is significantly influenced by hormonal changes associated with menstruation. By monitoring anterior tibiofemoral acceleration during the course of a game, the relative susceptibility of the athlete to the development of high ACL strains and potential injuries can be assessed in real time.

Significance

These results have significant implications as they establish a definitive relation between ACL modulus (stiffness or laxity) and ACL strain during impact loading. These results also provide insight into how ACL modulus implicates itself through the development of poor knee kinematics, particularly anterior tibiofemoral accelerations, and potential injury causing situations. In conclusion, we accept the hypothesis that low ACL modulus (high laxity) would cause the ligament to have poor restraining capabilities, resulting in an inability to provide the necessary force to sufficiently oppose anterior translation of the tibia relative to femur. This increase in anterior tibiofemoral acceleration would lead to greater stretch being induced in the ACL resulting in manifestation of higher ACL strain.

Chapter VI

Effect of Tibial Surface Geometry on ACL Strain during Impact Loading

Introduction

In this chapter, a mechanically plausible manner in which tibial surface geometry factors into an ACL loading is investigated. Tibial surface geometry dictates to a large extent the tibiofemoral articulation and subsequently, 3-D knee biomechanics. Specifically, three factors pertaining to the tibial surface geometry influence this articulation viz. medial tibial depth (MTD), medial tibial slope (MTS) and lateral tibial slope (LTS). During a single limb landing, large anterior tibiofemoral accelerations and potentially hazardous frontal and transverse plane rotations of the knee joint are possible at impact that cannot be adequately countered by the neuromuscular strategy. For instance, shallow MTD, greater MTS or greater LTS would tend to compound the anterior motion of tibia relative to femur resulting in unsustainable anterior tibiofemoral acceleration manifesting as greater stretch in ACL. A combination of shallow MTD and greater LTS could result in valgus loading of the knee joint that would exacerbate the adverse effect of anterior tibiofemoral acceleration. The objective of this chapter, thus, is to demonstrate the main effect of MTD, LTS and MTS as well as the interaction effect of these three factors on ACL strain through a definitive link between impact-induced anterior tibiofemoral accelerations, varus-valgus rotation, internal-external rotation and ACL strain during a single limb landing.

To achieve this objective, the hypothesis that *anterior tibiofemoral acceleration, varus-valgus angle and internal-external rotation angle during a simulated dynamic landing impact are*

proportional to relative anteromedial bundle ACL strain was tested. Further, it was hypothesized that shallow MTD, greater MTS and greater LTS will each result in greater peak relative anteromedial bundle ACL strain. It was also hypothesized that a combination of these three factors (shallow MTD, greater LTS and greater MTS) will result in the worst case scenario with higher strain being manifested in the antero-medial bundle of the ACL. On the contrary, a separate combination (deeper MTD, lower MTS and lower LTS) will result in least strain developing the antero-medial bundle of the ACL. The rationale for this goal is that establishing a link between impact-induced sagittal plane tibiofemoral accelerations, valgus-varus angle, internal-external rotation and ACL strain provides immediate insights into the influence of MTD, MTS and LTS, jointly and separately, on ACL loading. Such knowledge is ultimately critical to improved understanding of the role played by the tibial surface geometry on development of knee kinematics and ACL loading.

Methods

To achieve the objectives outlined above, a range for each of the three parameters, MTD, MTS and LTS was identified (Table 3). Mean values served as the baseline measures and each of the three parameters was either increased or decreased by 1 standard deviation (SD). To account for all the main effects and the interaction effects, 27 simulations were developed to account for each combination (Table 4). The tibial surface geometry was modified by changing the MTD, LTS and MTS each using morphing tools in Hypermesh®. The material properties of all the tissues were defined and the model was configured as described in Chapter IV. An impulsive impact load was applied for duration of 100ms, with the peak occurring at 55ms. Relative ACL strain in the anterior-medial bundle, anterior tibiofemoral acceleration, varus-valgus angle and internal-external rotation data were extracted for analysis in a manner similar to that outlined in Chapter IV.

Table 3: Values of MTD, MTS and LTS applied to test the hypotheses (Hashemi et al. 2011)

	Mean – SD	Mean	Mean + SD
Medial Tibial Depth (mm)	0.93	1.91	2.89
Medial Tibial Slope (degrees)	2.9	5.9	8.9
Lateral Tibial Slope (degrees)	3.9	7.0	10.1

Table 4: Different combinations of MTD, MTS and LTS tested

Test #	MTD	MTS	LTS
1	Mean	Mean	Mean
2	SD+	Mean	Mean
3	SD-	Mean	Mean
4	Mean	SD+	Mean
5	SD+	SD+	Mean
6	SD-	SD+	Mean
7	Mean	SD-	Mean
8	SD+	SD-	Mean
9	SD-	SD-	Mean
10	Mean	Mean	SD+
11	SD+	Mean	SD+
12	SD-	Mean	SD+
13	Mean	SD+	SD+
14	SD+	SD+	SD+
15	SD-	SD+	SD+
16	Mean	SD-	SD+
17	SD+	SD-	SD+
18	SD-	SD-	SD+
19	Mean	Mean	SD-
20	SD+	Mean	SD-
21	SD-	Mean	SD-
22	Mean	SD+	SD-
23	SD+	SD+	SD-
24	SD-	SD+	SD-
25	Mean	SD-	SD-
26	SD+	SD-	SD-
27	SD-	SD-	SD-

Results

Change in strain in the anterior-medial bundle of the ACL, anterior tibiofemoral acceleration, varus-valgus angle and internal-external rotation angle data were extracted from the simulation solutions and statistical analyses performed. The change in ACL strain varied over a range extending from the smallest peak ACL strain of 0.66% (knee 20) to the largest peak ACL strain of 1.3% (knee 12). Figure 25 shows the variability in the change in strain in the antero-medial bundle of the ACL observed for each of the morphed FE models.

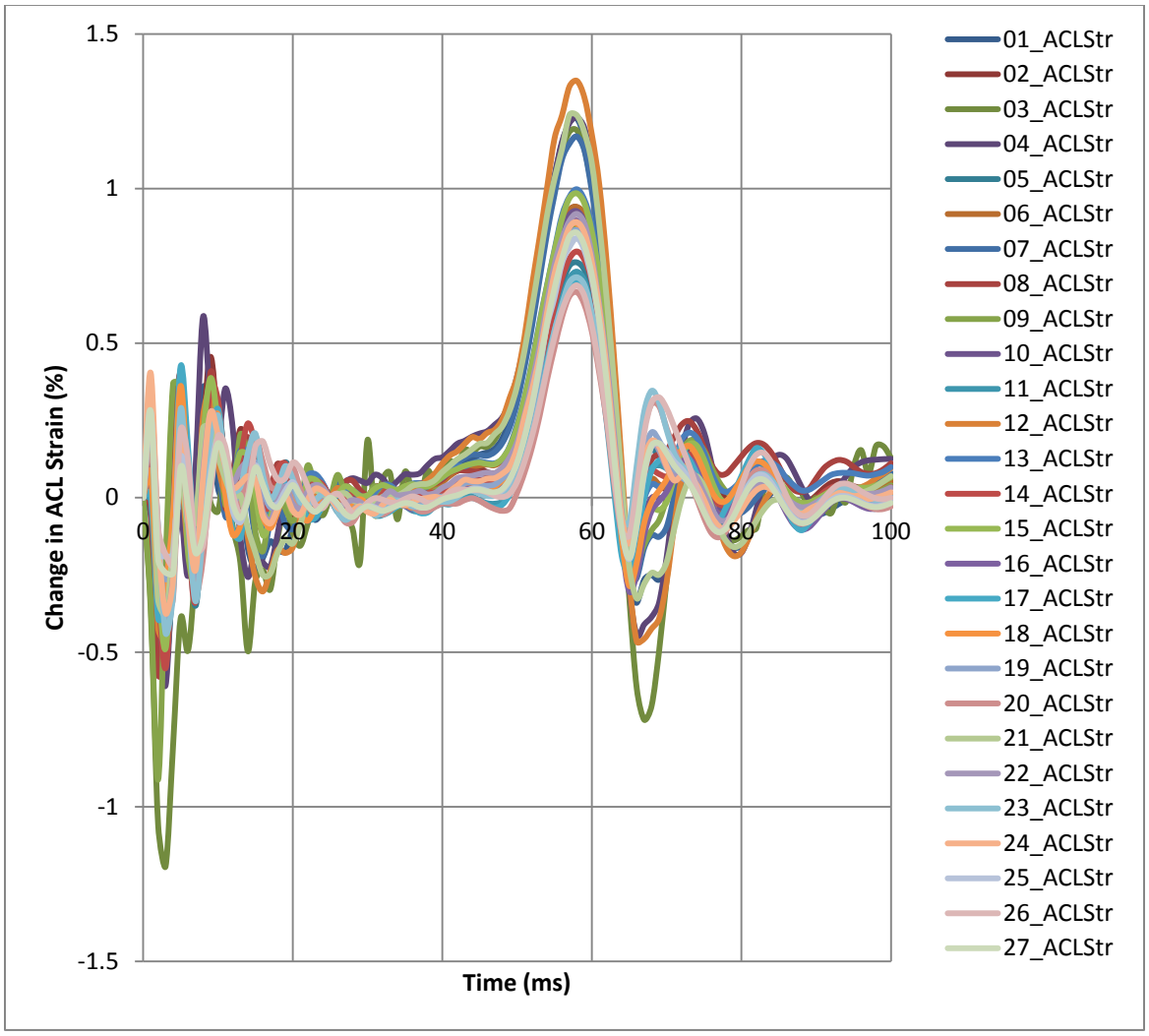

Figure 25: Variation in change in ACL strain with respect to different tibial surface geometries

Test of model effects showed a significant effect of the interaction of MTD, MTS and LTS on anterior-posterior tibiofemoral acceleration, varus-valgus angle and internal-external rotation angle ($p < 0.01$). The geometrical factors individually did not have any significant effect on the manifestation of these kinematics variables but in combination introduced statistically significant variability in the frontal and transverse plane rotations. To highlight this effect, rotations in the frontal and transverse planes from the control knee (Test# 1), hypothesized worst knee (Test# 15), FEA-predicted worst knee (Test# 12), hypothesized best knee (Test# 26) and FEA-predicted best knee (Test# 20) were plotted (Figures 26 and 27).

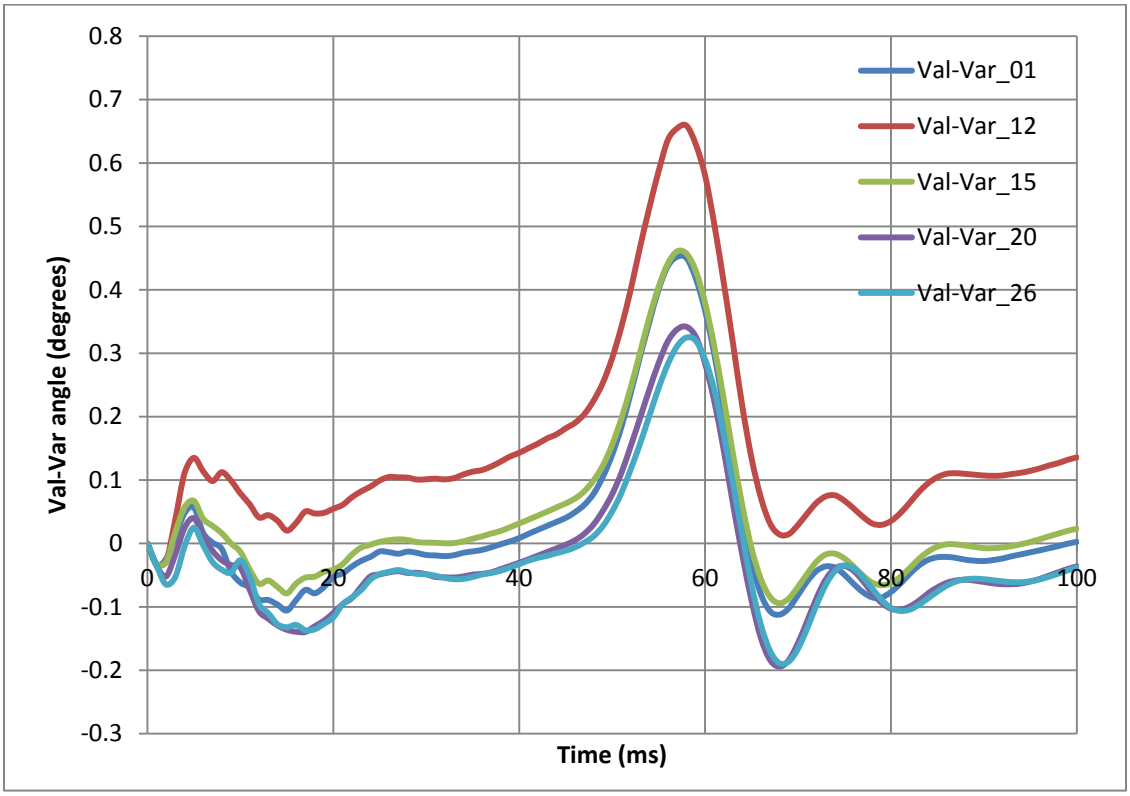

Figure 26: Variability in valgus(+) angle with change in tibial surface geometry

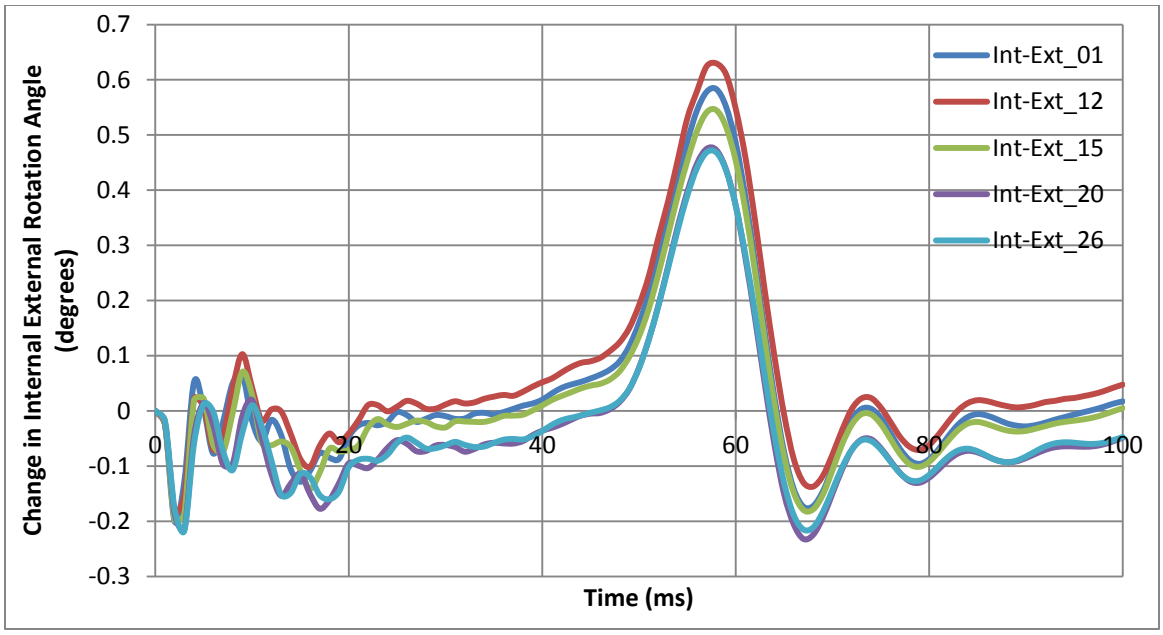

Figure 27: Variability in internal rotation (+) with change in tibial surface geometry

The kinematic variables viz. anterior-posterior tibiofemoral acceleration, varus-valgus angle and internal-external rotation angle were analyzed using a stepwise regression model to determine predictor importance and generate the regression equation to predict ACL strain. The internal-external rotation angle was found to be most important predictor of ACL strain with a predictor importance of 65% followed by varus-valgus angle at 24% and anterior-posterior tibiofemoral acceleration at 10%. The regression equation generated to predict the change in ACL strain, with an accuracy of 94%, was as follows:

$$Change\ in\ ACL\ Strain = \ 0.599IntExt + 0.325ValVar - 0.115APAcc$$

A P-P plot (Figure 28) compares the distribution of the residuals to a normal distribution. The solid black line represents the normal distribution. The closer the observed cumulative probabilities of the residuals are to this line, the closer the distribution of residuals is to the normal distribution.

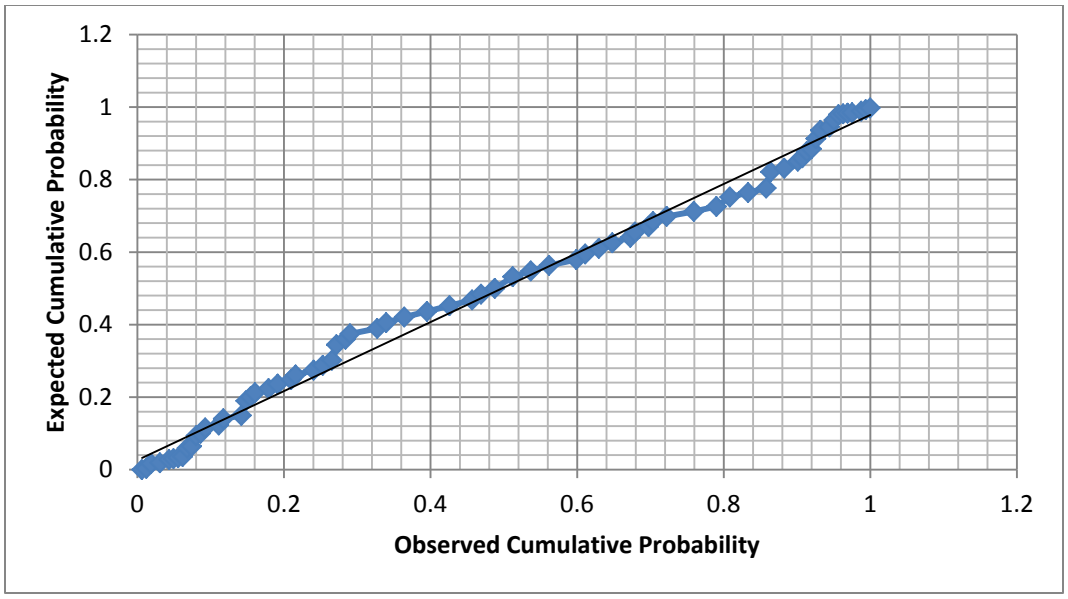

Figure 28: Comparison of distribution of residuals to normal distribution

Correlation tests were also performed on ACL strain against anterior-posterior tibiofemoral acceleration, varus-valgus angle and internal-external rotation angle independently to obtain Pearson's coefficient of correlation. The ACL strain was correlated with anterior-posterior acceleration with a Pearson's coefficient of 0.611 ($p < 0.01$), with varus-valgus angle with a coefficient of 0.917 ($p < 0.01$) and with internal-external rotation angle with a coefficient of 0.955 ($p < 0.01$). A correlation test was also performed to determine the relationship of peak change in ACL strain with the peak anterior tibiofemoral acceleration, peak varus-valgus angle and peak internal-external rotation angle. The Pearson's coefficient of correlation obtained between peak change in ACL strain and peak anterior tibiofemoral acceleration, peak valgus angle and peak internal rotation angle was 0.483 ($p < 0.05$), 0.779 ($p < 0.01$) and 0.678 ($p < 0.01$) respectively.

Discussion

Tibial surface geometry has long been understood to contribute significantly to 3-D knee joint kinematics and subsequently kinetics particularly during the execution of dynamic activities.

Despite the influence of geometry on knee joint biomechanics, this factor has been largely ignored in the study of ACL injuries due to its categorization as a non-modifiable factor. However, over the recent years, morphometric factors have been investigated to gain insight into the mechanism for ACL injuries and to understand the prevailing conditions that cause female population generally to be more susceptible to ACL injuries. In a blind study on injured and uninjured skiers, Hashemi et al (2010) were able to correlate risk of ACL injury to shallow medial tibial depth and high lateral slope. Recent work by McLean et al (2011) on cadaver knees establishes a significant correlation between posterior tibial slope, anterior-posterior tibiofemoral acceleration and ACL strain. These studies successfully demonstrate the significance of investigating tibial surface geometry and its effect on ACL strain. In this chapter, we take the analysis further by breaking down the effect of tibial surface geometry and analyzing the main and interaction effect of lateral tibial slope, medial tibial slope and medial tibial depth. Given the complexity of their interaction and the subsequent effect on 3D knee mechanics, a reasonable assumption would be that ACL strain depends on knee kinematics in three dimensions i.e. sagittal plane tibiofemoral acceleration, frontal and transverse plane rotations. The analysis within this chapter provides a new understanding of the role tibial surface geometry plays in the loading of ACL.

As the results indicate, peak change in ACL strain was observed to vary with change in tibial surface geometry (Figure 25). No statistically significant main effect of the MTD, MTS or LTS on the change in ACL strain was found. However, a significant interaction effect of MTD, MTS and LTS was observed which indicates that the tibial surface geometry dictates complex 3-D knee biomechanics encompassing the consequent loading of ACL (Figures 26 and 27). The development of ACL strain was influenced to a greater extent by frontal and transverse plane rotations than by sagittal plane kinematics. The regression equation clearly indicates a larger

effect of internal-external rotations and varus-valgus angle on ACL strain. Thus, the hypothesis that anterior tibiofemoral acceleration, varus-valgus angle and internal-external rotation angle during a simulated dynamic landing impact are proportional to relative anteromedial bundle ACL strain is accepted.

An unexpected observation from the results was that the greatest ACL strain was observed in a knee with shallow MTD, high LTS and *average* MTS and not in the hypothesized knee with shallow MTD, high LTS and high MTS. Similarly, the smallest ACL strain was observed in a knee with deep MTD, low LTS and *average* MTS and not in the hypothesized knee with deep MTD, low LTS and low MTS. This suggests a coupled action of LTS and MTS in dictating the 3-D rotations that subsequently determine the manifestation of ACL strain. Thus, it is critical to consider the effect of MTS and LTS jointly rather than separately when studying its effect on ACL loading during impact.

Implications

In the previous chapter, investigating the effect of ACL modulus, a strongly coupled relationship was observed between the peak change in ACL strain and peak anterior acceleration (Pearson's coefficient of correlation 0.999, $p < 0.01$). No such relationship between those variables was determined when controlling for the tibial surface geometry (Pearson's correlation coefficient of 0.483, $p < 0.05$) suggesting that sagittal plane kinematics are more dependent on ACL modulus whereas the frontal and transverse plane rotations are determined by tibial surface geometry. Yet another interesting observation was the lack of effect that the lateral tibial slope, medial tibial slope and medial tibial depth individually had on the tibiofemoral kinematics and ACL strain. Only the combined effect of these three geometric factors significantly influenced the kinematics and ACL strain suggesting that ACL injury is a multi-factorial mechanism.

Significance

Tibial surface geometry has a significant effect on the manner in which the ACL is loaded during the course of impact loading. Considering that the strain in the ACL can be predicted within reasonable accuracy using anterior-posterior tibiofemoral acceleration, internal-external rotation angle and varus-valgus angles, it is plausible to pursue development of a surveillance technique to monitor 3-D knee joint kinematics in real-time to predict the ACL strain. While tibial slope itself is non-modifiable, neuromuscular mechanism developed from training typically prevails and controls the kinematics of the knee joint. However, the neuromuscular control is susceptible to failure under conditions of stress and fatigue and the inherent knee joint biomechanics may emerge supplanting biomechanics from learned neuromuscular strategies. Monitoring the knee joint behavior in real-time may help identify when the athlete is reverting back to his or her potentially risky biomechanical profile. Additionally, the results establish that ACL injury mechanism is dictated by multiple factors, a consideration that must be addressed when studying ACL injury.

Chapter VII

Combined Effect of Tibial Surface Geometry and ACL Modulus on ACL Strain during Impact Loading

Introduction

In this chapter, the interactive effect of tibial surface geometry and ACL modulus is examined to explore the interaction of these factors and its implication in an ACL loading mechanism. In chapters V and VI, ACL strain was definitively linked to the anterior-posterior tibiofemoral acceleration, varus-valgus rotation and internal-external rotation angle. Solutions from separate simulations extracted to isolate the main effect of ACL modulus and tibial surface geometry on ACL strain suggest very distinctive effects of these two risk factors. ACL modulus was found to have a profound effect on ACL strain through the development of high anterior tibiofemoral acceleration whereas the tibial surface geometry predominantly influenced the varus-valgus and internal-external rotations. The objective of this chapter was, therefore, to elucidate the sensitivity of the kinematics to variations in both ACL modulus and tibial surface geometry. Female athletes are typically attributed with ACL of low modulus and tibial surface with shallow, highly sloped contours. These factors have been classified as risk factors for ACL injuries and have frequently been cited as a cause for higher rate of ACL injury observed within the female athlete population (Griffin et al. 2006). The underlying mechanism, however, through which these factors influence the strain response of the ACL, is poorly understood. It is therefore imperative to elucidate the extent to which variation in these factors viz. ACL modulus and tibial surface geometry influence the kinematic response of the knee through its effect on the

anterior–posterior tibiofemoral acceleration, frontal plane rotation and transverse plane rotation angles. Understanding the mechanism could potentially enable us to monitor ACL strain through parameters observable during the course of gameplay.

Methods

To test the effect of ACL modulus and tibial surface geometry, 5 knees of the 27 simulated in chapter VI were selected. The control knee (Test# 1), the FEA-predicted worst knee (Test# 12), the hypothesized worst knee (Test# 15), the FEA-predicted best knee (Test# 20) and the hypothesized best knee (#26) were chosen for this analysis.

Table 5: List of simulations run to test the effect of ACL modulus and tibial surface geometry

Test#	Knee#	MTD	MTS	LTS	ACL Modulus
1	1	Average	Average	Average	50%
2					75%
3					100%
4					125%
5					150%
6	12	Shallow	Average	High	50%
7					75%
8					100%
9					125%
10					150%
11	15	Shallow	High	High	50%
12					75%
13					100%
14					125%
15					150%
16	20	Deep	Average	Low	50%
17					75%
18					100%
19					125%
20					150%
21	26	Deep	Low	Low	50%
22					75%
23					100%
24					125%
25					150%

The explicit response of each knee was obtained at every level of ACL stiffness (50%, 75%, 100%, 125% and 150%) culminating in a total of 25 simulations set-up for analysis (Table 5). Each simulation was set up as previously described with muscle forces, boundary conditions and impact loads similar to those implemented by Oh et al (2011) in their cadaveric experiments.

Results

Change in strain in the anterior-medial bundle of the ACL was extracted as well as kinematic data including sagittal plane tibiofemoral acceleration, varus-valgus angle and internal-external rotation angle data. Change in ACL strain varied considerably (Figure 29) with an observed maximum change in strain of approximately 2.4% (Knee 12, modulus 50%) and an observed minimum of 0.3% (knee 26, modulus 150%).

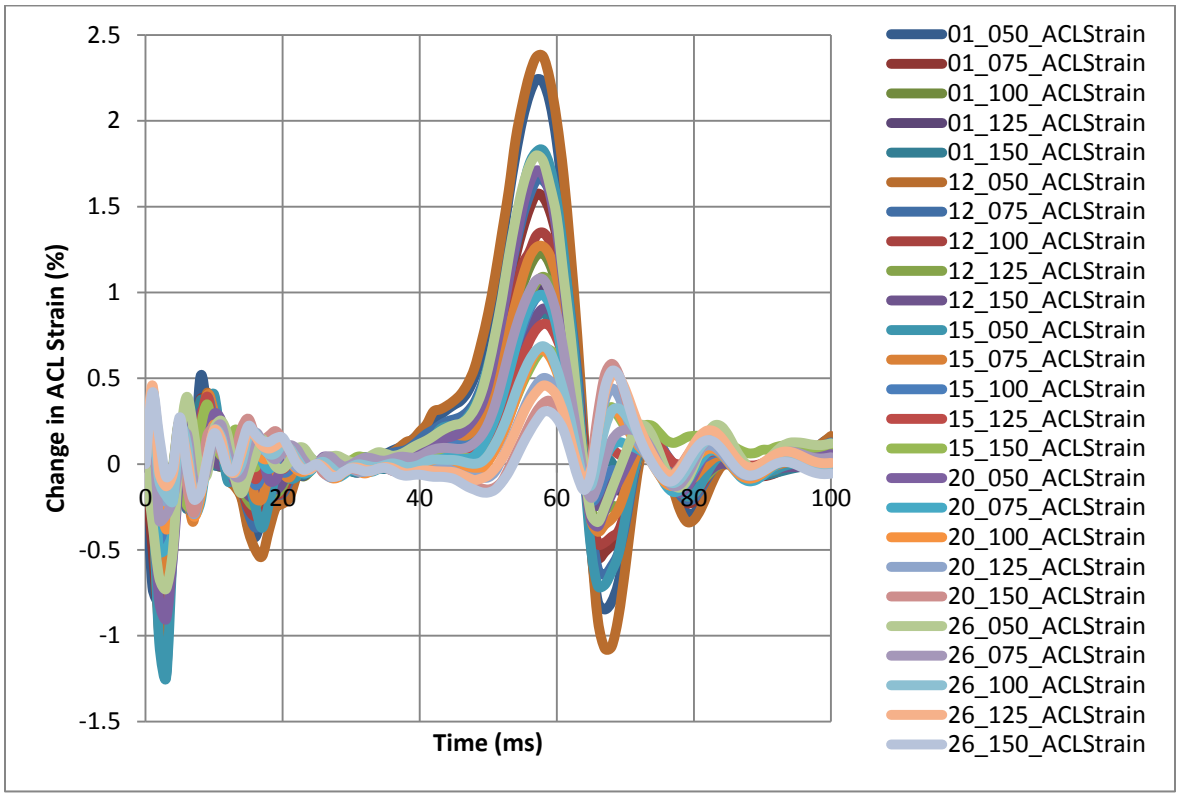

Figure 29: Change in ACL strain profiles for the 25 cases simulated

Peak anterior tibiofemoral acceleration, peak valgus angle, peak internal rotation angle and peak relative ACL strain were plotted together to understand how these variables vary relative to one another (Figure 30 – a, b, c, d and e).

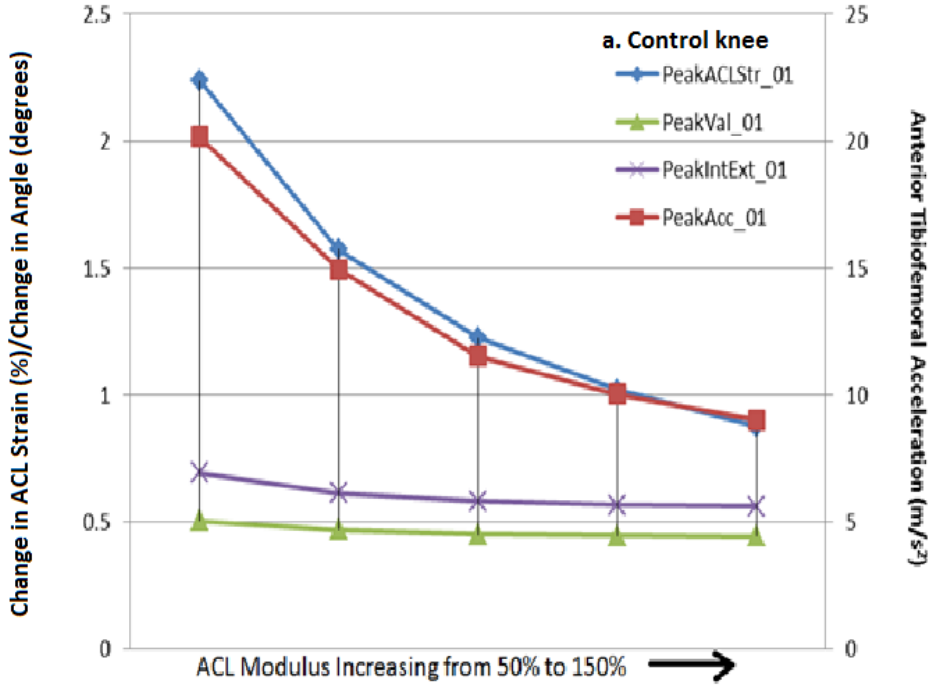

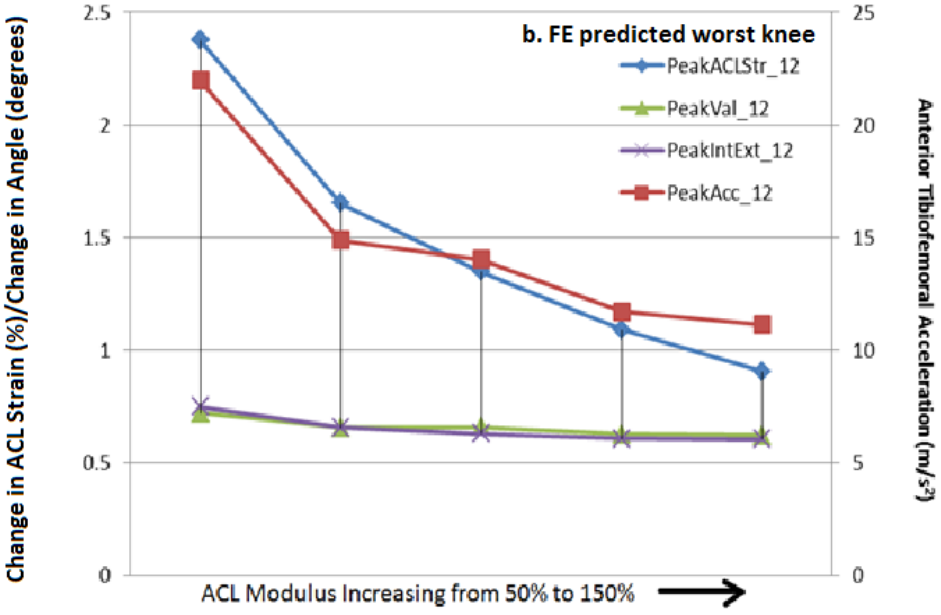

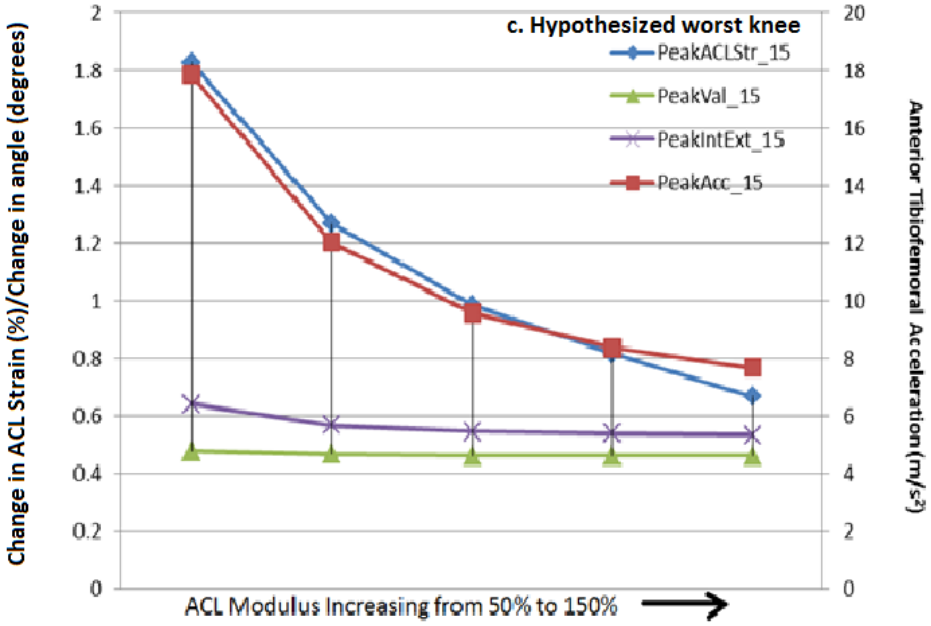
c. Hypothesized worst knee
PeakACLStr_15
PeakVal_15
PeakIntExt_15
PeakAcc_15
Change in ACL Strain (%)/Change in angle (degrees)
Anterior Tibiofemoral Acceleration (m/s²)
ACL Modulus Increasing from 50% to 150%
0
0.2
0.4
0.6
0.8
1
1.2
1.4
1.6
1.8
2
0
2
4
6
8
10
12
14
16
18
20

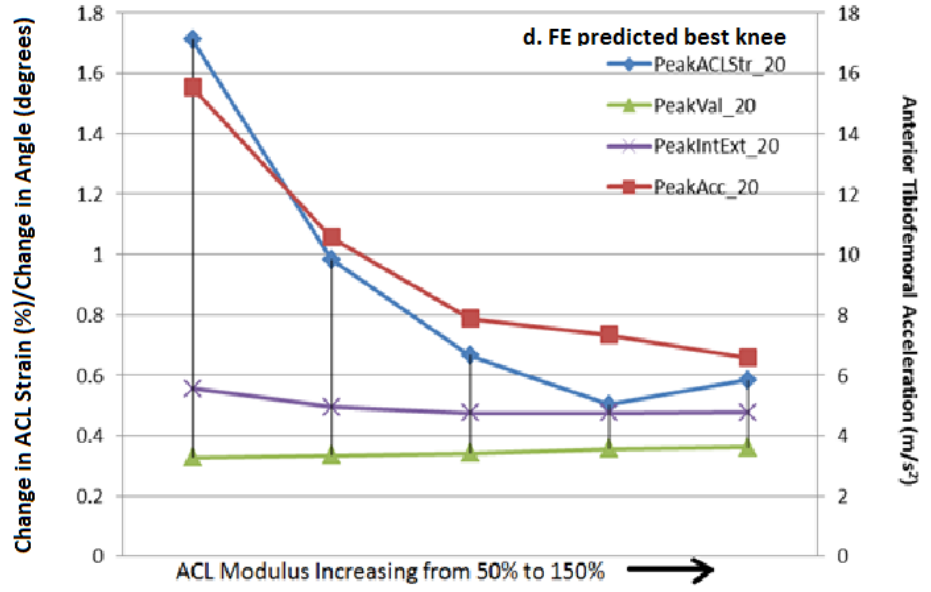
d. FE predicted best knee
PeakACLStr_20
PeakVal_20
PeakIntExt_20
PeakAcc_20
Change in ACL Strain (%)/Change in Angle (degrees)
Anterior Tibiofemoral Acceleration (m/s²)
ACL Modulus Increasing from 50% to 150%
0
0.2
0.4
0.6
0.8
1
1.2
1.4
1.6
1.8
0
2
4
6
8
10
12
14
16
18

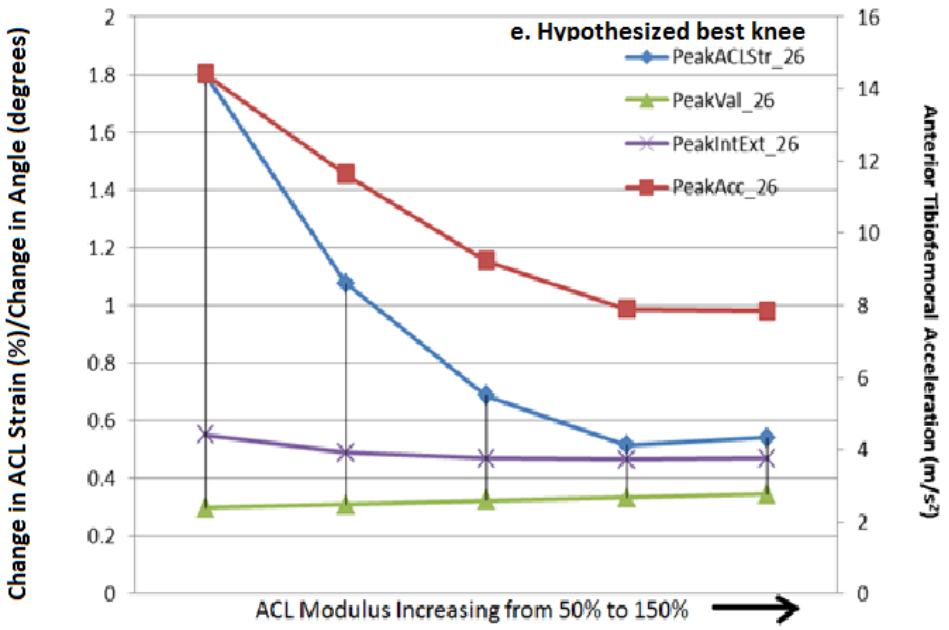

Figure 30 (a-e): Variation of peak ACL strain graphed with variation in peak anterior tibiofemoral acceleration, peak valgus angle and peak internal rotation angle for each of the five cases

Correlation tests were performed to determine the coefficient of correlation of peak change in ACL strain with peak anterior tibiofemoral acceleration, peak valgus angle and peak internal rotation angle. A significant correlation was found for all three pairs with a Pearson's coefficient of correlation of 0.979 between peak relative ACL strain correlated and peak anterior tibiofemoral acceleration ($p < 0.01$), coefficient of 0.853 between peak relative ACL strain and peak internal-rotation angle ($p < 0.01$) and a coefficient of 0.458 between peak relative ACL strain and peak valgus angle ($p < 0.05$).

Test of model effects indicate a significant main effect of both the tibial surface geometry and ACL modulus ($p < 0.01$). However, no significant interaction effect of these two factors was found. Significant model effects were also found for main effects of anterior-posterior tibiofemoral acceleration ($p < 0.01$), varus-valgus angle ($p < 0.05$) and internal-external rotation angle ($p < 0.01$) on relative ACL strain. A significant interaction effect of varus-valgus and internal-external rotation angle on relative ACL strain ($p < 0.01$) was also observed. The

kinematic variables were then fed into a stepwise regression analysis to generate an equation of regression to determine the predictor importance and to predict the relative ACL strain. Of the kinematic predictors, viz. anterior-posterior tibiofemoral acceleration, varus-valgus angle and internal-external rotation angles, the least important predictor was determined to be valgus-varus angle at 2% importance followed by anterior-posterior tibiofemoral acceleration at 16% and internal-external rotation angle with a predictor importance of 81%. The regression equation generated with an accuracy of 80% was as follows:

$$Change\ in\ ACL\ Strain = 0.917IntExt - 0.161\ APAcc - 0.138ValVar$$

A P-P plot (Figure 31) compares the distribution of the residuals to a normal distribution. The solid black line represents the normal distribution. The closer the observed cumulative probabilities of the residuals are to this line, the closer the distribution of residuals is to the normal distribution.

Correlation tests were also run to determine the coefficient of correlation between the kinematics and the relative ACL strain that develop during the course of impact. Change in ACL strain had a Pearson's coefficient of correlation of 0.64 with anterior-posterior tibiofemoral acceleration ($p < 0.01$), a coefficient of 0.811 with varus-valgus angle ($p < 0.01$) and a coefficient of 0.883 with internal-external rotation angle ($p < 0.01$).

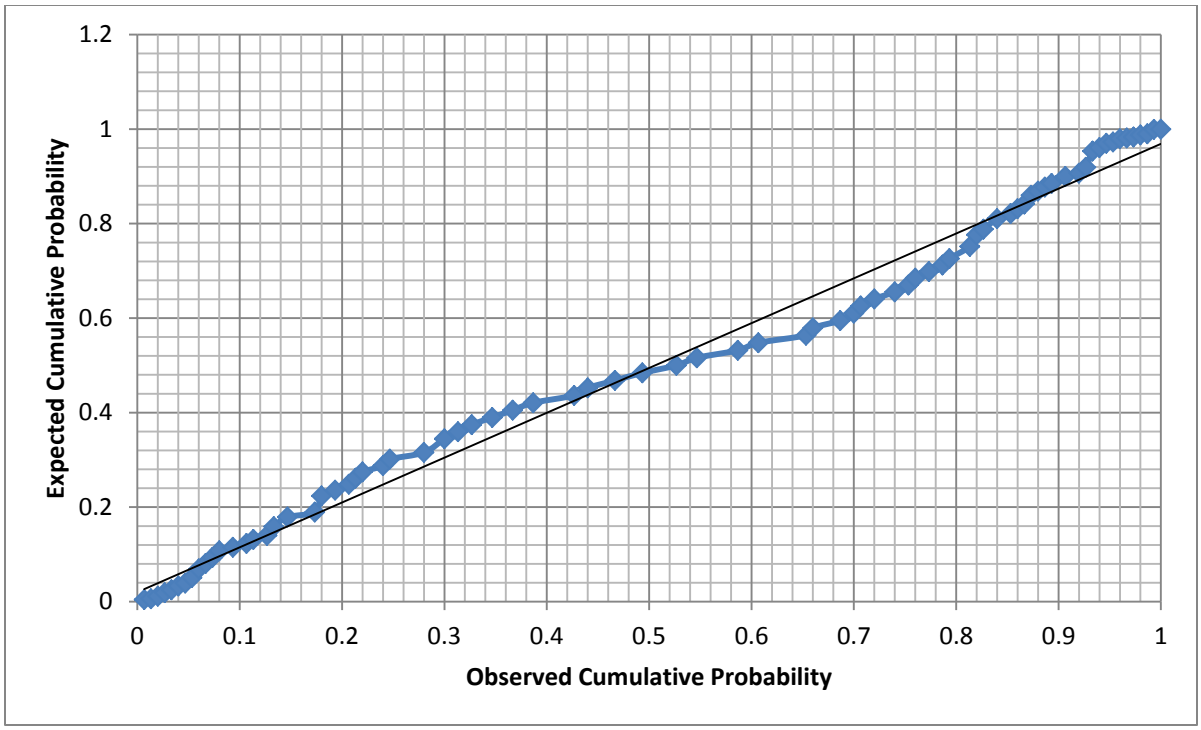

Figure 31: Comparison of distribution of residuals to normal distribution

Discussion

ACL modulus and tibial surface geometry have been recognized as non-modifiable risk factors for ACL injuries rendering an athlete inherently susceptible to potentially hazardous knee biomechanics. As the results indicate, these factors implicate through the effect of sagittal plane tibiofemoral acceleration and frontal and transverse plane knee rotation. Figure 30 depicts a clearly coupled relationship between peak relative ACL strain and peak anterior tibiofemoral acceleration, further supported by the Pearson's coefficient of correlation of 0.98. The fact that such a high coefficient of correlation was not observed when varying only the tibial surface geometry (chapter VI) suggests that anterior tibiofemoral acceleration is governed largely by the modulus of the ACL. However, as can be observed from the graphs in Figure 30, peak anterior tibiofemoral acceleration and ACL strain were highly correlated for knees # 1, 12 and 15 (Figure 30 – a, b and c) but deviated at higher moduli for knees # 20 and 26 (Figure 30 – d and e),

implying sensitivity of anterior tibiofemoral acceleration is sensitive to the tibial surface geometry at higher ACL moduli.

Tibial surface geometry predominantly influenced ACL strain through its effect on frontal and transverse plane kinematics, supported by the high coefficient of correlation of ACL strain with varus-valgus angle (0.811) and internal-external angle (0.883). The regression equation and analysis of predictor importance, however, suggest a significantly greater effect of internal-external rotation and a relatively negligible effect of varus-valgus angle. Considering the fact that transverse plane motions and frontal plane motions are never independent these results suggest that changes in varus-valgus angle are a consequence of internal-external rotation angles.

Implications

These results clearly highlight the influence of ACL modulus and tibial surface geometry on knee joint kinematics and consequentially on manifestation of ACL strain. The fact that ACL modulus predominantly affects sagittal plane tibiofemoral accelerations whereas tibial surface geometry primarily influences frontal and transverse plane kinematics suggests that monitoring specific kinematics during the course of a game can help predict the change in strain in the ACL. The specificity and impact elucidated in the results above suggest that the kinematics can also be used to estimate the physiological characterization of ACL and the tibial surface geometry. For instance, by monitoring sagittal plane tibiofemoral acceleration, varus-valgus rotation and internal-external rotation during the execution of a dynamic maneuver, not only can the change in strain that manifests in an ACL be predicted but estimates can also be made about the ACL modulus and tibial surface geometry.

Significance

A considerable challenge encountered in determining an athlete's susceptibility to ACL injuries is the significant effect of stress and fatigue on the neuromuscular response in the course of executing a complex maneuver. So, while at the start of a game, an athlete may have a strong and safer biomechanical and neuromuscular profile, these could likely deteriorate as the game progresses and the athlete may tend to revert to his or her inherent biomechanical and neuromuscular profile, often dictated by knee morphology. This is especially true for female athletes as hormonal conditions associated with menstrual cycle have been known to significantly influence not just their biomechanics and neuromechanics but also the strength of the ligament at the structural level (Schultz et al. 2005, Slauterbeck et al. 1999). These arguments therefore make a compelling case supporting the development of a surveillance tool that could monitor an athlete real time and predict risk of ACL injury during the course of game. The analyses presented in this chapter provide proof of concept and establish a framework within which the modality for a surveillance tool can be developed and employed.

Chapter VIII

General Discussion

Significance and Innovation

Injury of the anterior cruciate ligament is one of the most frequently encountered events in sports with nearly 200,000 occurrences per year. A vast majority of these incidents are experienced by athletes 15-20 years of age causing short term morbidity, trauma and rendering them vulnerable to potentially debilitating degenerative knee disease such as osteoarthritis manifesting as early as 10-15 years after the injury. These statistics imply that a large population of otherwise healthy people will require knee joint replacements when in their 30s or 40s significantly impacting their quality of life. Yet another characteristic of ACL injury epidemiology is the gender disparity in the rate of ACL injuries. Various studies have established that female athletes, even when matched for height, weight and sport, have a rate of ACL injury 2-8 fold greater than their male counterparts. This discriminate behavior paved the way for a lot of research in elucidating the role of gender in risk of ACL injury. Gender disparate factors were identified and considered for their role in ACL injuries. Such an approach led to the delineation of a number factors including (i) divergence in knee kinematics and kinetics – females, for instance, tend to have a larger valgus rotation and torque, and tend to land with knee in extension, (ii) divergence in neuromuscular behavior – females tend to have a greater quadriceps to hamstrings muscle activation ratio and a weaker hamstring response, and (iii)

divergence in knee morphology and physiology – female knees typically are shallower with higher anterior-posterior slope and female ligaments have weaker mechanical properties heavily influenced by sex-hormones associated with their menstrual cycle. The first two factors i.e. knee mechanics and neuromuscular control have been categorized as modifiable and therefore investigated extensively to facilitate mitigating risk factors by training athletes to employ biomechanical and neuromechanical profiles to minimize ACL loading. Various training programs have been established to help athletes execute dynamic motions safely. However, despite these programs, the rate of ACL injuries persists owing to various factors including high attrition rate of athletes in training programs, lack of long term follow up programs, inability to target specific, idiosyncratic factors that render an athlete susceptible to ACL injuries, lab environment not accurately recreating the fatigue and stress experienced on field etc. The need of the hour, therefore, is to pre-emptively identify risk factors specific to an individual and develop surveillance and intervention tools to target those risk factors explicitly. A considerable challenge to this approach especially within the female population, however, is accounting for the effect of fatigue, stress on neuromuscular control and sex-hormone levels associated with menstrual cycle on the mechanical behavior of soft tissues including ACL. This challenge can be addressed by actively monitoring knee joint mechanics to identify risky behavior that could potentially render the athlete susceptible to ACL injuries during the course of a game. Thus, it is imperative to develop a framework within which a pre-screening and surveillance tool can be developed to identify early on an athlete's propensity for ACL injury and monitor knee kinematics on-field during gameplay to determine their evolving risk for injury.

This thesis takes the initial step to address the void as it demonstrates a potential for being able to use kinematic measures to predict ACL strain during the course of a dynamic activity. The thesis also highlights the significant role of knee joint morphology and physiology in the

kinematic response of the knee and subsequent ACL strain development. Two non-modifiable factors viz. ACL modulus and tibial surface geometry were shortlisted for the scope of this investigation. These factors are especially dissimilar between the genders with female ACLs typically of a lower modulus and a tibial surface geometry with shallower concavity and higher slopes than their male counterparts. Segmental analysis suggested that these morphological parameters would significantly affect sagittal plane acceleration, frontal and transverse plane rotations and subsequently, ACL strain. Results from the analyses presented in chapters V, VI and VII support this concept. ACL modulus was found to heavily influence the sagittal plane tibiofemoral acceleration whereas the tibial surface geometry determined the frontal and transverse plane rotations to a larger extent. Of particular interest is the observation that LTS, MTS and MTD considered individually minimal to negligible effect on the kinematic and ACL strain measures. However, the combined effect of these three parameters demonstrated a more pronounced, significant effect on the kinematic and ACL strain measures. Additionally, while a statistically significant interaction effect of ACL modulus and tibial surface geometry was not observed, a large variability in the relative ACL strain and kinematic measures were evident. These observations suggest that ACL injury is dictated by a multi-factorial effect and an investigation into injury mechanism can be construed to be incomplete without this consideration.

A CT or MR image dataset can be used to prescreen athletes based on their tibial surface geometry and results from a simple anterior drawer test could be used to estimate the stiffness or laxity of the ACL. Tri-axial accelerometers and goniometers can then be used to track the athlete's knee kinematics in real time and fed into a predictive model to gain an estimate of ACL strain. Thus, the proclivity of an athlete to ACL injury can be predetermined and actively monitored to check for risky behavior and manifestation of potentially hazardous loads.

Summary of Results

The main results from chapters IV, V, VI and VII have been summarized in Table 6 to 9 below.

Table 6: Summary of results from Chapter IV

Analysis	Parameters	Statistical Test	Result	Significance <
Validation of FEM	ACL Strain (FEA)	Pearson's Correlation	0.861	0.01
	ACL Strain (Experiment)			
	Flexion-Extension (FEA)	Pearson's Correlation	0.80	0.01
	Flexion-Extension (Experiment)			
	AP-Translation (FEA)	Pearson's Correlation	0.829	0.01
	AP-Translation (Experiment)			

Table 7: Summary of results from Chapter V

Analysis	Parameters	Statistical Test	Result	Significance <
Effect of ACL Modulus	AP-Acceleration (FEA)	Pearson's Correlation	0.685	0.01
	ACL Strain (FEA)			
	Peak Anterior Acceleration (FEA)	Pearson's Correlation	0.999	0.01
	Peak ACL Strain (FEA)			

Table 8: Summary of results from Chapter VI

Analysis	Parameters	Statistical Test	Result	Significance <
Effect of Tibial Surface Geometry	AP-Acceleration (FEA)	Pearson's Correlation	0.611	0.01
	ACL Strain (FEA)			
	Valgus-Varus (FEA)	Pearson's Correlation	0.917	0.01
	ACL Strain (FEA)			
	Internal-External Rotation (FEA)	Pearson's Correlation	0.955	0.01
	ACL Strain (FEA)			
	Peak Anterior Acceleration (FEA)	Pearson's Correlation	0.483	0.05
	Peak ACL Strain (FEA)			
	Peak Valgus (FEA)	Pearson's Correlation	0.779	0.01
	Peak ACL Strain (FEA)			
	Peak Internal Rotation (FEA)	Pearson's Correlation	0.678	0.01
	Peak ACL Strain (FEA)			
	Internal-External Rotation (FEA)	Predictor Importance	65%	0.01
	Valgus-Varus (FEA)	Predictor Importance	24%	0.01
	AP-Acceleration (FEA)	Predictor Importance	10%	0.01
	Regression Equation	Prediction Accuracy	94%	0.01

Table 9: Summary of results from Chapter VII

Analysis	Parameters	Statistical Test	Result	Significance <
Effect of ACL Modulus and Tibial Surface Geometry	AP-Acceleration (FEA)	Pearson's Correlation	0.64	0.01
	ACL Strain (FEA)			
	Valgus-Varus (FEA)	Pearson's Correlation	0.811	0.01
	ACL Strain (FEA)			
	Internal-External Rotation (FEA)	Pearson's Correlation	0.883	0.01
	ACL Strain (FEA)			
	Peak Anterior Acceleration (FEA)	Pearson's Correlation	0.979	0.01
	Peak ACL Strain (FEA)			
	Peak Valgus (FEA)	Pearson's Correlation	0.458	0.01
	Peak ACL Strain (FEA)			
	Peak Internal Rotation (FEA)	Pearson's Correlation	0.853	0.01
	Peak ACL Strain (FEA)			
	Internal-External Rotation (FEA)	Predictor Importance	81%	0.01
	Valgus-Varus (FEA)	Predictor Importance	2%	0.05
	AP-Acceleration (FEA)	Predictor Importance	16%	0.01
	Regression Equation	Prediction Accuracy	80%	0.01

Assumptions and Limitations

Finite element modeling provides a versatile method to analyze complex biomechanical problems. However, the modality requires making certain assumptions and has inherent limitations that must be considered and acknowledged when interpreting the results. For instance, the interacting surfaces were defined as frictionless, sliding type interfaces in the FEM. Certain assumptions were made about the constitutive laws governing the behavior of different structures in the FEM. The ligaments were all represented as homogeneous, single bundled structures governed by an isotropic constitutive law. The physiological ACL is actually a double bundled, anisotropic structure with mechanical properties changing along its length. Similarly, the cartilage and menisci were assumed to be homogeneous governed by an isotropic, linearly elastic material law. The strain rate dependency effects, observable in physiological soft tissue, were not included in the material model definition of the ligaments, cartilage and menisci. Yet

another characteristic of the simulations that must be acknowledged as a limitation is that any temporal shifts in the ACL strain and impulse loads that ought to accompany any changes in the compliance and dynamic behavior of the knee joint were unaccounted for. These assumptions are fairly common within the realm of finite element analyses and are considered acceptable.

A significant consideration when interpreting the results is that the FE models were simulated to test the effects of ACL modulus and tibial surface geometry on ACL loading response during dynamic loading. The impact load to simulate single-limb landing were approximately 2 body weights in magnitude and are not representative of the forces experienced by the body during an actual landing which could be 4-15 body weights. The model therefore did not recreate the loading condition consistent with injury. However, the results indicate that knee morphology and physiology play a significant role in the ACL loading mechanism and must be considered when investigating ACL injuries.

When exploring the effect of ACL modulus on ACL strain, for instance, only the ACL modulus was varied and the moduli of PCL, MCL and LCL were left unchanged. In a knee with a low modulus ACL, it is likely that other ligaments (PCL, MCL and LCL) would be of considerably lower stiffness. However, not accounting for variation in the moduli of PCL, MCL and LCL enable us to isolate the exclusive effect of ACL modulus on ACL strain and anterior tibiofemoral acceleration.

When testing the effect of tibial surface geometry, the meniscal thickness was left unchanged between different test conditions. The effect of high tibial slope or shallow concavity can be offset by a thick meniscus increasing the effective tibial surface depth and providing stability to the femoral condyles articulating with the tibial surface. The objective of this thesis, however, is to provide proof-of-concept supporting the development of a surveillance tool to predict ACL

strain from real-time 3-D knee kinematics and does not require including the effect of meniscal thickness.

Another limitation arises from the linear muscle response model employed. The muscles simulated in our computational model and in the experiment were represented by passively pre-tensioned linear elastic cables. This implies that despite the predicted knee joint kinematics mirroring those observed in real life, the joint force due to the quadriceps-hamstring activity ratio varied linearly with flexion angle. By not including the non-linear dynamics of muscles, we expect that this model underestimates the destabilizing effects of quadriceps. Thus, the effect of "over-activation" of quadriceps or delayed activation of hamstrings in females is not represented in the model.

Future Work

The results presented in this thesis are unique and provide a compelling premise for the development of a surveillance and monitoring tool to identify athletes at risk in real-time. A significant aspect of any such research is its clinical applicability and translation from a theoretical construct to real life application. Before this is achieved, however, more data and information pertaining especially to neuromuscular control are required. The next step would be to use the FEM and test the knee and ACL response by varying the muscle forces. The quadriceps to hamstring ratio can be changed to simulate different muscle control functions. This would serve two purposes – (i) establish the role of muscle forces on knee kinematics and ACL strain and (ii) determine the sensitivity of this role to change in ACL modulus and change in tibial surface geometry. To achieve the first purpose, various simulations can be performed on the control knee. This analysis would enable us to explore the relationship between knee kinematics and ACL strain under the influence of different muscle loads. For the second

purpose, simulations can be performed to test the influence of ACL modulus, tibial surface geometry and the combination of these two parameters on the muscle forces – knee kinematics – ACL strain relationship. The study design can be similar to that used in this thesis. The analysis from such a study will help us identify the morphology and characterization of the knee most sensitive to changes in muscle load and therefore more amenable to targeted intervention. Additionally, such an analysis would also help us identify the morphology least likely to be helped by neuromuscular training.

The study could then be taken further by extending the analysis to performing clinical tests on human subjects. Active young people, 18-25 years old can be recruited to perform single limb landings in a biomechanical lab. An MRI of the subjects' knee joint can be obtained and an anterior drawer test performed to determine the tibial surface geometry and estimate anterior laxity of the knee. Electromyography (EMG) and knee kinematic data can then be assessed while the subjects perform single-limb landing. Such an analysis would enable us to clinically estimate (i) the correlation of kinematics on tibial surface geometry and anterior knee laxity; (ii) correlation of the muscle forces or activity with knee kinematics, tibial surface geometry and anterior laxity of the knee. The results from this analysis can then be compared to the predictions made by the FEM to determine its power of prediction.

The FEM can also be simulated to test effect of meniscal tears or resection, non-anatomical ACL reconstruction, graft properties etc. Another aspect of future work could include the development of a more complex FEM. For instance, the ACL, PCL, MCL and LCL could all be setup as multiple bundled structures with anisotropic, non-homogeneous, hyperelastic constitutive laws defined to dictate their behavior. Further modifications include a non-linear muscle response, complex meniscal and cartilage constitutive law, including effect of friction at

interacting interfaces etc.

BIBLIOGRAPHY

Al-Turaiki M.H.S., "The Human Knee", First Edition, 1986.

Alm A, Ekstrom H, Stromberg B. Tensile strength of the anterior cruciate ligament in the dog. *Acta Chir Scand Suppl* 445:15-23, 1974

American Academy of Orthopedic Surgeons. ACL reconstruction, October 2000.

Amis, AA; Dawkins, GPC, Functional-Anatomy of the Anterior Cruciate Ligament – Fiber Bundle Actions Related to Ligament Replacements and Injuries. *Journal of Bone and Joint Surgery – British Volume* 73:2 260-267, 1991.

Anderson AF, Dome DC, Gautam S, Awh MH, Rennirt, GW. Correlation of anthropometric measurements, strength, anterior cruciate ligament size, and intercondylar notch characteristics to sex differences in anterior cruciate ligament tear rates. *American Journal of Sports Medicine* 29:1 58-66, 2001.

Andriacchi TP, Mikosz RP, Hampton SJ, Galante JO. Model studies of the stiffness characteristics of the human knee joint. *Journal of Biomechanics* 16:1 23-29, 1983.

Andriacchi TP, Andersson GBJ, Ortengren R, Mikosz, R. Study of the interaction between knee-joint position, joint loads and muscle activity at the knee. *Journal of Biomechanics* 16:4 295-296, 1983.

Arendt EA, Agel J, Dick R. Anterior cruciate ligament injury patterns among collegiate men and women. *Journal of Athletic Training* 34:2, 86-92, 1999.

Arendt E A. Anterior cruciate ligament injuries. *Curr Womens Health Rep* 1:3 211-217, 2001.

Aspden R.M., A Model for the Function and Failure of the Meniscus, *Engineering in Medicine*, Vol.199, 1985, pp.119-122.

Baldwin MA, Langenderfer JE, Rullkoetter PJ, Laz PJ. Development of subject-specific and statistical shape models of the knee using an efficient segmentation and mesh-morphing approach. Comput Methods Programs Biomed. 2009

Barnett C. H., Davies D. V., and MacConnail M. A., Synovial Joints. Their Structure and Mechanics. *London, Longman, Green and Co.*, 1961.

Beynnon BD, Fleming BC. Anterior cruciate ligament strain in-vivo: A review of previous work. *Journal of Biomechanics* 31:6 519-525, 1998.

Blankevoort L, Huiskes R. Ligament-bone interaction in a 3-dimensional model of the knee. *Journal of Biomechanical Engineering – Transactions of the ASME* 113:3 262-269, 1991.

Blankevoort L, Kuiper JH, Huiskes R, Grootenboer HJ. Articular contact in a 3-dimensional model of the knee. *Journal of Biomechanics* 24:11 1019-1031, 1991.

Blankevoort L, Huiskes R, Delange A. Recruitment of knee-joint ligaments. *Journal of Biomechanical Engineering – Transactions of the ASME* 113:1 94-103, 1991.

Boden BP, Dean SG, Feagin JA, Garrett WE. Mechanisms of anterior cruciate ligament injury. *Orthopedics* 23:573-578, 2000.

Brandon ML, Haynes PT, Bonamo JR, Flynn MI, Barrett GR, Sherman MF, *The association between posterior-inferior tibial slope and anterior cruciate ligament insufficiency.* Arthroscopy, 2006. **22**(8): p. 894-9.

Brandt KD, Braunstein EM, Visco DM, OConnor B, Hech D, Albrecht M. Anterior (Cranial) Cruciate Ligament Transection in the dog - A Bona-Fide Model of Osteoarthritis, not merely of cartilage injury and repair. Journal of Rheumatology, 1991.

Brantigan O.C. and Voshell A.F., The Mechanics of the Ligaments and Menisci of the Knee Joint, *Journal of Bone and Joint Surgery*, Vol. 23 - American volume, 1941, pp.44-46.

Bullough P.G., Munuera L., Murphy J., and Weinstein A.M., The Strength of Menisci of the Knee as it Relates to Fine Structure, *Journal of Bone and Joint Surgery*, Vol.52-B, 1970, pp.564-570.

Chandrashekar N, Slauterbeck J, Hashemi J. Sex-based differences in the anthropometric characteristics of the anterior cruciate ligament and its relation to intercondylar notch geometry - A cadaveric study. *American Journal of Sports Medicine* 33:10, 1492-1498, 2005.

Chandrashekar N, Mansouri H, Slauterbeck J, Hashemi J. Sex-based differences in the tensile properties of the human anterior cruciate ligament. *Journal of Biomechanics* 39:16, 2943-2950, 2006.

Cochrane JL, Lloyd DG, Besier TF, Elliott BC, Doyle TLA, Ackland TR. Training Affects Knee Kinematics and Kinetics in Cutting Maneuvers in Sport. Medicine and Science in Sports and Exercise, 2010.

Crowninshield R., Pope M.H., and Johnson R.J., An Analytical Model of the Knee, *Journal of Biomechanics*, Vol.9, 1976, pp.397-405.

Daniel DM, Stone ML, Dobson BE, Fithian DC, Rossman DJ, Kaufman KR. Fate of the ACL-injured patient: A prospective outcome study. *Am J Sports Med* 22:632-644, 1994.

Danylchuk K., Studies on the Morphometric and Biomechanical Characteristics of Ligaments of the Knee Joint, *M.Sc Thesis, University of Western Ontario*, London, Ontario, Canada, 1975.

Darcy SP, Kilger RHP, Woo SLY, Debski RE. Estimation of ACL forces by reproducing knee kinematics between sets of knees: A novel non-invasive methodology. *Journal of Biomechanics* 39:13 2371-2377, 2006.

Deie M, Sakamaki Y, Sumen Y, Urabe Y, Ikuta Y. Anterior knee laxity in young women varies with their menstrual cycle. *International Orthopaedics* 26:3 154-156, 2002.

Dorlot JM, Aitbasidi M, Tremblay GM, Drouin G. Load elongation behavior of the canine anterior cruciate ligament. *Journal of Biomechanical Engineering – Transactions of the ASME* 102:3 190-193, 1980.

Englund M, Roos EM, Lohmander LS. Impact of type of meniscal tear on radiographic and symptomatic knee osteoarthritis - A sixteen-year followup of meniscectomy with matched controls. Arthritis and Rheumatism, 2003

Escamilla RF, Zheng N, Imamura R, MacLeod TD, Edwards WB, Hreljac A, Fleisig GS, Wilk KE, Moorman CT, Andrews JR. Cruciate Ligament Force during the Wall Squat and the One-Leg Squat. *Medicine and Science in Sports and Exercise* 41:2 408-417, 2009.

Evans P., "The Knee Joint: A Clinical Guide", Churchill Livingstone, First Edition, 1986.

Ford KR, Myer GD, Hewett TE. Valgus knee motion during landing in high school female and male basketball players**.** *Med Sci Sports Exercise* 35:1745-1750, 2003.

Freeman M.A.R., Swanson S.A.V. and Manley P.T., Stress-Lowering Function of Articular Cartilage, *Med. Biol. Eng.*, Vol.13, 1975, pp.245-251.

Fukubayashi T. and Kurosawa H., The Contact Area and Pressure Distribution Pattern of the Knee, Acta Orthopaedica Scandinavica, Vol.51, 1980, pp.871-879.

Gelber AC, Hochberg MC, Mead LA, Wang NY, Wigley FM, Klag MJ. Joint injury in young adults and risk for subsequent knee and hip osteoarthritis. Annals of Internal Medicine, 2000.

Gianotti SM, Marshall SW, Hume PA, Bunt L. Incidence of anterior cruciate ligament injury and other knee ligament injuries: A national population-based study. Journal of Science and Medicine in Sports, 2009.

Girgis F.G., Marshall J.L., and Al Monajem A.R.S., The Cruciate Ligaments of the Knee Joint. Anatomical, Functional and Experimental Analysis, Clinical Orthopaedics, Vol. 106, 1975, pp.216-220.

Gray H. Gray's Anatomy", Magpie Books Limited, London, 1993.

Griffin LY, Agel J, Albohm MJ et al. Non-contact anterior cruciate ligament injuries: Risk factors and prevention strategies. *J Am Acad Orthop Surg* 8:3, 141-150, 2000.

Griffin LY, Albohm MJ, Arendt EA et al. Understanding and preventing noncontact anterior cruciate ligament injuries - A review of the Hunt Valley II Meeting, January 2005. *American Journal of Sports Medicine* 34: 1512-1532, 2006.

Grood E.S., Noyes F.R, Butler D.L. and Suntay W.J., Ligamentous and Capsular Restraints Preventing Medial and Lateral Laxity in Intact Human Cadavers Knees, Journal of Bone and Joint Surgery, Vol.63-A(8), Oct. 1981,pp.1257-1269.

Grood E.S. and Hefzy M.S., An Analytical Technique for Modelling Knee Joint Stiffness – Part I: Ligamentous Forces, ASME Journal of Biomechanical Engineering, Vol.104, Nov. 1982, pp.330-337.

Gwinn DE, Wilckens JH, McDevitt ER, Ross G, Kao TC. The relative incidence of anterior cruciate ligament injury in men and women at the United States Naval Academy. *Am J Sports Med* 28:98-102, 2000.

Han SK, Federico S, Epstein M, Herzog W. An articular cartilage contact model based on real surface geometry. J Biomech. 2005;38:179-84.

Hashemi J, Chandrashekar N, Jang T, Karpat F, Oseto M, Ekwaro-Osire S. An alternative mechanism of non-contact anterior cruciate ligament injury during jump-landing: In-vitro simulation. *Experimental Mechanics* 47:3 347-354, 2007.

Hashemi J, Chandrashekar N, Gill B, Beynnon BD, Slauterbeck JR, Schutt RC, Mansouri H, Dabezies E. The Geometry of the Tibial Plateau and Its Influence on the Biomechanics of the Tibiofemoral Joint. *Journal of Bone and Joint Surgery – American Volume* 90A:12 2724-2734, 2008.

Hashemi J, Chandrashekar N, Mansouri H, Gill B,Slauterbeck JR, Schutt RC, Dabezies E, Beynnon BD. Shallow Medial Tibial Plateau and Steep Medial and Lateral Tibial Slopes New Risk Factors for Anterior Cruciate Ligament Injuries. American Journal of Sports Medicine, 2010.

Hefzy M.S. and Grood E.S., An Analytical Technique for Modelling Knee Joint Stiffness – Part II: Geometrical Non-Linearities, *Journal of Biomechanical Engineering - Transactions of the ASME*, Vol.105, 1983, pp.145-153.

Hefzy M.S., Grood E.S. and Zoghi M., An Axisymmetric Finite Element Model of the Meniscus, *Advances in Bioengineering*, Edited by A. Erdman, BED-3, ASME, New York, 1987.

Hefzy M.S. and Grood E.S., Review of Knee Models, *Applied Mechanics Review*, Vol.41(1), Jan. 1988, pp.1-13.

Heiderscheit BC, Hamill J, Caldwell GE. Influence of Q-angle on lower-extremity running kinematics. *Journal of Orthopaedic and Sports Physical Therapy* 30:5 271-278, 2000.

Heitz NA, Eisenman PA, Beck CL, Walker JA. Hormonal changes throughout the menstrual cycle and increased anterior cruciate ligament laxity in females. *Journal of Athletic Training* 34:2 144-149, 1999.

Hewett TE, Myer GD, Ford KR, Heidt RS, Colosimo AJ, McLean SG, van den Bogert AJ, Paterno MV, Succop P. Biomechanical measures of neuromuscular control and valgus loading of the knee predict anterior cruciate ligament injury risk in female athletes. *American Journal of Sports Medicine* 33:4, 492-501, 2005.

Hewett TE, Ford KR, Meyer GD. Anterior cruciate ligament injuries in female athletes. Part 2: A meta-analysis of neuromuscular interventions aimed at injury prevention. *Am J Sports Med* 34:1-9, 2006.

Hirokawa S, Tsuruno R. Hyper-elastic model analysis of anterior cruciate ligament. *Medical Engineering & Physics* 19:7 637-651, 1997.

Hirokawa S, Tsuruno R. Three-dimensional deformation and stress distribution in an analytical/computational model of the anterior cruciate ligament. *Journal of Biomechanics* 33:9 1069-1077, 2000.

Hughes G, Watkins J. A risk-factor model for anterior cruciate ligament injury. *Sports Medicine* 36:5 411-428, 2006.

Hughston J.C. and Eilers A.F., The Role of the Posterior Oblique Ligament in Repairs of Acute Medial (Collateral) Ligament Tear of the Knee, *Journal of Bone and Joint Surgery*, Vol.51-A, 1965, pp.1045.

Huston LJ, Greenfield ML, Wojtys EM. Anterior cruciate ligament injuries in the female athlete: Potential risk factors. *Clin Orthop Rel Res* 372:50-63, 2000.

Ireland ML, Wall C. Epidemiology and comparison of knee injuries in elite male and female United States basketball athletes. *Med Sci and Sports Exercise* 22:582, 1990.

Kempson G.E., The Mechanical Properties of Articular Cartilage, 'The Joints and Synovial Fluid', Vol.II, edited by L. Sokoloff, Academic Press, New York, pp.117-238.

Kennedy J.C. and Grainger R.W., The Posterior Cruciate Ligament, Journal of Trauma, Vol.7(3), 1967, pp.367-376.

Kennedy J.C. and Fowler P.F., Medial and Anterior Instability of the Knee, Journal of Bone and Joint Surgery, Vol.53-A(7), Oct. 1971, pp.1257-1270.

Krause W., Pope M.H., Johnson R., Weistein A. and Wilder D., Mechanical Changes in the Knee Postmenisectomy, Orthop. Research Society, Vol.34, 1975.

Kupper JC, Loitz-Ramage B, Corr DT, Hart DA, Ronsky JL. Measuring knee joint laxity: a review of applicable models and the need for new approaches to minimize variability. Clin Biomech (Bristol, Avon). 2007;22:1-13.

Kwan MK, Lin THC, Woo SLY. On the viscoelastic properties of the anteromedial bundle of the anterior cruciate ligament. *Journal of Biomechanics* 26:4-5 447-452, 1994.

LaPrade RF, Burnett QM. Femoral intercondylar notch stenosis and correlation to anterior cruciate ligament injuries - A prospective study. *American Journal of Sports Medicine* 22:2 198-203, 1994.

LeRoux, MA, Setton, LA., Experimental and biphasic FEM determinations of the material properties and hydraulic permeability of the meniscus in tension. *Journal of Biomechanical Engineering* 124:3 315-321, 2002

Li G, Gil J, Kanamori A, Woo SLY. A validated three-dimensional computational model of a human knee joint. *Journal of Biomechanical Engineering – Transactions of the ASME* 121:6 657-662, 1999.

Li G, Suggs J, Gill T. The effect of anterior cruciate ligament injury on knee joint function under a simulated muscle load: A three-dimensional computational simulation. *Annals of Biomedical Engineering* 30:5 713-720, 2002.

Liu SH, AlShaikh R, Panossian V, Yang RS, Nelson SD, Soleiman N, Finerman GAM, Lane JM. Primary immunolocalization of estrogen and progesterone target cells in the human anterior cruciate ligament. *Journal of Orthopaedic Research* 14:4 526-533, 1996.

Loch DA, Luo ZP, Lewis JL, Stewart NJ. A theoretical model of the knee and ACL – Theory and Experimental verification. *Journal of Biomechanics* 25:1 81-90, 1992.

Lohmander, L.S., Ostenberg, A., Englund, M., Roos, H., High prevalence of knee osteoarthritis, pain, and functional limitations in female soccer players twelve years after anterior cruciate ligament injury. *Arthritis Rheuatismm* 50(10): 3145-52, 2004.

MacConnail M. A., The Movement of Bones and Joints, III. The Synovial Fluid and its Assistance, *Journal of Bone and Joint Surgery*, Vol.32-B, 1950, pp.244-252.

McLean SG, Lipfert SW, Van Den Bogert AJ. Effect of gender and defensive opponent on the biomechanics of sidestep cutting. *Medicine and Science in Sports and Exercise* 36:6 1008-1016, 2004.

McLean SG, Oh, YK, Palmer, ML, Lucey, SM, Lucarelli, DG, Ashton-Miller, JA, Wojtys, EM., The relationship between anterior tibial acceleration, tibial slope and ACL strain during a simulated jump landing task. *Journal of Bone and Joint Surgery (American)* 93A:14 1310-1317, 2011.

Mizuno Y, Kumagai M, Mattessich SM, Elias JJ, Ramrattan N, Cosgarea AJ, Chao EYS. Q-angle influences tibiofemoral and patellofemoral kinematics. *Journal of Orthopaedic Research* 19:5 834-840, 2001.

Myer GD, Ford KR, Palumbo JP, Hewett TE. Neuromuscular training improves performance and lower extremity biomechanics in female athletes. *J Strength Cond Res* 19:51-60, 2005.

Myer GD, Ford KR, Paterno MV, Nick TG, Hewett TE. The effects of generalized joint laxity on risk of anterior cruciate ligament injury in young female athletes. *American Journal of Sports Medicine* 36:6 1073-1080, 2008.

Myklebust G, Holm I, Maehlum S, Engebretsen L, Bahr R. Clinical, functional, and radiologic outcome in team handball players 6 to 11 years after anterior cruciate ligament injury. *Am J Sports Med* 31:981-989, 2003.

National Collegiate Athletic Association (NCAA) Sports Sponsorship Participation Report: 1982-2002. Indianapolis, Indiana, National Collegiate Athletic Association, 2002.

NFHS 2003-4 High school participation survey. Indianapolis, IN, National Federation of State High School Associations, 2004.

Nordin M. and Frankel V.H., Basic Biomechanics of the Musculoskeletal System, Philadelphia, *Lea and Febiger*, 1989.

Norwood, L A; Cross, M J., Anterior cruciate ligament: functional anatomy of its bundles in Rotatory instabilities, *American Journal of Sports Medicine* 7:1 23-26, 1979.

Noyes FR, Grood ES. Strength of anterior cruciate ligament in humans and rhesus-monkeys. *Journal of Bone and Joint Surgery – American Volume* 58:8 1074-1082, 1976.

Oh YK, Kreinbrink, JL, Ashton-Miller, JA, Wojtys, EM., Effect of ACL transection on internal tibial rotation in an in vitro simulated pivot landing. *Journal of Bone and Joint Surgery (American)* 93A:4 372-380, 2011.

Olsen OE, Myklebust G, Engebretsen L, Bahr R. Injury Mechanisms for Anterior Cruciate Ligament Injuries in Team Handball. *Am J Sports Med* 32:1002-1012, 2004.

Pandy MG, Shelburne KB. Dependence of cruciate-loading on muscle forces and external load. *J Biomech* 30:1015-1024, 1997.

Papaioannou G, Nianios G, Mitrogiannis C, Fyhrie D, Tashman S, Yang KH. Patient-specific knee joint finite element model validation with high-accuracy kinematics from biplane dynamic Roentgen stereogrammetric analysis. J Biomech. 2008;41:2633-8.

Pioletti DP, Heegaard JH, Rakotomanana RL, Leyvraz PF, Blankevoort L. Experimental and mathematical methods for representing relative surface elongation of the ACL. *Journal of Biomechanics* 28:9 1123-1126, 1995.

Pioletti DP, Rakotomanana LR, Benvenuti JF, Leyvraz PF, Bumgardner JD, Puckett AD. Visco-elastic constitutive laws of soft tissues: Combination of short and long time memory effects. *Proceedings of the 1997 16th Southern Biomedical Engineering Conference* 67-69, 1997.

Piziali RL, Rastegar JC, Nagel DA. Measurement of non-linear coupled stiffness characteristics of human knee. *Journal of Biomechanics* 10:1 45-51, 1977.

Piziali R.L., Seering W.P. and Shurman D.J., The Functions of the Primary Ligaments of the Knee in Anterior-Posterior and Medial-Lateral Motions, *Journal of Biomechanics*, Vol.13, 1980, pp. 777-784.

Roos PJ, Neu CP, Hull ML, Howell SM. A new tibial coordinate system improves the precision of anterior-posterior knee laxity measurements: a cadaveric study using Roentgen stereophotogrammetric analysis. *Journal of Orthopedic Research*, 2005.

Schreppers G.J.M.A., Sauren A.A.H.J. and Husin A., A Numerical Model of the Load Transmission in the Tibio-Femoral Contact Area, *J. Engng. Med, Proc. Instn Mech.. Engrs*, Vol.204, 1990, pp.53-59.

Seering W.P., Piziali R.L., Nagel D.A., and Schurman D.J., The Function of the Primary Ligaments of the Knee in Varus-Valgus and Axial Rotation, *Journal of Biomechanics*, Vol.113, 1980, pp.785-794.

Shelbourne KD, Kerr B. The relationship of femoral intercondylar notch width to height, weight, and sex in patients with intact anterior cruciate ligaments. *American Journal of Knee Surgery* 14:2 92-96, 2001.

Shelburne KB, Pandy MG. A musculoskeletal model of the knee for evaluating ligament forces during isometric contractions. *Journal of Biomechanics* 30:2 163-176, 1997.

Shelburne KB, Pandy MG. Determinants of cruciate-ligament loading during rehabilitation exercise. *Clinical Biomechanics* 13:6 403-413, 1998.

Shelburne KB, Pandy MG, Andserson FC, Torry MR. Pattern of anterior cruciate ligament force in normal walking. *Journal of Biomechanics* 37:797-805, 2004.

Shin, CS, Chaudhari, AM, Andriacchi, TP., The influence of deceleration forces on ACL strain during single-leg landing: A simulation study. *Journal of Biomechanics* 40:5 1145-1152, 2007

Shin CS, Chaudhari, AM, Andriacchi, TP., The effect of isolated valgus moments on ACL strain during single-leg landing: a simulation study. *Journal of Biomechanics* 42:3 280-285, 2009

Shultz SJ, Perrin DH. The role of dynamic hamstring activation in preventing knee ligament injury. *Athletic Therapy Today* 4:49-53, 1999.

Shultz SJ, Sander TC, Kirk SE, Perrin DH; *Sex differences in knee joint laxity change across the female menstrual cycle*; JOURNAL OF SPORTS MEDICINE AND PHYSICAL FITNESS; 2005; 45, 4, 594-603.

Slauterbeck J, Clevenger C, Lundberg W, Burchfield DM. Estrogen level alters the failure load of the rabbit anterior cruciate ligament. *Journal of Orthopaedic Research* 17:3 405-408, 1999.

Slauterbeck JR, Hickox JR, Beynnon B, Hardy DM. Anterior cruciate ligament biology and its relationship to injury forces. *Orthopedic Clinics of North America* 37:4 585, 2006.

Smith, MP; Sizer, PS; James, CR., Effects of fatigue on frontal plane knee motion, muscle activity, and ground reaction forces in men and women during landing. *Journal of sports science and medicine,* Vol.8:3, 2009, pp.419-427

Soni A; Chawla A; Mukherjee S; Malhotra R., Response of lower limb in full-scale car-pedestrian low-speed lateral impact – influence of muscle contraction, *International Journal of Crashworthiness*, Vol. 14:4, 2009, pp.339-348

Souryal TO, Freeman TR, Daniel DM. Intercondylar notch size and anterior cruciate ligament injuries in athletes – a prospective study. *American Journal of Sports Medicine* 21:4 535-539, 1993.

Stijak L; Herzog, RF.; Schai, P., Is there an influence of the tibial slope of the lateral condyle on the ACL lesion? *Knee Surgery Sports Traumatology Arthroscopy* 16:2 112-117, 2008

Taylor, R., Interpretation of the correlation coefficient: A basic review. *Journal of Diagnostic Medical Sonography* 1:35-39, 1990

Taylor, KA, Terry, ME, Utturkar, GM, Spritzer, CE, Queen, RM, Irribarra, LA, Garrett, WE, DeFrate, LE., Measurement of in vivo anterior cruciate ligament strain during dynamic jump landing. *Journal of Biomechanics* 44:3 365-371, 2011

Thomas, AC; McLean, SG; Palmieri-Smith, RM., Quadriceps and Hamstrings Fatigue Alters Hip and Knee Mechanics. *Journal of Applied Biomechanics*, 2010.

Todd R., Freeman M.A.R., and Pirie C., Isolated Trabecular Fatigue Fractures in the Femoral Head, *Journal of Bone and Joint Surgery*, Vol.53-B,1972, pp.723-728.

Uhorchak JM, Scoville CR, Williams GN, Arciero RA, St Pierre P, Taylor DC. Risk factors associated with noncontact injury of the anterior cruciate ligament - A prospective four-year evaluation of 859 West Point cadets. *American Journal of Sports Medicine* 31:6 831-842, 2003.

von Porat A, Roos EM, Roos H. High prevalence of osteoarthritis 14 years after an anterior cruciate ligament tear in male soccer players: a study of radiographic and patient relevant outcomes. *Annals of Rheumatic Diseases*, 2004

Wang C. and Walker P.S., Rotary Laxity of the Human Knee, *Journal of Bone and Joint Surgery*, Vol.65-A, 1974, pp.161.

Warren, LF; MARSHALL, JL; GIRGIS, F., Prime static stabilizer of medial side of knee. *Journal of Bone and Joint Surgery (American)* A56:4 665-674, 1974.

Weightman B.O. and Kempson G.E., Load Carriage, '*Adult Articular Cartilage*', Edited by M.A.R. Freeman, Pitman Medical, London, pp.293.

Weiss JA., Gardiner JC., Ellis BJ, Lujan TJ., Phatak NS., Three-dimensional finite element modeling of ligaments: Technical aspects. *Medical Engineering and Physics* 27: 845-861, 2005.

Wirtz DC, Schiffers N, Pandorf T, Radermacher K, Weichert D, Forst R. Critical evaluation of known bone material properties to realize anisotropic FE-simulation of the proximal femur. *Journal of Biomechanics* 33:10 1325-1330, 2000.

Wismans J, Veldpaus F, Janssen J, Huson A, Struben P. A 3-dimensional mathematical model of the knee joint. *Journal of Biomechanics* 13:8 677, 1980.

Withrow TJ. Anterior cruciate ligament strain: An investigation of muscle and postural constraints in a cadaver impact model. Doctoral Dissertation. Department of Biomedical Engineering, The University of Michigan, Ann Arbor, 2005.

Withrow TJ, Huston LJ, Wojtys EM, Ashton-Miller JA. The relationship between quadriceps muscle force, knee flexion and ACL strain in and *in vitro* simulated jump landing. *Am J Sports Med* 34:269-274, 2006.

Withrow TJ, Huston LJ, Wojtys EM, Ashton-Miller JA. Effect of valgus loading on *in vitro* relative ACL strain during a simulated jump landing. Clin Biomech , 21:977-83, 2006.

Woo S.L.Y., Gomez M.A. and Akeson W.H., The Time and History-Dependent Viscoelastic Properties of the Canine Medial Collateral Ligament, *ASME Journal of Biomechanical Engineering*, Vol. 103, 1981, pp.293-298.

Woodford-Rogers B, Cyphert L, Denegar, CR. Risk factors for anterior cruciate ligament injury in high school and college athletes. *Journal of Athletic Training* 29:4 343-346, 1994.

Yao J, Snibbe J, Maloney M, Lerner AL. Stresses and strains in the medial meniscus of an ACL deficient knee under anterior loading: A finite element analysis with image-based experimental validation. *Journal of Biomechanical Engineering – Transactions of the ASME* 128:1 135-141, 2006.

Yoo JH, Chang CB, Shin KS, Seong SC, Kim TK. Anatomical References to Assess the Posterior Tibial Slope in Total Knee Arthroplasty: A Comparison of 5 Anatomical Axes. *The Journal of Arthroplasty* 23:4 586-592, 2008.

Yoshioka Y, Siu D, Cooke TDV. The anatomy and functional axes of the femur. *Journal of Bone and Joint Surgery – American Volume* 69A:6 873-880, 1987.

Yoshioka Y, Siu DW, Scudamore RA, Cooke TDV. Tibial anatomy and functional axes. *Journal of Orthopaedic Research* 7:1 132-137, 1989.

Zazulak BT, Paterno M, Myer GD, Romani WA, Hewett TE; *The effects of the menstrual cycle on anterior knee laxity – A systematic review*; SPORTS MEDICINE; 2006; 36, 10, 847-862.

Zhang X, Jiang G, Wu C, Woo SL. A subject-specific finite element model of the anterior cruciate ligament. Conf Proc IEEE Eng Med Biol Soc. 2008;2008:891-4.